MODELING OF THE THERMOPHYSICAL PROPERTIES OF HYDROLYSED URINE AND ITS CONCENTRATES

Khonzaphi Dube
BEng (Hons) Chemical Engineering (NUST)

Submitted in fulfilment of the requirements for the degree of MScEng in Chemical Engineering in the Faculty of Engineering at the University of KwaZulu Natal, Durban

February 2017

Supervisors: Prof C Buckley

Co-supervisor Prof D. Ramjugernath

DECLARATION

I, **Khonzaphi Prosper Dube** declare that:

(i) The research reported in this thesis, except where otherwise indicated, is my original work.

(ii) This thesis has not been submitted for any degree or examination at any other university.

(iii) This thesis does not contain other persons' data, pictures, graphs or other information, unless specifically acknowledged as being sourced from other persons.

(iv) This thesis does not contain other persons' writing, unless specifically acknowledged as being sourced from other researchers. Where other written sources have been quoted, then:

  (a) their words have been re-written but the general information attributed to them has been referenced;

  (b) where their exact words have been used, their writing has been placed inside quotation marks and referenced;

(v) Where I have reproduced a publication of which I am an author, co-author or editor, I have indicated in detail which part of the publication was actually written by myself alone and have fully referenced such publications.

(vi) This thesis does not contain text, graphics or tables copied and pasted from the Internet, unless specifically acknowledged, and the source being detailed in the thesis and in the References sections.

Signed :…….

As the candidate's Supervisor I have approved this thesis for submission.

1) ……..	……	…….
Name	**Signature**	**Date**
2) ……..	……	…….
Name	**Signature**	**Date**

ACKNOWLEDGEMENTS

My immerse gratitude goes to the following:

God Almighty	First and foremost, I would like to thank God, for everything and yet another achievement in my pursuits in the Chemical Engineering field
Chris Buckley	Thank you for the expert knowledge, tireless support and wisdom shown not only in this work, but also in the opportunities you granted me which aided in my personal and professional development
Prof D. Ramjugernath	Thank you for your guidance work and providing valuable comments throughout the course of this work
Santiago	Thank for your close supervision and willingness to help at each and every call.
Chris Brouckaert	Thank you for sharing your expertise in the modelling of this work.
PRG family	To the PRG staff and colleagues, your support and companionship during this study is sincerely appreciated.
Thermodynamics research unit	Thank for offering the experimental equipment and lab space for this work
Bill & Melinda Gates Foundation	For funding this work
Family	Finally I seize this opportunity to express my sincere gratitude to my parents for their unreserved support and encouragement. They showed great understanding for my long hours of work, sometime with reduced attention to them, to accomplish this work

ABSTRACT

In 2011, the Bill and Melinda Gates Foundation launched the Reinvent the Toilet Challenge (RTTC) to provide sustainable, sanitary amenities for 2.6 billion people who lack access to suitable toilet facilities. 16 research groups, including the Pollution Research Group, were awarded grants to develop concepts and to design prototypes of a toilet that would provide safe and sustainable treatment of human waste. To this end, various technologies were proposed and developed for the treatment of urine, to recover valuable nutrients and water.

However knowledge of the thermophysical properties of urine is key in the engineering design and optimization of urine treatment technologies. The aim of this project was to provide the RTTC grantees with experimental data that will inform optimised designs of their urine treatment units, particularly those required for the design and optimum operation of thermal and membrane separation processes. The properties investigated include: vapour pressure; osmotic pressure; electrical conductivity; and density.

To investigate the thermophysical properties of urine, synthetic solutions of hydrolysed urine were prepared at a series of concentrations, up to 10 fold. High precision measurements were undertaken for each property at temperatures ranging from 293 to 373 K. Vapour pressure was measured using a static apparatus and osmotic pressure data was calculated from the vapour pressure measurements. The density of the solutions was measured using an Anton Parr DMA 5000 densimeter that uses the vibration principle and electrical conductivity measurements were performed using a commercially available dip style cell (YSI model 3200).

Modeling of the experimental data was undertaken to assist the design engineer to calculate the thermophysical properties from the composition of hydrolysed urine. Two existing techniques for modeling were applied. In the first method, a geochemical speciation software, PHREEQC, was used to determine the chemical equilibria and distribution of the ions in the urine solutions at varying temperatures and concentrations. The speciation data was incorporated into thermodynamic models to predict the properties of the urine solutions. In the second technique, existing correlative models were used to fit the experimental data to best fit equations. These models can be incorporated into computer software used in chemical engineering design processes.

The accuracy of both techniques was verified by comparing the model calculations to the experimental data. The calculated properties, using both modelling techniques, were in good agreement with experimental data, and the average deviations were within ±2.0% for the studied concentration and temperature ranges. In conclusion, cases studies were done, to demonstrate the use of the urine data and models in the design of a multiple effect evaporator, thermal recompression evaporator, forward osmosis and reverse osmosis processes.

TABLE OF CONTENTS

LIST OF FIGURES

LIST OF TABLES

NOMENCLATURE

a	Activity
å	Distance of closest approach
A_γ, B_γ	Debye-Hückel parameters
a, b, c, d, e	empirical constant
Ḃ	B-dot coefficient
A, B, C, D, E,	Regression constants
c_P	specific heat capacity (kJ kg^{-1} K^{-1})
D_w	Diffusion coefficient ($m^{-2}s$).
F	Faradays number (C mol^{-1})
G	Gibb's free energy (J mol^{-1})
H	Enthalpy in (kJ kg^{-1})
k	relative molal vapour pressure depression
k_B	Boltzmann's constant (m^2 kg s^{-2} K^{-1})
K	Equilibrium constant
K_{cell}	cell constant
I	Ionic strength (mol kg^{-1})
m	Molality (mol kg^{-1})
M	Molecular weight (g mol^{-1})
M_T	Mean equivalent weight
N_A	Avogadro's constant
R	gas constant in (J mol^{-1} K^{-1})
P	Pressure (kPa)
S	Entropy ($J.K^{-1}.mol^{-1}$)
V	Molar volume (cm^3 mol^{-1})
T	Absolute temperature (K)
V	molar volume of the water (m^3 mol^{-1})
x	mole fraction
z	electric charge

Greek letters

α	Temperature compensation factor
ε	Relative permittivity
κ	Specific conductance (S m^{-1})
ρ	Density (kg m^{-3})
Λ	Equivalent conductivity (S cm^2 mol^{-1})
γ	Activity coefficient
μ	Chemical potential
λ	Equivalent conductivities
ϕ	osmotic coefficient
π	Osmotic pressure (MPa)
ν	Stoichiometric coefficient

Subscript

H_2O	water
i, j, k	Component i, j, k
g	gas
l	liquid
s	solute
SOL	Solution
T	Total property

Superscript

a	Anion
A,B	component A and B
c	Cation
o	standard state superscript

1 INTRODUCTION

In Chapter One, the Reinvent the Toilet Challenge (RTTC), a program initiated by the Bill and Melinda Gates Foundation (BMGF) to tackle sanitation problems in developing countries - the reason for this research - will be explained. The current treatment options for human urine are summarised. The aims and objectives are provided, and an outline of this thesis is given.

1.1 SANITATION CRISIS

In 1990, the World Health Organisation (WHO) and the United Nations Children's Fund (UNICEF) estimated that 46% of the global population had no access to improved sanitation facilities. The term "improved sanitation" is a term used by WHO / UNICEF in referring to a toilet that separates human waste from human contact. In 2000, the United Nations during the Millennium Summit established 8 Millennium Development Goals (MDGs) with set targets and indicators for the reduction of poverty for the next 15 years. The MDG target for sanitation was to halve the number of people without access to proper sanitation facilities, by 2015. At the end of 2015, global coverage of people with access to improved sanitation improved by 14% and fell short of the target by 9%. This meant that 2.5 billion people still lacked access to a proper toilet. The MDGs sanitation target was missed in the following developing regions Southern Asia, sub-Saharan Africa and Eastern Asia where only 27% of their population gained access to improved sanitation facilities since 1990 (UNICEF, 2015).

Poor sanitation has a direct impact on health and consequently on the socio-economic development of a country. Lack of sanitation is strongly linked to diseases such as diarrhoea, cholera, schistosomiasis, trachoma and intestinal nematode infections (Prüss-Üstün et al., 2008). In 2008, approximately 8% of the diseases and 7% of the global deaths were associated with poor sanitation (Mathers et al., 2008). An estimate of about 700 000 child deaths was reported per year due to diarrhoea which is more than the deaths caused by HIV/AIDS, malaria and measles combined (Black et al., 2010). Children affected with chronic diarrhoea suffer from poor development due to reduced absorption of vital nutrients, malnutrition and missed schooling. WHO estimates that in 2014, at least 200 million people suffered from schistosomiasis and that at least 1 billion people were treated for soil-transmitted helminth diseases (Mathers et al., 2008). Additionally, poor sanitation has a significant impact on budgetary resources especially in developing countries. An economic impact analysis conducted by the World Bank in South-East Asian countries Philippines, the Lao People's Democratic Republic, Cambodia, Vietnam, and. Indonesia, showed that the countries lost a combined total of 9 billion dollars as a result of unsafe sanitation (Hutton et al., 2007).

Poor management of human waste also poses an environmental risk if the faecal sludge and urine are disposed directly into the environment. About 1.1 billion people practise open defaecation (EMBARGO, 2014) which results in the contamination of the environment and compromises the usability of the water from nearby water bodies. The mismanagement of urine containment and disposal can therefore lead to environmental alterations such as eutrophication in water bodies, ammonia poisoning of aquatic life and pH adjustment of the soil and water bodies which results in the formation of aquatic dead zones. In 2012, 13 million tonnes of faeces and 122 million cubic meters of urine were discharged into inland water bodies in south-east Asia alone. The continual disposal of urine not only pollutes the environment, but results in the loss of valuable nutrients (Udert et al., 2006). Nitrogen and phosphorus are crucial nutrients that are continually exploited for food production and the reserves for are fast becoming scarce (Lagreid, et al 1999; Smil 2000; Fokes, 2007; Botheju, et al 2010).

Despite the positive progress observed in global sanitation as a result of the MDG goals set in 2000, there is still more work to be done given that the 2015 MDG target was not achieved. Poor sanitation for the 2.5 billion people who still lack access to improved sanitation is causing diseases, loss of lives, polluting the environment, disrupting ecological processes and is costing billions of dollars in dealing with the associated health and environmental costs. In the post 2015 period, the MDGs have been replaced by the Sustainability Development Goals (SDGs) which target to achieve access the improved sanitation facilities for all and end open defaecation by 2030 (NATIONS, 2015)

1.2 THE REINVENT THE TOILET CHALLENGE (RTTC)

In 2005, the Bill & Melinda Gates Foundation launched the Water, Sanitation and Hygiene (WSH) program which was involved in research, monitoring and field implementation on sustainable sanitation facilities for the poor and marginalised populations. Between 2005 and 2011, the foundation has committed in excess of $265 million on water, sanitation and hygiene projects (BMFG, 2011). In 2011, the BMFG foundation through the WSH program, initiated the Reinvent the Toilet Challenge (RTTC) to improve sanitation in the developing world by funding research projects into delivering a “reinvented toilet”. The aim of the challenge was to use fundamentals of chemical engineering processes to design and develop a new generation toilet that could sanitize the waste and recover valuable components like nutrients, water and energy. The sanitation infrastructure in developed countries requires large amounts of capital, and are expensive to maintain as it requires a lot of water and energy, hence they cannot be adopted in the developing world. Therefore, another important feature of the toilet was that it should cost less than 5 US-cents per user per day and that it should not be connected to the water or sewer or electricity grid. The foundation in 2011 awarded eight universities with grants totalling USD3 million in the first phase of grants and since then, the number of RTTC-funded research groups has increased

to 16. In 2011 and 2014, the foundation facilitated the RTTC fairs in Seattle and India respectively, which showcased the prototypes and technological innovations developed by the research groups, designers, partners and other grantees of the BMGF.

1.3 THE ROLE OF THE POLLUTION RESEARCH GROUP

The Pollution Research Group (PRG), was one of the recipients of the grants awarded in the first and second rounds of the Reinvent the Toilet Challenge in 2011 and 2012, respectively. PRG is a professional research centre in the Faculty of Engineering at the University of KwaZulu-Natal in South Africa. In the first phase, PRG collaborated with the eThekwini Water and Sanitation (EWS) in carrying out an extensive sampling and analyses of the mechanical, chemical and biological properties of excreta streams from on-site sanitation systems. Building on their lessons and experience from the first phase, PRG motivated and was awarded a grant in the second phase to assume a central role in assisting other RTTC research groups and product developers by: collecting experimental data for a wide range of excreta streams, performing process investigations in the treatment of human excreta streams and facilitating pilot and field trials in their laboratory (PRG, 2014). The experimental and characteristic data provided by PRG are expected to assist and support the RTTC grantees in the design, evaluation and optimisation of their prototypes. Informed by the data requirements of the RTTC grantees, the Pollution Research Group performed specific tests on faecal sludge which included analysing the physical, chemical and mechanical properties of different excreta streams, determining the rheological properties and drying characteristics of faecal sludge. Tests for the treatment of urine included analysing the chemical and physical properties of urine, obtaining vapour / liquid equilibrium data of urine at different temperatures, and investigating the use of nanofiltration, microfiltration and forward osmosis in the treatment of urine.

1.4 SCOPE OF THE PROJECT

This study was conducted at the Pollution Research Group in collaboration with the Thermodynamic Research Group, to provide data required for the design, evaluation and scaling up of urine processing units developed by the RTTC grantees. This section reviews the experimental data required by the RTTC designers and researchers and the purpose of modeling the data.

1.4.1 Required urine data

Table 1-1 shows the sanitation projects funded by the Gates Foundation on urine treatment. The table also shows the experimental data required by each grantee for their project.

Fresh human urine is an aqueous mixture of inorganic salts, urea, organic compounds and organic ammonium salts (Putnam, 1971). However in the urine solution the salts do not exist as binary molecules but exist as ions, complexes and neutral molecules. The distribution of these species is referred to as speciation, which is affected by temperature, pH and concentration. All the grantees listed in Table 1-1 require the knowledge of the speciation in urine, mainly because the species – species interactions and the species –water interactions have a significant bearing on the behaviour and characteristics of the urine.

Since the bulk of the urine, near 96%, is water, it can be assumed as a first approximation that the properties of urine closely resemble that of water. However as the concentration of the urine increases, the deviations between the properties of urine and water differ significantly, and these may greatly affect the design of the urine processing units. Four grantees, National University of Singapore, Eawag-the Swiss Federal Institute of Aquatic Science and Technology, University of Colorado Boulder, University of Toronto have processes that require the vaporisation of urine to obtain a concentrate of nutrients and water. The presence of non-volatile solids in urine has the effect of increasing the boiling temperature of urine. The vapour pressure data will assist in establishing the optimum process design.

Table 1-1: Urine sanitation projects funded by the Gates Foundation

Grantee	Project Title	Objective	Required urine data
Pollution Research Group	Investigation of membrane processes in the treatment of urine	Use of microfiltration, nanofiltration and forward osmosis	Osmotic pressure Speciation
National University of Singapore	Low-cost Decentralized Sanitary System for Treatment, Water and Resources Recovery	Three-way urine diversion sanitary system • transforms faeces into biochar through pyrolysis, • recovers energy via microbial fuel cells • Recovers and cleanses water from urine via evaporation, condensation, and sand/zeolite filtration and produces fertilizers from fertilizer	Vapour pressure Density Electrical Conductivity Speciation
Eawag	Valorisation of Urine Nutrients in Africa (VUNA)	Stabilisation of urine using the nitrification process followed by concentration using the distillation process. Complete nutrient recovery, the concentrate is used as a fertiliser and 95% water is recovered.	Speciation Vapour pressure Density Electrical Conductivity
Eawag	Blue Diversion	A grid-free dry diversion toilet, in which undiluted urine, faeces and wash water are collected separately. Water is recovered from urine by electrochemical treatment to remove colour and prevent pathogen growth	Speciation Electrical conductivity
University of Toronto	NoWater! NoWatts! NoWaste! No Sanitation	The liquid stream is separated from the solid and heated in a counter-current heat exchanger to produce a sanitised liquid for agricultural use	Vapour pressure Speciation Specific heat capacity
University of West England, Bristol		Urine from a urinal facility is directed to a Microbial Fuel Cell, which generates electricity as a natural respiratory by-product of microorganisms	Speciation Electrical Conductivity

The Pollution Research Group is investigating the use of membrane technology in the treatment of human urine. The specific membrane processes include ultrafiltration, nanofiltration and forward osmosis. Membrane processes work by selectively rejecting specific ionic species and hence the speciation data will be useful in selection of the membranes with the appropriate pore size. Forward osmosis employs the natural process of osmosis based on the osmotic pressure difference between two solutions separated by a membrane to extract water. PRG selected ammonium bicarbonate as a draw solution mainly because after extracting water from urine, the ammonium bicarbonate can be regenerate using low grade heat. In order to facilitate the extraction of water from urine, the osmotic pressure of the draw solution must be greater than urine at all times. The osmotic pressure of ammonium bicarbonate is available in literature hence the need for the osmotic data of urine in order to evaluate the feasibility of using ammonium bicarbonate as a draw solution and also evaluating the amount of water that can be extracted from urine.

Density is an important parameter in the design calculations and sizing of transfer equipment such as piping, pumps, heat and mass transfer equipment such as heat exchangers, evaporators and crystallizers. This explain why density data are required by all the grantees in their projections.

Electrical conductivity is a property that quantifies the ability of a solution to conduct an electric current. The electric current in urine is facilitated by the movement of the charged species in the solution. The magnitude of the charge is dependent of the nature of the charged species in the solution. Electrochemical treatment methods developed by the University of the West of England (UWE) and Eawag greatly depend on the ability of urine to conduct an electric charge. The University of the West of England (UWE), Bristol designed a microbial fuel cell integrated with a urinal facility which generates electricity as a respiratory by-product of the metabolizing microorganisms. While Eawag, in collaboration with PRG and eThekwini Water and Sanitation developed electrolysis reactor which sanitised and removed nitrogen and organic compounds from urine. The electrical conductivity is directly proportional to the concentration of ions in a solution and in evaporation processes, the conductivity is used as a simple, accurate and reliable means for monitoring and control.

Based on the data required by the RTTC grantees in Table 1-1, this study will be focused on the following physical properties; vapour pressure, osmotic pressure, density and electrical conductivity.

1.4.2 Modeling

Data presented in tabular form presents challenges if the property of interest is not at the specified conditions presented in the tabulated data. The researcher and the designer is faced with the challenge of having to interpolate and at times, extrapolate tabulated data to attain the required value of the property. Mathematical models which can accurately describe the data within the specified conditions assist the designer and researcher to calculate the necessary property at any point of interest. The models can be conveniently integrated into designing and modeling software.

Two modeling techniques were be used to calculate the thermophysical properties of urine from its composition, and these models include the correlative models and the thermodynamics models. In correlative modeling, the experimental data will be regressed and fit into semi-empirical equations where each property will be correlated to the total dissolved solids (TDS) in urine. The total dissolved solids is the measure of all inorganic and organic components in a solution. Urine has a total of at least 158 chemical constituents (Putnam, 1971), which may be too many and some too difficult to analyse. The purpose of using TDS, is that it is a relatively easy property to measure.

In thermodynamic modeling, a thermochemical equilibrium model based on the Debye-Hückel equation was used to calculate the physical properties of the urine. Unlike, the correlative model which was based on the TDS, the thermochemical equilibrium model will use the chemical speciation of the urine solution. The speciation of the urine will be limited to the predominant components in urine which include ammonia, ammonium, sodium, chlorides, potassium, phosphorus, sulphates, magnesium calcium and carbonates.

Both models will be evaluated at different concentrations and temperature, and the model calculations will be compared with the experimental data.

1.5 AIM AND SPECIFIC OBJECTIVES

The successful development, design and operation of urine treatment processes requires knowledge of the physical properties and characteristics of the urine solution and its concentrates. There is very little data in literature which presents the physical properties of urine. The aim of this project is to investigate the thermophysical properties of urine which are required for the design of thermal, membrane and electrochemical separation processes. The overall aim of the project was achieved through the following specific objectives

- Performing high precision measurements for temperatures ranging between 298 K to 398 K and concentrations ranging between 4.5 to 32 wt%.
- Correlation of data using best-fit regression equations as functions of temperature and concentration
- Simulate the chemical equilibrium and speciation of the urine and its concentrates at varying temperatures
- Use the thermochemical equilibrium model based on the Debye-Hückel equation was used to calculate the physical properties of the urine
- Demonstrate the use of the models in the design and evaluation of urine processing units.

The accuracy of the modelling techniques was verified by comparing the model calculations to the experimental data.

1.6 THESIS OUTLINE

Chapter One – introduces the research work in this thesis. A brief overview of how the Reinvent the Toilet Challenge was initiated to alleviate the sanitation crisis in the world is given. The chapter concludes with the motivation, scope, and the aims and objectives of this work.

Chapter Two – focuses on the composition and chemistry of the urine and how the spontaneous processes result in the transformation of urine in urine collecting systems and storage tanks

Chapter Three - reviews the modelling techniques used in calculating the physical properties of multicomponent aqueous solutions similar to urine. The models reviewed include correlative equation and predictive thermodynamic models

Chapter Four – reviews the measurement equipment used for aqueous solutions as well as the inherent pros and cons of each method.

Chapter Five – outlines the equipment and the methodology used in measuring the properties of urine

Chapter Six – presents the results conducted on test solutions and the physical properties of urine.

Chapter Seven – is the discussion of the results in relation to the models discussed in chapter Three. The accuracy of each model over the studied concentration and temperature ranges is assessed and discussed.

Chapter Eight – briefly concludes this research work by stating the major findings and outcomes.

2 URINE COMPOSITION, CHEMISTRY & TREATMENT

Urine treatment technologies must take into account the spontaneous transformative processes that change the composition of source separated urine (Udert et al., 2006). The aim of this chapter is to review the chemical composition of fresh urine presented in literature, and outline how spontaneous transformative process result in a change in composition of urine.

2.1 CHEMISTRY OF URINE

Research in reclaiming water from urine has been extensively undertaken in space ship technology studies, because it is expensive to ferry water from earth (Adam et al., 2012, Putnam, 1971, Tamponnet et al., 1999). This culminated in the collection of chemical, physical and engineering data on fresh urine (Putnam, 1971). Fresh urine refers to urine that has not gone through any chemical, physical and biological alterations. Spaceships have a highly controlled environment, where immediately after expression from the body, the urine can be pre-treated and stored for further processing before it breaks down. The next section reviews the composition of fresh urine found in literature.

2.1.1 Fresh human urine composition

Fresh human urine is a complex aqueous solution that consists of 1.3% urea, 1.4% inorganic salts, 0.5% organic compounds, 0.4% organic ammonium salts and 96.4% water (Putnam, 1971). The concentrations of the constituents of urine vary for each individual and for each region, and they are affected by feeding habits, drinking water consumed, physical activities, body size and environmental factors (Vinnerås et al., 2003, Karak and Bhattacharyya, 2011).

The major components in fresh urine consist of the following: urea, sodium, potassium, calcium, magnesium, sulphates, phosphates and chlorides and chemical oxygen demand (COD) (Udert et al., 2006, Lind et al., 2000). Table 2-1 shows the urine compositions for fresh urine reported in various literatures sources.

Freshly expressed urine has a slightly acidic to neutral pH (Höglund et al., 1998). Urea is the single, largest constituent in urine. About 75 - 90% of the nitrogen in urine is in the form of urea while the remainder exists as ammonia and organic nitrogenous compounds such as creatinine, amino acids and uric acid (Table 2-1). The concentrations of calcium, magnesium and phosphorus are dependent on the precipitation reactions in urine, which will be discussed later. Nearly 95 - 100 % of the phosphorus in human urine exists as $H_2PO_4^-$ and HPO_4^{2-} complexes (Ciba-Geigy et al., 1970). Approximately 90% of the sulphur is in the form of sulphates and 10% is found in sulphuric acid, esters and other organic compounds(Ciba-Geigy et al., 1970).

Chemical oxygen demand (COD) is used as a measure of the organic compounds in urine. In fresh urine, the COD can be as high as 10 000 mg/L of urine (Udert et al., 2006, Ciba-Geigy et al., 1970). The predominant compounds contributing to the COD include long chain organic acids, creatinine, amino acids and carbohydrates.

Table 2-1: Literature values for the compositions of fresh urine from various sources

	Major components of fresh urine (mg/L)				
	Putnam (1971)	**CIBA Geigy (1977)**	**Udert (2003)**	**Rink (1964)**	**Roempp (1997)**
pH	6.6	6.2	7.2	6.1	5.7
Urea	13400	7700	5810	7700	6200
Total Nitrogen	8123	9200	6064	9150	-
Phosphate	349	326	367	715	-
Calcium	210	170	129	113.6	330
Magnesium	196	100	77	167.5	270
Sodium	3151	420	2670	3666.5	3930
Potassium	2484	2200	2170	4216.5	1800
Chloride	5627	3800	3830	5500	5930
Sulphate	2074	960	748	-	1600
COD	7530	1200	8150	-	-

* Units for all in mg/L

2.1.2 Spontaneous transformation processes in urine

Unlike fresh urine in spaceships, urine cannot be immediately treated in normal sanitation facilities, even where it is collected as a separate stream, uncontaminated by faecal matter, and especially so in low income areas which rely on on-site sanitation (OSS) facilities (Montangero, 2004). On-site sanitation, also known as a decentralised system, refers to facilities where human excreta is treated at the same location it is generated.

When OSS facilities are full, the excreta needs to be collected and transported for either safe disposal or treatment. During the process of collection and storage, the fresh urine undergoes spontaneous transformative processes that result in hydrolysis of urea, precipitation of phosphate-based solids and volatilization of ammonia (Udert et al., 2006). These spontaneous processes are initiated by bacteria which are found in urine collecting and storage systems.

Hydrolysis is the chemical breakdown of a compound due to the addition of water. Fresh urine is regarded as being biologically unstable as a result of the high content of urea. Urea is readily hydrolysed into ammonia and bicarbonate, by the enzyme urease produced by most bacteria found in faeces and urine collecting systems (Hellström et al., 1999, Mobley and Hausinger, 1989).

Since urea makes up about 37% (Putnam, 1971) of the total dissolved solids, its breakdown results in significant changes to the composition of urine. The hydrolysis of urea is shown in equation (2.1):

$$CO(NH_2)_{2(aq)} + 3H_2O_{(l)} \rightarrow 2NH_{4\,(aq)}^{+} + HCO_{3(aq)}^{-} + OH^{-}{}_{(aq)} \qquad (2.1)$$

The breakdown of urea results in an increasing concentration of ammonia, which raises the pH of the urine to 9. High pH values prompt the precipitation of struvite ($MgNH_4PO_4 \cdot 6H_2O$), hydroxyapatite ($Ca_5(PO_4)_3(OH)$) and calcite ($CaCO_3$), found in urine collecting systems (Udert et al., 2003b). After complete hydrolysis of the urea, 90% of the nitrogen is fixed as ammonia. At a pH of 9, a significant proportion about 33% (Udert et al., 2006) of the dissolved ammonia ion exists in equilibrium with the ammonium ion:

$$NH_{4\,(aq)}^{+} + OH_{-(aq)} \leftrightarrow NH_{3(aq)} + H_2O_{(l)} \qquad (2.2)$$

Volatilisation of the ammonia will occur when the urine is in contact with air. Equation (2.3) shows the equilibrium equation between the gaseous ammonia and the aqueous ammonia:

$$NH_{3(aq)} \leftrightarrow NH_{3(g)} \qquad (2.3)$$

The deprotonated ammonia is highly soluble in water, with a high Henry coefficient at 25 ˚C of 0.00071 $M_{(g)}/M_{(aq)}$ (Pronk and Kone, 2009). The gaseous ammonia is responsible for the odour problems in hydrolysed urine, and if not contained may result in nitrogen losses (Hellström et al., 1999).

During precipitation, most of the calcium and magnesium is used up to form struvite and hydroxyapatite. Approximately 30% of the dissolved phosphorus is integrated into the solid structure of the precipitates. Struvite formation uses less than 1% of the total ammonia in urine. Lind et al. (2000) and Wilsenach et al. (2007) noted that, to a lesser extent, potassium could replace ammonium in the struvite precipitate and could replace calcium in hydroxyapatite. The loss of potassium to the formation of precipitates in urine is expected to be less than 7%. Organic substances are also incorporated into precipitates. (Udert et al., 2003b) measured about 0.18gCOD/gTSS in the urine sludge from a collection tank.

The hydrolysis of urea, which is unavoidable in urine collecting systems, results in the precipitation of urine components and potential volatilisation of ammonia. This significantly changes the composition and the characteristics of the urine. (Rose et al., 2015) performed an extensive literature review on the composition of hydrolysed urine. Table 2-2 shows the final composition of urine after complete hydrolysis.

Table 2-2: Composition of hydrolysed human urine

	Major Components of hydrolysed Urine (mg/L)		
	Kirchmann et al (1995)	**Udert (2012)**	**Udert (2002)**
pH	8.9 - 8.96	8.69	9.1
COD		4500	10000
Ammonium	1526 - 2219	-	5100
Ammonia	1436 - 2219	2390[(a)]	2700
Phosphorus	-	208	540
Potassium	875 - 1150	1410	2200
Calcium	13.34 - 15.75	16	0
Magnesium	1.5- 1.63	5	0
Sodium	9.38 - 982	1740	2600
Carbonate	-		3200
Sulphate	175 - 225	778	1500
Chloride	2.24 - 225	3210	3800

(a) Total ammonia
*-Units for all in mg/L except for pH

2.2 TREATMENT OF HYDROLYSED URINE

In order for urine to be treated, it needs to be separated from the faeces at the toilet and as discussed in the previous section, the urine undergoes transformative processes and is hydrolysed. Treatment technologies for urine must take into account the spontaneous transformative processes that change the composition of source separated urine(Udert et al., 2006). At a pH of 9, the hydrolysed urine is susceptible to ammonia losses, if it is heated or stored in open containers. Mismanagement of hydrolysed urine can result in ammonia loss which reduces the quality of the urine if it is going to be used as a fertiliser (Botheju et al., 2010). Therefore, urine pre-treatment is necessary for complete nutrient recovery.

The next section outlines how hydrolysed urine is separated at the source and pre-treated prior to major urine processing operations outlined in the objectives in **Chapter 1** which include evaporation, membrane and electrochemical treatment.

2.2.1 Source Separation

Urine treatment processes require urine to be separated from the faeces at the toilet. The treatment of source separated urine using chemical engineering principles has received increasing attention over the years (Maurer et al., 2006b). This concept has been investigated as early as the 1990s as a sustainable option, since urine is abundant with nutrients which can be used as a fertiliser (Kirchmann and Pettersson, 1994, Larsen and Gujer, 1996, Otterpohl et al., 1999). This is because urine in waste water constitutes about 1% of the wastewater volume, yet contributes about 80% of nitrogen and 50% of phosphorus to domestic wastewater (Larsen and Gujer, 1996).

In decentralised sanitation facilities, the separation of urine at the source can be achieved through the use of urine diversion (UD) toilets, shown in Figure 2-1, which have separate collection systems for urine and faeces.

(a) Pedestal UDT

(b) Squat UDT

Figure 2-1: Types of urine diversion toilets

Urine diversion was initially investigated by the Stockholm Water Company in 1995, as a sustainable initiative that would meet the MDG sanitation goal (Kvarnström et al., 2006). Apart from collecting pure urine, UD toilets have several advantages that include: reduced water consumption, reduced odours and the production of relatively dry faecal sludge which is easy to handle.

2.2.2 Pre-treatment of hydrolysed urine

The presence of ammonia and mineral precipitates in hydrolysed urine presents several operational challenges. The ammonia nitrogen in urine exists in two forms: free ammonia (NH_3) and ammonium ion (NH_4^+). At a pH value of 9, 33% of the ammonia is in it unionised form (NH_3).

Increasing the temperature of hydrolysed urine results in a loss of ammonia in gaseous form and this hinders the capability of using evaporation and other thermal process in concentrating urine. Urine hydrolysis in urine-collecting systems is a relatively fast process which takes less than 24 hours (Udert et al., 2003b). Since the urea-hydrolysing bacteria are found everywhere (Mobley and Hausinger, 1989), this means urine hydrolysis cannot be avoided in on-site sanitation facilities.

Hydrolysed urine needs to be stabilised in order to prevent ammonia loss through volatilisation. Stabilisation can be done either through acidification (Ek M, 2006, Tettenborn et al., 2007) or biological nitrification (Sun et al., 2012, Udert and Wächter, 2012). Acidification of urine converts the ammonia into an ammonium form which is stable even at high temperatures. Biological nitrification converts

about 50% of the ammonia into nitrates which are non-volatile (Udert et al., 2003a). The remaining ammonia is converted into ammonium form by the low pH of 6 caused by the nitrification process.

2.2.3 Evaporation

Both acidification and nitrification have been used as a pre-treatment method for evaporation of hydrolysed urine. Ek et al. (2006) evaporated hydrolysed urine under vacuum at various levels of pH using glass equipment. The urine was evaporated until a volume reduction factor of 20 was achieved. Quantities of 12 and 13 kg H_2SO_4/m^3 urine were required to reduce the pH of the urine to 5.5 and 4.5, respectively. A nitrogen recovery of 89% was achieved in concentrate from a pH of 5.5 and 95% from pH of 4.5.

Tettenborn et al. (2007) evaporated hydrolysed urine at a pH of 6 using a 'Prowadest mini' evaporation unit at a pressure of -300mbar and temperatures of 70 – 80 ˚C. The pH was lowered using concentrated sulphuric acid and phosphoric acid. The evaporation process was driven until a 12 fold concentrate was obtained.

Udert et al. (2012) recovered all nutrients from source-separated urine by combining biological nitrification with distillation. The hydrolysed urine was nitrified in a membrane-aerated biofilm reactor, to produce a nitrified urine. 50% of the ammonia in the urine was converted to nitrates and the final pH of the nitrified urine was 6.2. A rotavapor was used to evaporate 99.2% of the water in urine at 200 mbar and 78 ˚C. A nitrogen recovery of 97% was achieved in the urine concentrate.

2.2.4 Membrane treatment

In membrane treatment processes, hydrolysed urine has been stabilised by acidification. The use of membrane technology is viewed as an energy efficient method for treating urine, with high nutrient recovery. Ammonium (NH_4^+) is readily retained by reverse osmosis membranes, compared to ammonia (NH_3) (Maurer et al., 2006a). Dalhammar (1997) lowered the pH of hydrolysed urine to 7.1, in order to prevent the permeation of ammonia through the membranes. The urine was filtered using reverse osmosis membranes at a pressure of 50 bars until a concentration factor of 5 was achieved. The following recoveries were obtained in the retentate: 70% ammonium, 73% phosphate and 71% potassium.

Ek et al. (2006) filtered hydrolysed urine using reverse osmosis at various pH levels to a concentration factor of 5, at a pressure of 5Pa and temperature of 29 ˚C. Nitrogen recoveries of 79%, 91% and 98% were obtained in the concentrate for pH values of 9.2, 7.0 and 6.0. A loss of nitrogen from the urine to the permeate was due to the better retention of NH_4^+ to NH_3.

2.2.5 Electrochemical treatment

Larsen and Maurer (2011) gives a comprehensive review of electrochemical treatment processes for human urine. The processes can be summarised as follows: oxidation and reduction of major pollutants, coagulation treatment processes, disinfection or targeted micropollutant removal.

In oxidation and reduction processes, when the voltage is applied to the solution, the chloride ions in urine are oxidised to form chlorine, which is a strong oxidant. The chlorine is responsible for the oxidation of compounds in the urine solution; hence the process is referred as indirect oxidation. Free ammonia is oxidised to molecular nitrogen in a process called breakpoint chlorination (Kapałka et al., 2010).

Udert (Udert et al.) used two types of anodes for indirect electrochemical oxidation in source-separated urine. These were: thermally decomposed iridium oxide film (TDIROF) and boron-doped diamond (BDD) electrodes. Although both electrodes can directly oxidise ammonia, Udert et al. (2015) observed a prevalence of indirect oxidation reactions. The process revealed COD removal rates of 500 g $COD \cdot m^{-2} \cdot d^{-1}$ and 1 000 g $COD \cdot m\text{-}^2 d^{-1}$ for TDIROF and BDD, respectively. Ammonia oxidation rates were greater than 400 g $N \cdot m^{-2} \cdot d^{-1}$ for TDIROF and 200 g $N \cdot m^{-2} \cdot d^{-1}$ for BDD respectively

The use of microbial fuel cells has attracted increasing attention in the sustainable treatment of wastewater, as revealed by the publication of experimental work: (Logan et al., 2006, Logan and Regan, 2006, Rabaey et al., 2003, Liu et al., 2004, Logan, 2008). The use of electroactive bacteria, in bioelectrochemical systems for wastewater treatment, has been extended to the treatment of urine.

Electroactive bacteria are able to convert organic substances in urine to electricity by transferring electrons through their cell walls and onto electron acceptors. They grow on the electrode surfaces and facilitate cathode (reductive) and anodic (oxidative) electrochemical processes. Santoro et al. (2013) used a novel membraneless single-chamber microbial fuel cell for the treatment of urine and was able to generate about 0.1 mA-0.23mA. The average COD decomposition rates was 1825 g $COD \cdot m\text{-}^2 d^{-1}$.The University of the West of England (UWE) in Bristol has designed a microbial fuel cell integrated with a urinal facility. The microbial fuel cell generates electricity as a respiratory by-product of the metabolizing microorganisms. The prototype from Bristol generates about 107mW of power from 2.4L$\cdot d^{-1}$ urine which is enough to charge a cell phone.

2.3 SYNTHETIC URINE SOLUTIONS

For this study, the experimental measurement of the properties of urine was conducted in the Thermodynamics Research Unit laboratory. The laboratory is not equipped and certified to handle biologically hazardous materials such as human waste. In such cases, where the use of real urine is not permitted, synthetic urine, simulating the chemical and physical ranges in normal human urine, is commonly used (Tilley et al., 2008). Most synthetic recipes used in urological research are based on a simulant prepared by (Griffith) which is based on fresh urine (Chutipongtanate and Thongboonkerd, 2010).

Table 2-3 shows the composition of synthetic urine recipes found in literature. Generally, all three formulations provided are in the composition range of hydrolysed urine presented in Table 2-2. The urine recipes show comparable chemical composition, except for Sendrowski‘s (2013) formula, which reports low values for chloride levels. All of the formulas assume that all the urea is converted to ammonia and carbonates, and that all the calcium and magnesium is precipitated as struvite.

Table 2-3: Composition of synthetic urine in literature

		Components in mg/L		
Chemical		**Sendrowski (2013)**	**Boyer (2014)**	**Udert et al. (2003a)**
Ammonia	NH_3	7000	8778	7938
Carbonate	CO_3^{2-}	3000	3192	3192
Sodium	Na^+	2162	2530	2300
Potassium	K^+	1600	1840	1800
Chloride	Cl^-	3550	6035	6000
Sulphates	SO_4^{2-}	1440	1536	1536
Phosphates	PO_4^{3-}-P	434	744	527

2.4 CHAPTER SUMMARY

The aim of this chapter was to present the chemical composition of urine and its chemistry, and explain how the transformative processes change the urine composition and the selection of the appropriate treatment technologies. Hydrolysis of source-separated urine is unavoidable as hydrolysing bacteria are prevalent in urine collecting systems.

The hydrolysis of urine results in the following changes; all urea is converted to ammonia and carbonates, pH raises to 9 and struvite (ammonium magnesium phosphate) is precipitated out of the urine solution. At a pH of 9, the nitrogen in urine exits in two forms; as ammonium (NH_4^+) and as ammonia (NH_3).

Pre-treatment of hydrolysed urine is important for evaporation and membrane processes if the aim it recover all nutrients present in urine. Approximately 33% of the ammonia is volatile and this presents treatment challenges when using evaporation or membrane separation processes. The ammonia will volatilise when heated and some of it will not be retained by membranes. In order to avoid ammonia losses via volatilisation or permeation, hydrolysed urine needs to be stabilised by nitrification or acidification. Acidification lowers the pH and converts the ammonia (NH_3) to ammonium (NH_4^+), which is stable at high temperatures. Nitrification converts 50% of the ammonia into nitrates which are non-volatile, and the final pH of 6 converts the remaining ammonia into ammonium

Since the use of real urine was not permitted in the Thermodynamics Research Group Laboratory, where the thermophysical properties were measured, a review of the synthetic recipes of hydrolysed urine found in literature was given.

.

3 MODELING OF AQUEOUS ELECTROLYTE SOLUTIONS

Chapter 3 focuses on the modeling techniques that can determine the thermophysical properties of hydrolysed urine from its concentration.

Modeling of the thermophysical properties of urine will assist the design engineer to derive a mathematical expression that can be used to interpolate and at times extrapolate the tabulated experimental data. These models can also be incorporated into computer software used for the design of chemical engineering processes.

Urine is a multicomponent aqueous solution with high ionic strength ranging between 0.3 – 0.6 M (Ronteltap et al., 2007). This chapter reviews two modelling techniques that can be applied to such a solution, such as natural water, seawater and industrial brines. The models include thermodynamic predictive models and correlative models.

In thermodynamic modeling, the chemical speciation of the hydrolysed urine is incorporated into thermodynamic equations used for the prediction of the thermophysical properties. In relation to aqueous solutions, chemical speciation is the distribution and concentration of physicochemically distinct entities at molecular level (Kot and Namieśnik, 2000). The speciation in the solution, which will be discussed in detail, is calculated from the nature of the species, temperature and the ionic strength. The advantage of this technique is that the contribution of each species or component in the urine solution can be quantified.

Correlative modeling is a relatively simple method compared to the thermodynamic models mentioned above which are difficult and cumbersome to calculate. It involves the use of regression equations to fit the experimental data. The thermophysical properties will be correlated to the total dissolved solids (TDS) in hydrolysed urine. Urine has a total of at least 158 chemical constituents (Putnam, 1971), which may be too many and some too difficult to analyse. In using the correlative method, the researcher only has to measure the TDS, which is a relatively easy property to measure.

Figure 3-1 shows how the thermophysical properties will be calculated from the urine composition. The underlying theories and principles employed for the development of these models are discussed in detail in this chapter, according to Figure 3-1, in order to justify the choice of models that have been made for the purposes of this study.

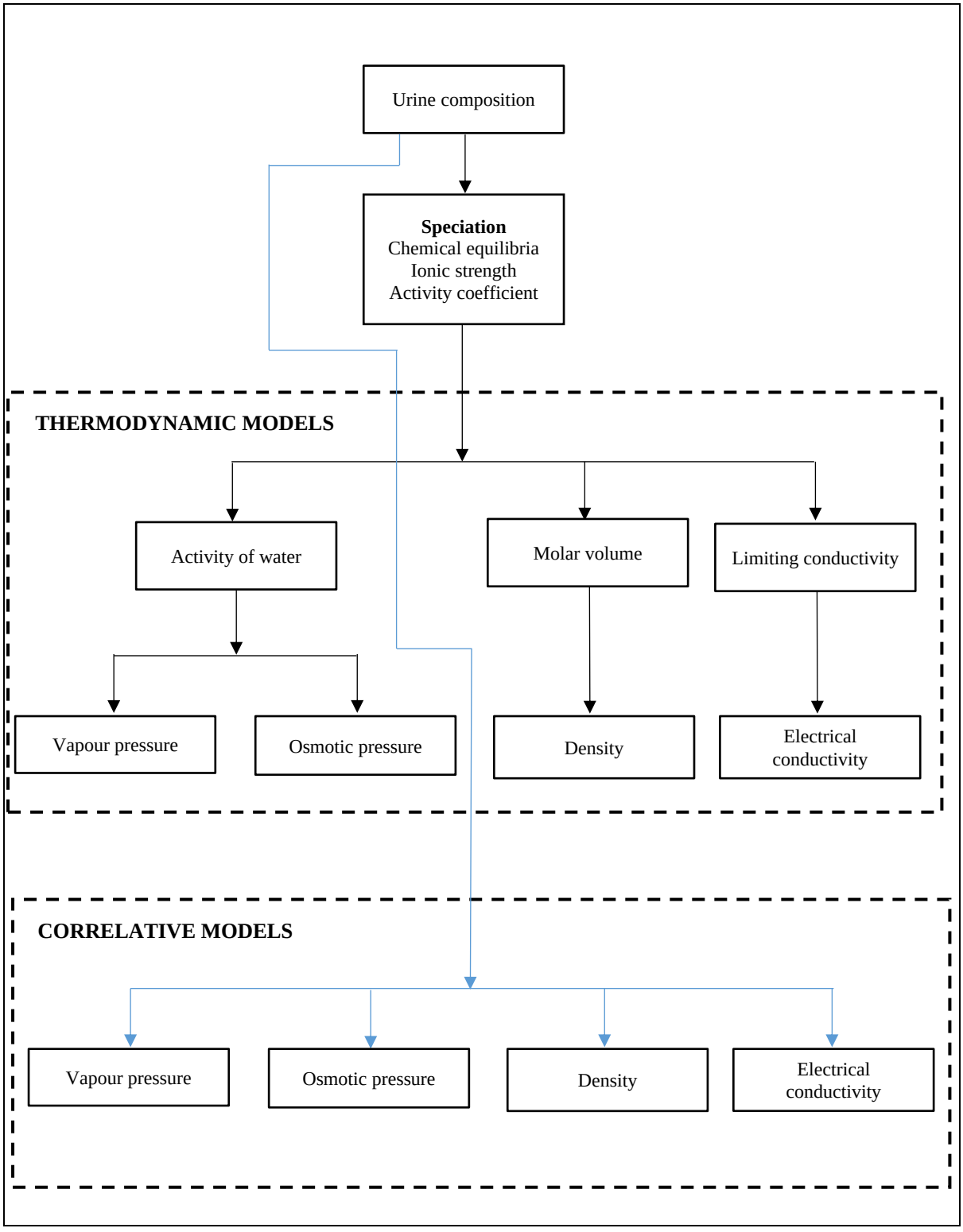

Figure 3-1: Calculation of the thermodynamic properties using thermodynamic equations.

3.1 SPECIATION

The need for ionic speciation is a preliminary step in determining its thermophysical properties. Ionic speciation refers to the determination and distribution of an element among different species in an aqueous solution (Kot and Namiesńik, 2000). This section reviews the equations used to calculate the speciation of an aqueous solution.

3.1.1 Ion-activity

Salts in multicomponent solutions, like urine, seawater and brines, do not exist as binary molecules, but as individual ions, ion-pairs and neutral molecules. Each given cation in the solution is surrounded by negatively charged ions due to the interionic attraction between ions. The electrostatic interactions of the ions can be described using Coulomb's law:

$$F = \frac{Q_1 Q_2}{\varepsilon r^2} \tag{3.1}$$

where Q_1 and Q_2 are the magnitudes of the electrical charges; ε is the relative permittivity of the medium; and r is the distance between the ions.

Due to the electrostatic attraction between the ions in solution, oppositely charged ions may collide to form a distinct entity known as an ion-pair. If the ions are closer than a certain critical distance, the electrostatic force between the ions maybe greater than the kinetic energy required to maintain the random motion of the ions in the solution. As a result of the ion pairing effects, the ionic species may not be fully dissociated. Examples of ion-pairs include $NaSO_4^-$, $NH_4SO_4^-$, $CaCl^+$, $NaHCO_3^-$, $H_2PO_4^-$ and $KHPO_4^-$.

In symmetrical electrolytes, the ion pair behaves as a neutral molecule. An ion pair does not share electrons in a single molecular orbital, like a covalent molecule. As a result, ion pairing reduces the number of free ions existing in the solution $CaSO_4$, $MgCO_3$, and $MgSO_4$.

Ion-pairing increases with an increase in the concentration of ions in solution. At very low concentrations (below 10^{-4} mol.dm^{-3}), the electrolytes are completely ionized and dissociated, and hence ion-ion interactions are negligible. At high concentrations, the interactions between ions become significant and result in ion-pair formation.

The accurate determination of the distribution of the species (speciation) is important for the calculation of the ionic strength of the solution. The ionic strength, *I*, of a solution is defined by equation (3.2):

$$I = \frac{1}{2}\sum m_i z_i^2 \tag{3.2}$$

where *m* and *z* are the molality, and electrical charge of the solute species, *i*, respectively.

The speciation in a solution depends on the law of mass action and the temperature dependency of the equilibrium of the species in the solution (Stumm and Morgan, 1996). At equilibrium, the law of mass action for each ion must be satisfied. A reaction between ion *A* and *B* to form a product *C*, at equilibrium, has the following relationships:

$$aA + bB \leftrightarrow cC \tag{3.3}$$

The relationship between the concentration of the products and the reactants is given by the equation:

$$K = \frac{m_C{}^c}{m_A{}^a m_B{}^b} \tag{3.4}$$

where *K* is an equilibrium constant.

The molal concentration of species, *i*, is related to the activity, a_i, and the activity coefficient, γ_i, demonstrated in equation (3.5):

$$a_i = \gamma_i m_i \tag{3.5}$$

Since m_i is the concentration measured in reality, and a_i is the effective concentration under ideal conditions, the activity coefficient is an *a* correction factor, which describes the non-ideality of a solution. The mass-action law equation (3.4) can be written in terms of activities of the species:

$$K_i = \prod_{m=1}^{N_i} a_m^{\pm \nu_m} \tag{3.6}$$

where N_i is the total number of aqueous ions; and *v* is the stoichiometric coefficient of the species *m*.

The equilibrium constants in equation (3.6) are not only dependent on the ionic strength of the solution, but are also influenced by changes in temperature. The effect of temperature is calculated using the van't Hoff equation (3.7):

$$\frac{\partial lnK}{\partial T} = \frac{\Delta H}{RT} \tag{3.7}$$

where ΔH is the reaction enthalpy, R is the gas constant and T is the temperature. If the enthalpy of the reaction, ΔH, does not change with temperature, then the integration of equation (3.7) gives:

$$logK_{T_1} - logK_{T_2} = \frac{\Delta H}{2.303R}\left(\frac{1}{T_1} - \frac{1}{T_2}\right) \tag{3.8}$$

The temperature dependency of the equilibrium constant K, can also be calculated using an analytical expression, equation (3.9), which requires knowledge of constants A_1 to A_6 (Parkhurst, 1995):

$$logK = A_1 + A_2T + \frac{A_3}{T} + A_4 logT + \frac{A_5}{T^6} + A_6T^2 \tag{3.9}$$

The process of determining the speciation is, in effect, an iterative process. Determining the individual ions, ion-pairs and neutral species in the solution requires knowledge of the interaction of the ionic species as shown in equation (3.3) and (3.4). The equilibrium constant in equation (3.4), is affected by ionic strength, which is in-turn affected by concentration of the species according to equation (3.2).

3.1.2 Activity Coefficients of multicomponent solutions

The determination of the speciation described in the previous **section (3.1)** requires the activity coefficient in order to complete the iterative computation of the species distribution. The activity coefficient is calculated using models which are based on the ionic strength of the electrolyte solution, which needed to be selected for this study. This, however, was not a simple task, owing to the peculiar nature of urine.

Urine is a multicomponent solution with an ionic strength ranging between 0.3 and 0.6 M. (Ronteltap et al., 2007). Hence, activity coefficient models used for multicomponent solutions and ionic strengths greater than 0.3 M, were selected for review:

- Davies equation (Davies, 1962)
- B-dot equation (Helgeson et al., 1969)
- specific ion models (Guggenheim and Turgeon, 1955)
- Pitzer model (Pitzer, 1973)

These models have their origins in the limiting law first developed by Debye and Hückel (1923), which is applicable only to single salt solutions over a limited range of ionic strengths up to 0.1M. Although the Debye-Hückel theory does not fully predict the activity coefficient of electrolyte solutions at high concentrations, the limiting law will be briefly discussed to offer a better understanding of the development and validity of the models mentioned above that have been extended for broader application.

Debye-Hückel Theory

The Debye-Hückel limiting law is a theoretical model that describes the non-ideal behaviour caused by ionic interactions in very dilute solutions. In the development of their mathematical model, Debye and Hückel (1923) proposed the following postulations in order to explain the electrostatic attractions between ions in solution at infinite dilution:

- All ions are completely ionised and there is no formation of ion association between positive and negative ions to form ion pairs, hence each ion contributes to the charge density and conductivity of the solution.
- The central ion is surrounded by several oppositely charged ions and the charge around the ion is represented as a statistically averaged, continuous-charge density of the surrounding ions.
- The only relevant ion-ion interactions are long range electrostatic forces governed by Coulomb's law, and short range effects, such as Van der Waals forces, are neglected.
- Where z_1 and z_2 are the magnitudes of the electrical charges; e is the electronic charge (C); ε_r is the ratio between the permittivity of the medium ε and the vacuum, ε_0 ; and r is the distance between the ions.
- The solvent plays no role other than to provide a constant relative permittivity for the interaction of interionic forces. The model does not take into account the interaction between the ions and the water molecules.

The original Debye-Hückel equation for a completely ionised electrolyte can be written as equation (3.10):

$$log_{10}\,\gamma_{\pm} = -\frac{|z_{+}z_{-}|A_{\gamma}\sqrt{I}}{1+\overset{o}{a}\,B_{\gamma}\sqrt{I}} \qquad (3.10)$$

where $\gamma_{\pm}$ is the mean activity coefficient; $\mathring{a}$ is the distance of closest approach of the ions; z is the ionic charge; + and – is the charge on the ion; and I is the ionic strength. A_{γ} and B_{γ} are parameters that depend on the permittivity and density of the solvent. These are given by the equations (3.11) and (3.12):

$$A_\gamma = \sqrt{\frac{2\pi}{1000}} \quad \frac{e^2}{2.303 k_B^{3/2}} \left(\frac{1}{(\varepsilon T)^{3/2}} \right) \tag{3.11}$$

$$B_\gamma = \left(\frac{8\pi N e_A^2}{1000\, k_B} \right)^{1/2} \left(\frac{1}{(\varepsilon T)^{1/2}} \right) \tag{3.12}$$

where N_A is Avogadro constant; and k_B is the Boltzmann's constant.

The assumptions made in the formulation of Debye-Hückel equation are oversimplified and thus they make the model valid for very dilute electrolyte solutions, typically less than 0.001M (Crowe and Longstaffe, 1987).

The assumption that there is complete dissociation of the ions does not hold at higher ionic concentrations because of the formation of ion pairs. Moreover the model does not take into account the ion-solvent interaction, because it considers the solvent as a structureless medium. However, all solvents are made up of molecules and in the case of water, they are dipolar and polarizable, which results in the solvation of the ions in the solution.

Table 3-1 shows the models used for calculating the activity coefficients of multicomponent solutions of high ionic strength.

Table 3-1: Activity coefficient models

Name	Equation	Eqn	Validity
Davies	$log_{10}\gamma_{\pm} = -z_{+}\lvert z_{-}\rvert A_{\gamma}\left(\frac{\sqrt{I}}{1+\sqrt{I}} + 0.2I\right)$	(3.13)	Ì < 0.5 mol kg^{-1}
B-dot	$log_{10}\gamma_{\pm} = -\frac{z_{+}\lvert z_{-}\rvert A_{\gamma}\sqrt{I}}{1+\overset{o}{a}B_{\gamma}\sqrt{I}} + \dot{B}I$	(3.14)	Ì < 1.0 mol kg^{-1}
Specific ion models	$log_{10}\gamma_{\pm} = -\frac{z^2 A_{\gamma}\sqrt{I}}{1+1.5\sqrt{I}} + \sum_{k}\varepsilon(j,k,I)m_k$	(3.15)	Ì < 4.0 mol kg^{-1}
Pitzer	$\ln\gamma_{\pm} = -\frac{A}{3}\frac{\lvert z_c z_a\rvert\sqrt{I}}{1+1.2\sqrt{I}} + 1.67\,\mathrm{In}\left(1+1.3\sqrt{I}\right) + \frac{2\nu_{c'}\nu_{a'}}{\nu_{c'}+\nu_{a'}}B(I)m + \frac{2(\nu_{c'}\nu_{a'})^{3/2}}{\nu_{c'}+\nu_{a'}}Cm$	(3.16)	Ì < 6.0 mol kg^{-1}

Davies Equation

The Davies equation, an empirical modification of the Debye-Hückel equation, was developed to predict the activity coefficient of electrolyte solutions at moderately high concentrations at 25°C. For the ionic size parameter, the term *å* in the Debye-Hückel equation is difficult to measure, and it has mostly been used to fit the model to experimental data (Samsonov et al., 1999).

This parameter fails to account for the increase in the activity coefficients of electrolytes at high ionic strengths as it does not take into account the phenomenon of solvation of the ions in solution. The term, $åB_{\gamma}$, in the Debye-Hückel equation was equated to one; and an empirical term proportional to the ionic strength of the solution was added to take into account solvation and short-range interactions. As a result, the Davies equation is largely dependent on ionic strength, and the only variable required to calculate the activity coefficient is the ionic charge of the species. This allows it to be applied to a wide range of species (Wolery, 1996). Hence, it is applied in geochemical models, such as, the WATEQ (Ball et al., 1979) and PHREEQC (Parkhurst et al., 1980). The Davies equation makes accurate predictions for concentrations ranging up to 0.5 M at 25°C.

The B-dot Equation

The B-dot equation is an extended Debye-Hückel model, presented by Helgeson (1969) that uses temperature-dependent A_γ, B_γ and $\dot{B}$ Debye-Hückel parameters. The model was developed to calculate the activity coefficient of hydrothermal solutions at high pressures and temperatures up to 300°C.

At high temperatures, the dielectric constant and the viscosity of water are low, which permits the formation of ion pairs and complexes in the solution. The presence and concentration of the ion pairs varies the ionic strength of the solution, which consequently alters the calculated activity coefficient by means of the Debye-Hückel model. According to Helgeson, the activity coefficient of the ions then depends on the association constants that determine the concentration of the ion pairs in the solution. In the extension in the Debye-Hückel model, the $\dot{B}I$ term is referred to as the salting out term. This term dominates at high ionic strengths and is a correction for short-range interactions.

Application of the B-dot equation to geochemical systems has been used by (Helgeson et al., 1981) and (Parkhurst, 1995). The model can accurately predict the activities of a sodium chloride-dominant solution up to 3 molal, with other salt solutions up to 300°C, and ionic strengths up to 1.5 M.

Specific ion theory (SIT) interaction models

Brönsted (1922) proposed a specific ion theory (SIT), which was further developed by Guggenheim (1935) and Scatchard (1936) into what is known as the Brönsted-Guggenheim-Scatchard model. The SIT theory can predict the activity coefficients of single ions in electrolyte solutions at high concentrations. In addition to the long range forces that are accounted for by the Debye-Hückel theory, these calculation methods include a virial expansion, to take into consideration the short-range specific ion-ion interactions.

The assumptions for the formulation of SIT methods are listed below:

- The interactions between ions *A* and *B* are specific for those particular ions, and are the same even in the presence of other ion species.
- The magnitude of the deviation from ideality depends on the concentration of the solutes.
- Deviations from ideality can be described by means of virial equations, where the first term is based on the Debye-Hückel theory.
- All methods for the estimation of deviations from ideality, such as activity coefficients, must approach, with increasing dilution, the Debye-Hückel limit.

Even though the SIT parameters have a theoretical basis, they have to be determined, using equilibrium constants or activity coefficient data established in different electrolyte solutions and ionic strengths.

Brönsted (1922), in the formulation of the activity equation, considered the ion interactions between ions of the same charge sign to be very negligible. This was because he presumed that, due to electrostatic repulsion forces, the ions would not reach close proximity to each other. The first term in the equation is the Debye-Hückel theory; and the second term is a correction of the limiting law when the concentrations exceed the range of validity of that law. The term $\varepsilon(j, k, I)$ in the model, is an interaction coefficient based on concentration; and the summation extends over the ions present in the solution. The Brönsted-Guggenheim-Scatchard model is valid for concentrations up to 4.0M.

The Pitzer Equations

The Pitzer model (1973) was developed as an improvement of the SIT approach proposed by Guggenheim (1935). Further work has been done by Pitzer and his co-workers to improve the predictions to higher ionic strengths, up to 6.0M (Pitzer, 1973, Pitzer, 1975, Pitzer and Mayorga, 1973, Pitzer and Kim, 1974, Silvester and Pitzer, 1977, Silvester and Pitzer, 1978).

Pitzer (1973) combined a modified version of the Debye-Hückel theory with a virial expansion of excess Gibb's energy. The virial series of the Gibb's excess energy is expressed as a power series written as a function of ionic strength that accounts for the short-range specific ion-ion interactions:

$$\frac{G^E}{n_w RT} = f(I) + \sum_i \sum_j \lambda_{ij}(I) m_i m_j + \sum_i \sum_j \sum_k \mu_{ijk} m_i m_j m_k \qquad (3.17)$$

where G^E is the excess Gibbs energy in *kJ*; R is the gas constant in *kJ* mol^{-1} K^{-1}; T is the temperature in *K*; n_w is the mass of water; m_i and m_j the molality of species *i* and *j*, respectively.

In mol kg^{-1} the function $f(I)$ is an electrostatic term that expresses the effect of long-range electrostatic forces between ions, taking into account the hard-core effects of the Debye-Hückel theory. The parameter $\lambda_{ij}(I)$ is the second virial coefficient, which represents the short-range interaction; and μ_{ijk} is the third virial coefficient. The coefficients $B(I)$ and C are empirical parameters that, to be determined, require a large amount of experimental data for many multicomponent solutions at varying temperatures over wide ranges of composition.

The Pitzer model is parameterized to cover a wide continuum of electrolytes over a wide range in temperature, pressure, and composition space (Millero et al., 1976). The model can accurately predict the activity coefficients for concentrations up to 6.0 molal ionic strength. This capability makes it the most popular model for the calculation of activity coefficients in geochemical processes.

Discussion – Activity coefficients

While all the models described above are derived from Debye-Hückel, they can be classified into two types, namely, the extended Debye-Hückel methods (Davies and the B-dot equation) and the virial methods (Specific ion approximations and the Pitzer model).

The extended Debye-Hückel methods have the advantage of being relatively simple models that can be readily extended to include new components, since they require few parameters for the species and the solution. The models can be applied to complex solutions since there is extensive literature available on ion association reactions. The B-dot equation, in particular, makes it possible to apply the models over a wide range of temperatures, up to 300 ˚C.

But, the extended Debye-Hückel methods break down at high ionic strengths, especially with solutions in which salts other than NaCl are present in high concentrations. Additionally, the Debye-Hückel methods assume the same set of activity coefficients for all ions in the solution, irrespective of the distribution of the species and regardless of the ionic strength of the solution.

The virial methods, on the other hand, have the ability to fit data at high ionic strengths, even for complex electrolyte systems. The drawback with specific virial methods is that they require extensive experimental data for many multicomponent electrolyte solutions, at varying temperatures and over a wide range of concentration, in order to generate the essential fitting parameters (Millero et al., 1976). Due to this complexity, the models have only been applied to systems with a limited number of components. Extension to other systems is difficult.

The specific ion approximations are limited to the following system of elements Na-K-Mg-Ca-H-Cl-SO_4-OH-HCO_3-CO_3-CO_2-H_2O (Pang, 2007). Interaction parameters for ammonium and phosphate are not available in literature and, hence, the models are not functional for urine solution applications. In addition, the virial methods do not offer any information on the distribution and concentration of the species in the solution.

As a result, the virial models cannot be used to calculate the activity coefficient of the species in urine because the interaction parameters for ammonium and phosphate are not available in literature. Hence, despite its limitations, the B-dot model was selected for calculation of the speciation because it has a wider validity range.

3.1.3 Chemical Speciation software - Phreeqc version 2.0

PHREEQC 2.0 was the software selected for the speciation of the urine solutions. The software program is used for simulating geochemical reactions and transport processes. The program calculates the distribution of the species from thermodynamic data sets, by simultaneously solving a set of non-linear equations from the equilibrium constants and mass balances in the system. Similar programs using the same modelling technique include EQ 3/6, WATEQ4F, and MINTEQA2.

PHREEQC was developed in 1980 and at the time it was named PHREEQE and was written in FORTRAN. Various versions of PHREEQE were developed between 1988 and 1994. PHRQPITZ (Plummer et al., 1988) was developed in 1988 and it included Pitzer equations, applicable for highly concentrated solutions with ionic concentrations greater than 1.0 molal. In 1994, Appelo and Postma developed PHREEQM, which had all the functions of PHREEQE but had an add-on module, PHRKIN that allowed for the modelling of kinetically controlled reactions. The program was rewritten in C programming language in 1995 by Parkhurst and was named PHREEQC. PHREEQC stands for PH Redox Equilibrium in C language.

The program employs various aqueous models that enable the program to undertake:

- Speciation- and saturation-index calculations;
- Reaction-path and advective-transport calculations, involving specified irreversible reactions, mixing of solutions, mineral and gas equilibria, surface-complexation reactions, and ion-exchange reactions, and;
- Inverse modelling, which finds sets of mineral and gas mole transfers that account for composition differences between waters, within specified compositional uncertainties.

The aqueous models implemented by PHREEQC for these calculations include the LLNL (Lawrence Livermore National Laboratory) model, the WATEQ4F model, the Pitzer specific-ion-interaction aqueous model, and the SIT (Specific ion Interaction Theory) aqueous model.

Program Limitations

Despite the wide range of capabilities of PHREEQC, knowledge of the limitations and assumptions inherent in the programme is essential for accurate modelling of aqueous solutions:

The databases have a limited spectrum of elements for which they are valid. For example, the Pitzer.dat database is limited to the following system of elements: Na-K-Mg-Ca-H-Cl-SO_4-OH-HCO_3-CO_3-CO_2-H_2O. Interaction parameters for ammonium and phosphate are not available in literature and, hence, the model cannot be functional for urine solutions

All the databases, except for the Pitzer.dat database, use the Debye-Hückel model for the approximation of the activity coefficients of the aqueous solutions. The applicability of this model is only valid for low ionic strength solutions. On the other hand, the Pitzer model can accurately calculate the thermodynamic properties of high ionic solutions, up to 6M.

There is a lack of internally consistent, validated thermodynamic data in the programme database. The log K and the enthalpy of reaction data were collected from various literature sources. But, the validity of the aqueous model, used to develop the log K, has not been undertaken. Nor has it been ensured that the aqueous model, defined in terms of the current database files, is consistent with the original experimental data.

Taking into consideration the above limitations, the PhreeqC.dat database was selected for the speciation calculation of hydrolysed urine as it contains the required ion pairing reactions, thermodynamics data for components present in urine. The database has analytical constants for the calculation of the equilibrium conditions for a wide range of temperature, between 0 and 300 °C.

3.2 THERMODYNAMIC PREDICTIVE MODELS FOR THE THERMOPHYSICAL PROPERTIES

Thermodynamic equations for calculating the physical properties of urine are presented. This section focuses on how the thermodynamic equations are used in conjunction with the chemical speciation of urine discussed in the previous **section 3.1,** to predict its physical properties.

3.2.1 Vapour Pressure and Osmotic Pressure

The vapour pressure and the osmotic pressure can be calculated from the activity of water using equations (3.18) and (3.19) respectively:

$$P_s = a_{H_2O} P_{H_2O} \tag{3.18}$$

where P_s is the vapour pressure of the solution in kPa; a_{H2O} is the activity of water; and P_{H2O} is the vapour pressure of water in kPa.

$$\pi = -\frac{RT}{v} ln a_{H_2O} \tag{3.19}$$

where π is the osmotic pressure in kPa; R is the universal gas constant (8.314 kJ mol^{-1} K^{-1}); a_{H2O} is the activity of water; T is the absolute temperature in K; and v is the partial molar volume of water (0.018067 m^3 mol^{-1} at 25 °C for dilute solutions).

The accurate calculation of the vapour pressure and osmotic pressure relies on the correct prediction of the activity of water. Models for calculating the activity of water from the speciated composition is available in literature and these include equations proposed by Garrels and Christ (1965), Brouckaert (1995), and Pitzer (1973), shown in Table 3-2.

Garrels and Christ (1965) developed a simple empirical equation (3.21) for calculating the activity of water based on Raoult's equation. This law assumes that there are no interactions between ions and that each species has the same effect on lowering the vapour pressure of water in a solution. The above assumptions can only be made at very dilute conditions where the effect of the size, nature and charge of the ions is minimal. Hence, equation (3.21) is only valid at very low ionic concentrations.

Brouckaert (1995) derived an expression for the activity of water by substituting the Davies equation (3.13) into the Gibbs-Duhem equation to give equation (3.20).

$$n_{H_2O} d ln a_{H_2O} = -\sum_{j=}^{n} n_j d\ ln a_j \tag{3.20}$$

The Gibbs-Duhem equation (3.20) was then integrated using a boundary limit of $a_{H_2O} = 1$, and the resultant equation was (3.21). Brouckaert (1995) used the equation to predict the osmotic pressures of a solution of Na_3PO_4. The osmotic pressure predictions were in good agreement with literature values up to 0.2 MPa. But the model became increasingly inaccurate with high concentrations. The equation is based on the Davies equation; and the theory of the Davies equation considers the coulombic forces that exist at larger distances. Similar to Raoult's law, the theory overlooks the ionic interactions between species. It also overlooks the nature of ions in the solution.

Table 3-2: Equations for calculating the activity of water

Reference	Equation	Eqn	Validity
Garrels & Christ (1965)	$a_{H_2O} = 1 - 0.017 \sum_{i=1}^{N} m_i$	(3.21)	Ì < 0.5 mol kg^{-1}
Brouckaert (1995)	$55.52 \ln a_{H_2O} = -\sum_i m_i - \sum_k mk - 2.303AbI^2 + 4.606A\left[I + I^{1/2} + 2\ln\left(1 - I^{1/2}\right) - \frac{1}{\left(1 + I^{1/2}\right)} \right]$	(3.22)	Ì < 1.0 mol kg^{-1}
Pitzer (1973)	$\ln a_{H_2O} = \frac{\varphi \sum_i m_i}{55.50837}$	(3.23)	Ì < 6.0 mol kg^{-1}

where a_{H2O} is the activity of water, m_i is the molality of charged species i, mol.kg^{-1}; m_k is the molality of uncharged species k, mol.kg^{-1}. I is the Ionic strength, mol kg^{-1}, ϕ is osmotic coefficient.

The activity of a solution for a multicomponent solution can be calculated from the knowledge of the osmotic coefficient ϕ, as shown by equation (3.23). The osmotic coefficient of a mixed ionic system can be calculated using the Pitzer model. Calculated using equation (3.24):

$$(\varphi-1)=\frac{2}{\left(\sum_i m_i\right)}\left\{\begin{array}{l}-\dfrac{A^{\varphi}I^{3/2}}{I+bI^{1/2}}+\sum_c\sum_a m_c m_a\left(B^{\varphi}_{ca}+ZC_{ca}\right)+\\ \sum_{c,c'}\sum m_c m_{c'}\left(\Phi^{\varphi}_{cc'}+\sum_a m_a\psi_{cc'a}\right)+\\ \sum_{a,a'} m_a m_{a'}\left(\Phi^{\varphi}_{aa'}+\sum_c m_c\psi_{aa'c}\right)\end{array}\right\} \quad (3.24)$$

where m_c is the molality of cation *c* with charge *z*; the subscripts of *m*, *c* and *c'* refer to cations; and *a* and *a'* refer to anions. The summation index *c* refers to the sum over all cations; and the double summation index, *c<c'*, is the sum of all distinguishable pairs of dissimilar cations, similar for the anions.

The equation proposed by Brouckaert (1995) is the model chosen for the calculation of the activity of water in urine. The equation developed by Garrels and Christ (1965) is based on the simplified assumptions of Raoult's law. This limits the model to solutions of low ionic strength. The equation developed by Brouckaert (1995) is based on the Davies equation, which has better prediction capacity compared to Raoult's law.

The Pitzer model, as discussed in the previous **section 3.1**, is used for the determination of thermodynamic properties of mixed electrolyte solutions, and it requires parameters obtained from ionic interactions between binary ions of the same sign. The Pitzer model cannot be applied due to insufficient data to generate the interaction parameters for the ammonium and phosphate ions in the urine solution.

3.2.2 Density

The density, or more precisely, the volumetric mass density of a liquid is the ratio of its mass to its volume. Density is a physical intrinsic property that is not only affected by the molecular mass, but also by the interactions and structures of the molecules in the substance. It is a pressure- and temperature-dependent property, where an increase in temperature results in a decrease in density, and vice versa.

The density of aqueous solutions has been studied using the concept of molar (equivalent) volume since a study by (Millero, 1971). When a solute is added to water, there is a volume change that is attributed to the dissolved salt. The change in volume is a result of the dipolar molecules in water being attracted to, and arranged and compacted around, the dissolved ions (Pang, 2007).

The molar volume of solutions provides essential information on the ion-ion, ion-solvent and solvent-solvent interactions occurring in the solution (Millero, 1971). Hence, the density of the salt solution can be calculated from the density of pure water and the apparent molar volume of a salt solution, using equation (3.25):

$$\rho = \rho^{\circ}\left(\frac{1000 + m_i M_i}{1000 + \rho^{\circ} m_i V_{m,i}}\right) \tag{3.25}$$

where V_m is the apparent molar volume (m^3 mol^{-1}); ρ and ρ^o are the densities of the solution and water (kg m^{-3}), respectively; m is the molarity of the solution (mol kg^{-1}); and M is molecular weight of the solute ($g.mol^{-1}$).

Several authors have devised methods for calculating the density of solutions containing more than one salt (Fabuss et al., 1966, Appelo et al., 2014, Laliberte and Cooper, 2004, Reynolds and Carter, 2008, Millero, 1985). The molar volumes of ions have been found to be additive, in that, they can be added to obtain the total volume of the salts, and the volumes can be added, or subtracted, to get the volume of the desired ions (Ellis, 1968, Monnin, 1999, Millero, 1972).

The general equation used for calculating the density of a multicomponent solution, containing an arbitrary number of ions, is shown in (3.26):

$$\rho = \rho^{\circ}\left(\frac{1000 + \sum m_i M_i}{1000 + \rho^{\circ}\sum m_i V_{m,i}}\right) \tag{3.26}$$

Equation (3.26) shows that, in order to calculate the density of an aqueous electrolyte solution, the molar volume of the ions must be known. The molar volume of an ion is dependent on the concentration and temperature of the solution. Various methods have been proposed for determining the molar volumes (Masson, 1929, Redlich and Meyer, 1964, Fabuss et al., 1966, Millero, 1985, Appelo et al., 2014), as shown in Table 3-3

Table 3-3: Equations for calculating the molar volume of salts in aqueous solutions

Name	Equation	Eqn
Mason (1929)	$V_m = V_m^o + k\sqrt{m}$	(3.27)
Redlich and Rosenfeld (1931)	$V_m = V_m^o + A_\gamma I^{0.5} \sum 0.5\, \nu_i z_i^2 + bI$	(3.28)
Millero (1973)	$V_m = \sum_M \sum_X E_M E_X V_{MX}$	(3.29)
	$E_i = \frac{e_i}{e_T} = \frac{m_i Z_i}{e_T}$	(3.30)
	$V_{MX} = A + BI^{0.5} + CI + DI^{1.5}$	(3.31)
Helgeson-Kirkham-Flowers-modified-Redlich-Rosenfeld (HKFmoRR)	$V_m = V_m^o + 0.5 A_\gamma z_i^2 \frac{I^{0.5}}{\left(1 + \overset{o}{a} B_\gamma I^{0.5}\right)} + \left(b_{1,i} + \frac{b_{2,i}}{T-228} + b_{3,i}(T-228)\right) I^{b_{4,i}}$	(3.32)
	$V_m^o = 41.84 \left(\begin{array}{l} 0.1 a_{1,i} + \frac{100 a_{2,i}}{2600 + P_{bar}} + \frac{a_{3,i}}{(T-228)} \\ + \frac{10^4 a_{4,i}}{(2600 + P_{bar})(T-228)} - \omega_i \frac{\partial \varepsilon_r^{-1}}{\partial P_{bar}} \end{array} \right)$	(3.33)

where Vm˚ is the apparent molar volume (m3 mol-1) at infinite dilution; and k is an empirical constant from fitting the experimental data. Aγ is the Debye-Hückel constants. ; ν is the stoichiometric coefficient of element I in the salt; z is the charge number of the ions; and b is an empirical coefficient for fitting at higher concentrations,a_1, a_2, a_3, a_4, b_1, b_2, b_3, b_4, ω, A, B, C and D are empirical coefficients for fitting experimental data

Masson (1929) (cited in Millero 1972) developed equation (3.27) that related the molar volume to the square root of the molar concentration, where *k* was an empirical constant. However Redlich and Rosenfeld (1931) developed a theoretical equation similar to the Masson equation (3.27), except that the *k* was replaced with Debye-Hückel constant, A_γ, and an empirical term, *bI*, was added for fitting at higher concentrations. Since the equation was derived from the limiting law (Debye-Hückel), it is valid only at very dilute concentrations, less than 0.2 $mol.kg^{-1}$ (Redlich, 1940, Millero, 1970, Millero, 1971).

Millero developed a method to estimate the density of multicomponent systems (seawater, lakes, natural waters and brines), from the contribution of the major salts in the solution (Millero, 1973, Millero, 2000, Rodriguez and Millero, 2013, Millero, 1985). The molar volume of the multicomponent solution, V_m, was calculated using Young's additivity rule that sums up the weighted contributions of the major components in the solution, as seen in equation (3.29): The molar volume of the salt was expressed as a function of ionic strength as shown in equation (3.31). This equation can predict the molar volume of multicomponent solutions from 0 – 90 ˚C (Rodriguez and Millero, 2013), and ionic strengths up to 6 M (Millero, 2000).

Helgeson and co-workers (Helgeson and Kirkham, 1976, Shock et al., 1992) developed the Redlich-Rosenfeld equation (3.28) in order to extend its validity to higher concentrations, to give equation (3.32), known as the Helgeson-Kirkham-Flowers-modified-Redlich-Rosenfeld (HKFmoRR) equation.

The second term of the HKFmoRR equation was obtained by differentiating the extended Debye-Hückel theory equation (3.10) with respect to pressure. This modification leads to excellent results for varying ionic size values, *å*, for the respective ions. The third term of the equation was added with the purpose of fitting the Redlich-Rosenfeld equation at high concentrations. The original coefficient, *b*, was replaced by a temperature dependent term with three parameters, in order to describe the temperature effects. This term gives constant values for temperatures up to 100˚C, but shows variation at higher temperatures.

The model chosen for the calculation of the density of urine is the equation proposed by Millero (1970), because it is valid over the wide temperature and concentration range investigated in this work. The equations used by Mason (1929) and Redlich & Rosenfeld (1931) were developed from the Debye-Hückel theory, which is valid at low concentrations less than 0.2 mol kg^{-1}. The HKFmoRR equation lacks parameters for key components such as ammonia and phosphates.

3.2.3 Electrical Conductivity

The conduction of an electrical current generally involves the movement of charged particles through a medium. This flow of electrical charge can occur in metallic conductors and electrolytic conductors. Metallic conduction, which is not relevant to this study, involves the flow of valence electrons from atom to atom in the conductor, while electrolytic conductance refers to the flow of ionic species in the solution medium.

Aqueous electrolyte solutions can conduct an electric current because they contain free ions. When an electrical potential field is applied on an electrolyte solution, positive ions migrate toward the cathode, and negative ions move toward the anode. This movement of charged species in a solution medium constitutes an electrical current. As the migrating ion moves with a certain velocity, it distorts the ionic atmosphere around it resulting in more ions of like charge at the front and oppositely charged ions at the back. This loss in symmetry of the ionic atmosphere produces a dipole moment which exerts a retarding force on the moving ion. This effect is referred to as the "asymmetry effect" or "relaxation effect". The effect lowers the conductivity of the ion below the infinite dilution value.

The applied electric field has the tendency to move the entire ionic atmosphere around the central ion. This motion exerts a drag force on the solvent molecules as a result of the attraction forces between the ions and the molecules. Consequently, a frictional force is exerted on the central ion in the direction of the pole opposite its ionic atmosphere. This effect is referred to as the "electrophoretic effect".

The total electrical conductivity of a solution is a function of the specific ions in the solution and the total concentration of all ions present (Pawlowicz, 2008), and various methods have been presented in literature for calculating the electrical conductivity of multicomponent solutions (McCleskey et al., 2012a). However, Talbot (1990) proposed a general equation used by various authors (Brouckaert, 1995, McCleskey et al., 2012a, Pawlowicz, 2008, Pawlowicz, 2010, Appelo, 2010) for the calculation of the conductivity of mixed salts as shown in (3.34):

$$\kappa = \sum_{i}^{N} m_i |z_i| \lambda_i \tag{3.34}$$

where z is the ionic charge; λ_i is the equivalent conductivity (S cm^2 mol^{-1}); and N is the number of ionic species.

According to equation (3.34), the equivalent conductance of the individual ions in the solution will have to be determined in order to calculate the total conductivity of the solution. The equivalent conductivity of a given ion is calculated using equation:

$$\lambda_i = \frac{\kappa_i}{m_i} \tag{3.35}$$

However the equivalent conductivity is conveniently expressed as a function of concentration and several empirical functions have been developed for fitting the conductivity data of electrolyte solutions (Jones and Dole, 1930). These correlations will be discussed in detail together with the various forms of the equations used for calculating the conductivity of the solution.

Table 3-4 shows the various models in literature used to calculate the conductivity of multicomponent solutions. These equations are based on Talbot's equation (3.34) and they differ in the methods in which they determine the specific conductance of the ions in the solution

Table 3-4: The electrical conductivity and specific conductivity equation

κ equation	Eqn.	λ equation	Eqn.	Reference
$\kappa = \sum_i^N \lambda_i^\circ m_i \lvert z_i \rvert - k \sum_i^N \lvert z_i \rvert m_i^{3/2}$	(3.36)	$\lambda_i = \lambda_i^\circ + k\sqrt{m_i}$	(3.37)	Taiji and Biggar (1972)
$\kappa = \sum_i^N m_i \lvert z_i \rvert \lambda_i(I)\overline{\alpha_i}\Gamma(p)$	(3.38)	$\lambda = \frac{\lambda^\circ}{1 + Az_i\sqrt{I}}$	(3.39)	Pawlowicz (2008)
$\kappa = A_0 + A_1 \sum_i^N \lambda_i^\circ m_i \lvert z_i \rvert$	(3.40)	$\lambda_i = \lambda_i^\circ + k\sqrt{m_i}$	(3.41)	Visconti et al (2010)
$\kappa = \sum_i^N m_i \lambda_i$	(3.42)	$\lambda = \lambda^\circ(T) + A(T)\frac{\sqrt{I}}{1 + B\sqrt{I}}$	(3.43)	McCleskey (2012)
$\kappa = \sum_i^N m_i \gamma_i \lambda_i^\circ$	(3.44)	$\lambda_i^\circ = \frac{z^2 F^2}{RT} D_w$	(3.45)	Appelo (2010)
$\kappa = \kappa^\circ + \sum_i^N A_i I_i$	(3.46	$\kappa^\circ = \sum_i^N m_i \lvert z_i \rvert \lambda^\circ{}_i$	(3.47)	Brouckaert (1995)

[κ, electrical conductivity (mS/cm); λ, equivalent conductivity (μS.cm^2.mol^{-1}); λ°, limiting conductivity (μS.cm^2.mol^{-1}); T, temperature (K); R, gas constant (J.mol^{-1}.K^{-1}); F, Faraday constant (C.mol^{-1}); c, concentration (mol/kg); D_w, Diffusivity (m^2/s); I, ionic strength (mol/kg); z, ionic charge; A_0-A_1 and k, constant]

Taiji and Biggar (1972) used the Kohlrausch's square root law, equation (3.37) to calculate the equivalent conductivity of the ionic species. This law is valid for very dilute concentrations as it postulates that at infinite dilution, there is complete dissociation of the electrolyte, such that the conductivity of each ion is independent of other ions present in the solution. The square root law was substituted into the Talbot's equation (3.34) to give equation (3.36) for calculating the electrical conductivity. The constant *k* in the equation, represents a concentration-weighted mean of each ion, which accounts for the ion association effects.

Pawlowicz (2008) developed an algorithm for calculating the specific conductance of mixed salt solutions from measured chemical compositions, as seen in equations (3.38) and (3.39). The method considers the multicomponent solution as a mixture of binary salts formed by the possible anion-cation combinations of the available ions, and not as individual ions.

The overall conductivity of the solution is then calculated by using the weighted sum of the binary electrolytes formed using equation (3.38). Since the multicomponent mixture is assumed to be a mixture of anion-cation combinations, Pawlowicz's (2008) method requires numerical parameters for the ion pairing interactions necessary for the calculation of electrical conductivity. The specific conductivity was calculated using Walden's (1924) equation, which accurately fits at concentrations close to 0.01M.

Visconti et al. (2010) modified Talbot's equation (3.34) to give a simple mathematical expression (3.40) based on the hypothesis that conductivity is proportional to analytical concentrations. Kohlrausch's equation was used to calculate the equivalent conductance of the species in the solution.

McCleskey (2012) developed a set of equations for the conductivity of a wide range of natural waters, drawn from the speciated concentration of ions in solution. The specific conductivity was calculated using equation (3.42) and the equivalent conductivity was calculated using equation (3.43) proposed by Lattey (1927). McCleskey (2011) used Lattey's equation to fit data for several salts solutions at varying temperature ranging from 5 to 90°C. The Lattey equation shows accurate predictions for a very wide range of concentrations from very dilute solutions up to concentrations of 1M. The speciated concentration of the ions used in McCleskey's method was calculated using U.S. Geological Survey geochemical speciation code WATEQ4F (Ball and Nordstrom, 1991).

Appelo (2010) proposed a unique method for calculating the specific conductivity of a multicomponent system from the speciated concentration, the activity coefficient and the diffusion coefficient. The equation is developed from Talbot's equation (3.34) where the equivalent conductance, λ, was replaced with the limiting equivalent conductance, which is calculated from diffusivity using equation (3.45).

Brouckaert (1995), similar to Appello (2010), calculated the conductivity from the limiting specific conductivities of the species in the aqueous solution, using equation (3.47), which is similar to the equation proposed by Talbot (1990). The conductivity of the solution was then calculated using a correction for concentration, using a polynomial-based equation for the ionic concentration of the solution.

In conclusion, the methods for calculating the electrical conductivity reviewed include the calculations proposed by Taiji and Biggar (1972), Pawlowicz (2008), Appelo (2010), Visconti et al (2010) and McCleskey (2012) and Brouckaert (1995). These methods require knowledge of the speciated composition of the solution as well as the equivalent conductivity of each ion.

The methods of Pawlowicz (2008) and Appelo (2010) provide accurate predictions for concentrations up to 0.1M. This is because the equations used to calculate the equivalent conductivity have poor predictions for concentrations above 0.1 M, and this makes them unsuitable for calculating the conductivity of urine, which has high concentrations greater than 0.3 M. While the method proposed

by McCleskey uses the Lattey equation which has good predictions up to 1.0 M, the method requires transport numbers for the phosphate ions, which are not available in literature. While Appelo's (2010) method includes a comprehensive list of up to 50 ions and ion pairs, including phosphate ions, the limitation of this method is that it cannot correctly predict conductivities greater 6 S/m (Appelo, 2010), which may be too low for the conductivities of the concentrates of urine.

Brouckaert's method was therefore selected as the model for calculating the electrical conductivity of urine solution. Apart from the ionic speciation, the method requires knowledge of the limiting conductivities of the species in the urine solution, which are widely available in literature (LIDE, 1999). The limiting conductivities of ion complexes not available in literature were calculated using an equation proposed by Anderko and Lencka (1997).

$$\lambda^{\circ}_{complex} = \frac{\left|z_{complex}\right|}{\left[\sum_{i=1}^{n}\left(\frac{z_i}{\lambda_i}\right)^3\right]^{\frac{1}{3}}} \tag{3.48}$$

The limiting conductivities in literature are given at 25 °C and since the change in the conductivity of a solution with temperature is mainly controlled by the viscosity of water (Miller et al., 1988) a viscosity-based equation proposed by (Sorensen and Glass, 1987) provides for the correction of temperature.

$$\kappa = \kappa_{25}\left(\frac{\mu}{\mu_{25}}\right)^{n} \tag{3-1}$$

where μ and μ_{25} are the viscosities of pure water at temperature T and 25 °C respectively; and n is an empirical constant.

3.3 CORRELATIVE MODELLING OF AQUEOUS ELECTROLYTE SOLUTIONS

The correlation equations for vapour pressure, osmotic pressure, density and electrical conductivity are reviewed.

3.3.1 Vapour Pressure

There are several correlation techniques available in literature for the modeling of aqueous salt solutions (Apelblat and Korin, 2009, Patil et al., 1992, Sako et al., 1985, Sharqawy et al., 2010, Sparrow, 2003, Wiesenburg and Little, 1988). However, this review of correlative equations was limited to simple, polynomial functions and to equations based on the Clausius-Clapeyron equation, shown in Table 3-5, because they are simple and fit data with accuracy.

Table 3-5: Correlative equations used for calculating vapour pressure

Equation name	Equation	Eqn	Validity	Reference
Polynomial	$P = A + BT + CT^2 + DT^3 + ET^4$	(3.49)	±2.0%	(Sparrow, 2003)
Kirchoff's equation	$ln\ P = A - \frac{B}{T} + C\ ln\left(\frac{1}{T}\right)$	(3.50)	±1.0%	(Apelblat and Korin, 1998, Apelblat and Korin, 2009, Apelblat and Korin, 2011)
Antoine equation	$ln P = A - \frac{B}{T + C}$	(3.51)	±1.0%	(Sako et al., 1985)
Extended Antoine equation	$ln P = A - \frac{B}{T} + \frac{C}{T^2}$	(3.52)	±1.0%	(Patil et al., 1992, Patil et al., 1990, Patil et al., 1991)

Sparrow (2003) used a fourth-order polynomial function, equation (3.49), to fit the vapour pressure data of sodium chloride solutions for temperatures ranging from 273 K to 573 K and concentrations up to the solution's saturation point. The equation was in good agreement with the vapour pressure data, with the percent error having a mean of 0.09% and maximum error of 2.21% over the entire range.

The equations developed by Kirchoff and Antoine are semi-empirical models based on the Clausius-Clapeyron equation, shown in equation (3.53):

$$\frac{d\ ln\ P}{dT} = \frac{\Delta H}{RT^2} \tag{3.53}$$

where P is the vapour pressures, (kPa); T is the temperatures (K); R is the gas constant (kJ mol^{-1} K^{-1}); and ΔH is the enthalpy of vaporization (kJ/kg).

Kirchoff's equation was developed by expressing the heat of vaporisation as a function of temperature as shown in equation (3.54).

$$\left(\frac{\partial H}{\partial T}\right)_P = a + bT + cT^2 + ... \tag{3.54}$$

Substitution of the polynomial function resulted in equation substitution and integration, proposed in equation (3.50). Apelblat and Korin (1998, 2009 and 2011) used Kirchhoff's equation to fit the data of several binary and quaternary aqueous salt solutions. The vapour pressure calculations were within an average error of ±1.0% of the experimental data.

Antoine (1988) Antoine (1888) proposed a modified but simpler version of the Clausius-Clapeyron equation by assuming that the heat of vaporisation remains constant with temperature, integrating equation (3.53) and addition of the term, *C*, to the temperature. A plot of ln P against 1/T gives a linear relationship which has a slight curve. The addition of the term, *C*, permits the model to fit the vapour pressure data. The Antoine equation is arguably the most widely used vapour pressure equation, given the extensive data of tabulated values for the parameters of A, B and C for several liquids (Dykyj et al., 1999, 2001, and 2001).

Sako et al. (1985) used the Antoine equation to fit data for binary electrolyte solutions with varying concentrations. The parameter C was equated to the experimental value for pure water, and values for A and B were evaluated for each concentration and then expressed as a polynomial function of concentration. The set of equations gave an excellent fit for the temperature and pressure ranges investigated, with calculated values within ±1.0% of the experimental value.

Patil (1990, 1991 and 1992) used an extended Antoine type equation (3.52) to fit vapour pressure data of aqueous electrolyte solutions at varying concentration and temperature. The constants A, B and C were expressed as cubic functions of concentration. The calculated values were within an average mean error of ±1.0% from the experiment data.

All equations presented in Table 3-5, can correlate experimental data with suitable accuracy. As discussed above, a plot of ln P against 1/T yields a linear relationship. Therefore the extended Antoine's equation was selected for the correlation of the vapour pressure of urine, because it can accurately describe the curvature of the log P against 1/T curve.

3.3.2 Osmotic Pressure

The osmotic pressure of a salt solution is calculated based on the theory proposed by the Van't Hoff equation:

$$\pi = RTm \tag{3.55}$$

where π is the osmotic pressure (kPa); R is the gas constant (kJ mol^{-1} K^{-1}); T is the temperature (K); and m is the molar concentration (mol kg^{-1}).

However the osmotic pressure of a concentrated solution can be expressed as an expanded power series of the solute concentration (Stigter and Hill, 1959):

$$\frac{\pi}{mRT} = 1 + Bm + Cm^2 + Dm^3 + ... \tag{3.56}$$

This expansion is identical to the virial expansion of the EOS for a real fluid, hence the coefficients B, C and D are referred to as the osmotic virial coefficients. For dilute solutions, the osmotic virial coefficients can be theoretically determined using freezing point depression data and the Gibbs-Duhem equation (Elliott et al., 2007). Theoretical models for calculating the virial coefficients do not exist for solutions of high concentration (Yokozeki, 2006), hence the coefficients are empirically determined by fitting the experimental osmotic pressure data. Fitting the equation up to the third term (C coefficient) has shown to be sufficient to accurately correlate the data.

Based on the virial equation, (3.56), a simple polynomial equation with as many terms as necessary can be used to fit osmotic pressure data (Wilson and Stewart, 2013):

$$\pi = A + Bm + Cm^2 + Dm^3 + ... \tag{3.57}$$

Equation (3.57) has been used by several authors to fit the osmotic pressure of multicomponent aqueous solutions (Elliott et al., 2007, Kaghazchi et al., 2010, Money, 1989, Wilson and Stewart, 2013)

3.3.3 Density

In general, density is a relatively easy property to measure with great accuracy and, hence, there is extensive density data for electrolyte solutions in literature. Similarly, numerous correlative models for electrolyte solutions have been developed to fit the density data with suitable accuracy (Covington, 1986).

Although studies into the density of electrolyte solutions date back as early as 1770, it was only in 1929 that simple correlative equations relating density to concentration were developed (Millero, 1971). Over the years, the equations have become more complex, to relate density, not only to concentration, but to temperature and pressure (Fofonoff, 1985, Sun et al., 2008, Wagner and Kleinrahm, 2004, Wagner and Pruß, 1995).

In literature, two-dimensional equations expressing density in terms of concentration and temperature are generally polynomial (Abdulagatov and Azizov, 2003a, Millero and Huang, 2009, Novotny and Sohnel, 1988, Patil et al., 1992, Sun et al., 2008). The equations can be expressed in the form:

$$\rho = A + Bm + Cm^2 + Dm^3 + ... \tag{3.58}$$

where the constants *A*, *B*, *C* and *D* are empirical constants, which are functions of temperature.

Variations of equation (3.58) express the polynomial as relative density, as given in equation:

$$\rho - \rho_{H_2O} = A + Bm + Cm^2 + Dm^3 + ... \tag{3.59}$$

These polynomial equations have been applied to single salt solutions and have been extended to multicomponent solutions such as brines and seawater.Generally, correlative equations calculate the density with good accuracy where the average errors are within ±0.5%.

3.3.4 Electrical Conductivity

This section reviews the empirical equations presented in Table 3-6, used to calculate the conductivity of multicomponent solutions. Unlike the predictive equations for electrical conductivity presented in **section 3.2.3,** the equivalent conductivities are not theoretically determined, but are defined by fitting the experimental data.

Fireman and Reeve (1948) proposed a simplified form of equation (3.60), by using an averaged specific conductivity for all species in the solution. This equation assumes a linear relationship between conductivity and the summation of the concentrations at very dilute concentrations. At high concentrations, the ion interaction effects, particularly the electrophoretic and relaxation effects, result in loss of linearity

Table 3-6: Correlative equations for calculating conductivity

Reference	Equation	Eqn
(Fireman and Reeve, 1948)	$\kappa = \lambda \sum_{i}^{N} m_i \lvert z_i \rvert$	(3.60)
(Richards, 1954)	$\kappa = \lambda \left(\sum_{i}^{N} m_i \lvert z_i \rvert \right)^{k}$	(3.61)
(McNeal et al., 1970)	$\kappa = \sum_{i}^{N} \lambda_i \left(m_i \lvert z_i \rvert \right)^{k}$	(3.62)
(McNeal et al., 1970)	$\kappa = A_0 + A_1 m + A_2 m^2 + A_3 m^3$	(3.63)
(Visconti et al., 2010)	$\kappa = \sum_{i}^{N} m_i \lambda \lvert z_i \rvert$	(3.64)

Richards (1954) proposed an exponential correction factor, *k*, to the equation proposed by Fireman and Reeve (1948), in order to describe the curvature in the relationship between conductivity and concentration at higher concentrations. Equation (3.61) can be linearized by plotting the graph of log κ versus $\Sigma c_i |z_i|$ to graphically obtain the values of κ and λ.

McNeal et al. (1970) derived two methods for calculating conductivity from concentration of the major ions, using equations (3.62) and (3.63). The first method is similar to the technique proposed by Richards (1954), except that McNeal considers the equivalent conductivity of each ion. In the second method, the authors replaced the product, λc, with a third order polynomial. The polynomial fit performed poorly for dilute solutions less than 200 µS/cm because the estimated conductivity approached A_0.

The empirical methods presented by Fireman and Reeve (1948), Richards (1954), McNeal et al, (1970) and Visconti et al, (2010) are simple mathematical relationships that calculate the conductivity directly, and are based on the hypothesis that the conductivity is proportional to the concentration. Although these methods were originally based on analytical concentrations, Visconti et al. (2010) tested these methods for both analytical and speciated concentrations. Their finding revealed that the use of a speciated concentration improved the prediction of the equations, especially at higher concentrations.

All methods presented in Table 3-6 have been applied to soil extract solution and natural waters whose conductivity does not exceed 20 000 μS/cm. However, the polynomial function presented by McNeal (1970) has been used to fit conductivity (De Diego et al., 1997, De Diego et al., 2001)data for concentrations up to saturation, and hence it was selected for fitting the conductivity data of urine solutions (De Diego et al., 1997, De Diego et al., 2001).

3.4 CHAPTER SUMMARY

In most cases, tabulated thermophysical data needs to be interpolated in order to obtain the required data at specific conditions. Models assist the designer to accurately determine thermophysical properties at any point of interest within the valid range of the model.

The review of urine composition in Chapter 2 revealed that it is a complex mixture of salts and has an ionic strength ranging between 0.3 – 0.6 M. In order to select the appropriate models to determine its properties, thermodynamic predictive and correlative equations used to model the thermophysical properties of ionic-strength multicomponent aqueous solutions, similar to urine, were reviewed in Chapter 3.

In addition, the speciation method was reviewed so that it could be coupled with the thermodynamic models in order to improve the accuracy of their predictions. Figure 3-2 shows the speciation of the urine sample and the thermodynamic equations which were selected for the calculation of its thermophysical properties. Selection of the models was based on the validity of the range of their application as well as their accuracy.

Speciation is an iterative process which requires knowledge of the concentration of the species, ionic strength and ionic activity coefficient of a given aqueous solution. The ionic activity of the species was calculated using the B-dot equation (3.14), which can model ionic strengths of up to 1.5 M and temperatures up to 300°C. Specific ion models, which can model activity coefficients up to 6.0 M, could not be applied to urine because they lack parameters for key components in urine which include phosphates and ammonia.

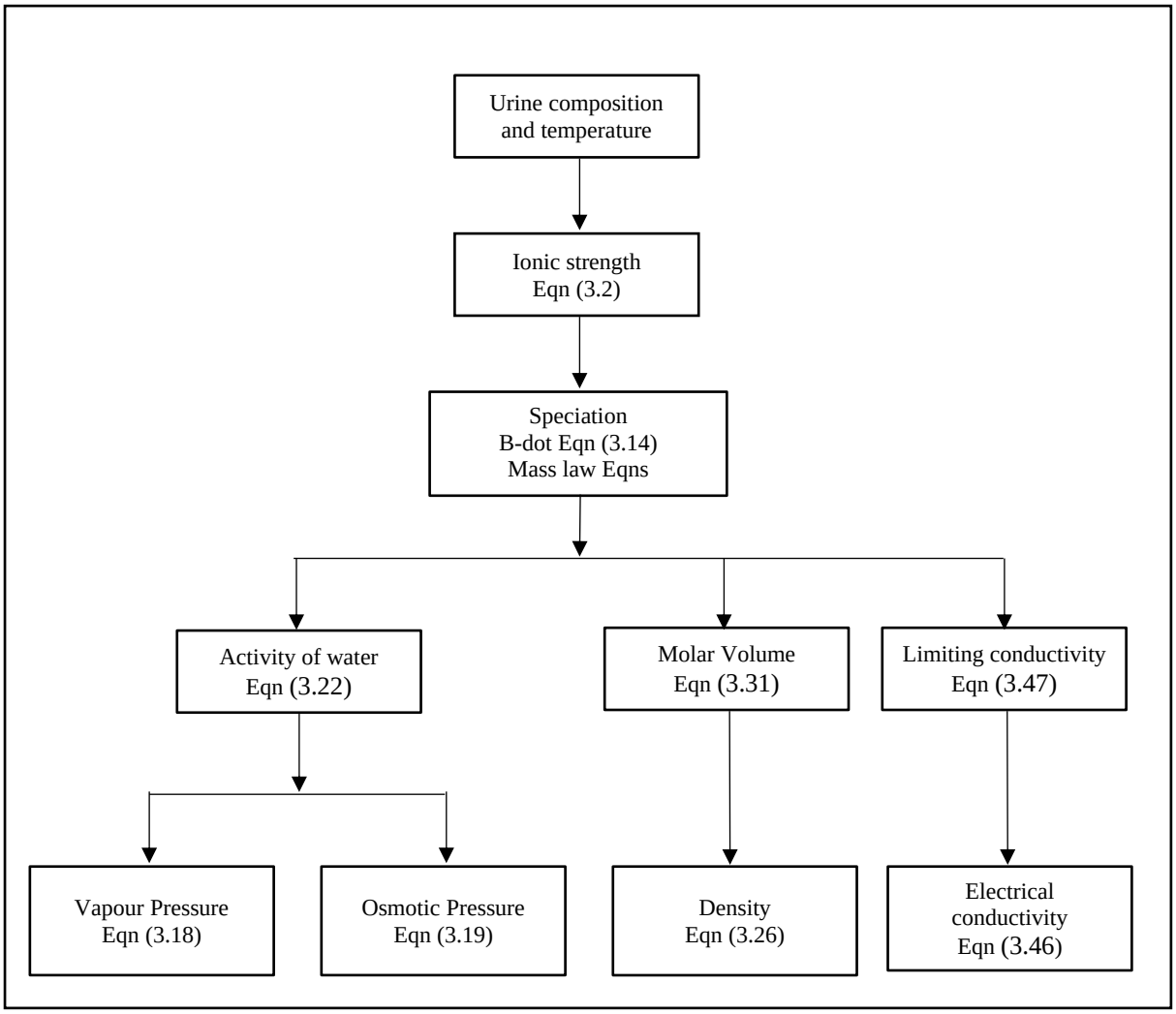

Figure 3-2: specific thermodynamics equations used for calculating the thermophysical properties of hydrolysed urine.

Vapour pressure and osmotic pressure of the urine solutions was calculated using equations (3.18) and (3.19), where the activity of water was calculated using an model developed by Brouckaert (1995) Density was calculated by adding the molar volumes of the ions in the solution and the molar volume of each ion was determined using the method proposed by Millero (1970). Brouckaert's (1995) method was selected for calculating the conductivity of urine. Corrections for temperature would be done using the viscosity-based equation proposed by Sorensen and Glass (1987)

The equations chosen for the correlation of the thermophysical properties of urine were generally polynomial in principle. This is because they are simple, and can fit data with suitable accuracy.

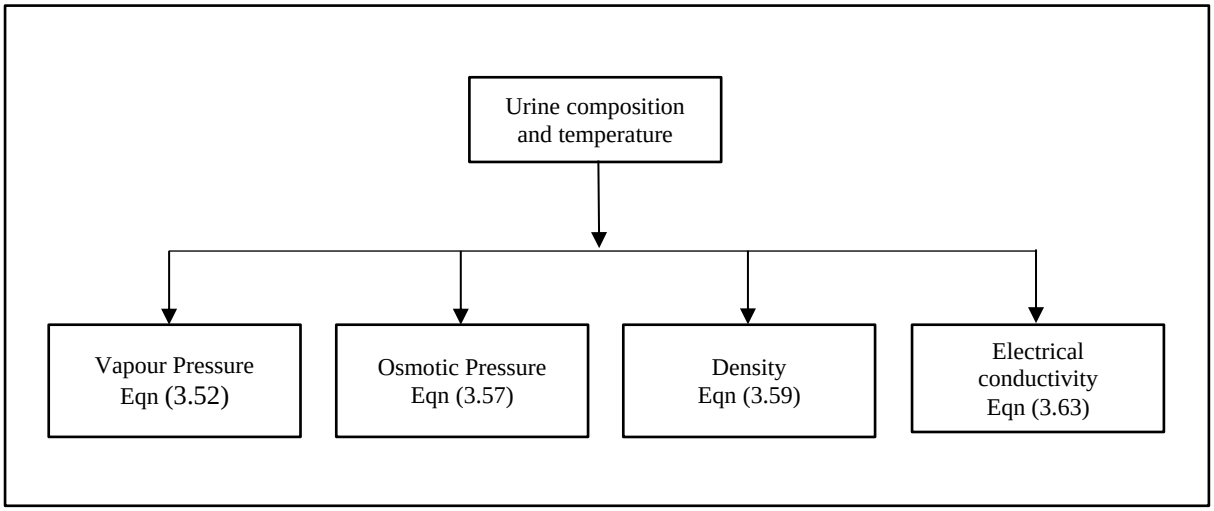

Figure 3-3: Selected correlative models for calculating the thermophysical properties of hydrolysed urine

4 EQUIPMENT REVIEW

The validity and reliability of experimental data is influenced by the quality of the measuring instrument used (Kimberlin and Winterstein, 2008). Equipment measuring the same thermophysical property may differ in the principle or technique in which they determine the property. A measurement obtained from any instrument consists of the "true" value which is not known and an error (Crocker and Algina, 1986). The "true" value is the measurement obtained if the instrument used were perfect. Knowledge of the measuring technique helps the researcher in identifying and reducing the inherent errors associated with a measuring method

Urological research on hydrolysed urine has mainly been focused on characterizing its chemical composition (Karak and Bhattacharyya, 2011, Kirchmann and Pettersson, 1994, Rose et al., 2015, Udert et al., 2006). Very little information is available on the studies focusing on measurements of the thermophysical and engineering data of hydrolysed urine investigated in this work which include; vapour pressure, osmotic pressure, density and electrical conductivity. As discussed in **Chapter 2** hydrolysed urine is a high-ionic strength aqueous solution containing a wide range of dissolved salts. Literature is abundant with measurements of thermophysical properties of multicomponent aqueous solutions such as seawater (Fabuss and Korosi, 1968, Millero and Huang, 2009, Wiesenburg and Little, 1988), industrial brines (Mariah et al., 2006) and natural waters (McCleskey, 2011, McCleskey et al., 2012b, Millero, 1985, Talbot et al., 1990).

The aim of this chapter is to review the equipment used for measuring the thermophysical properties of multicomponent aqueous systems. The review outlines the principle of measurement and the associated uncertainty for each equipment. After discussing the advantages and disadvantages inherent in each technique, the equipment suitable for measuring the thermophysical properties of hydrolysed urine are selected.

4.1 VAPOUR PRESSURE

(Muhlbauer, 1997) gives a detailed review for vapour pressure phase equilibrium measurements. This review will focus on pressures below and up to atmospheric pressure which can be classified into five groups, which are namely: dynamic methods, static methods, semimicro techniques, measurement of infinitely dilute activity coefficients, dew-point and/or bubble point methods. Widely used techniques used for low vapour pressure measurement of aqueous electrolyte solutions include:

- Isopiestic methods (Hefter et al., 1997, Lin et al., 1996, Miladinović et al., 2008, Rush and Johnson, 1966);
- Vapour pressure lowering (Patil et al., 1992, Patil et al., 1990, Patil et al., 1991);
- Ebulliometry (de Azevedo and de Oliveira, 1984, de Oliveira and Meites, 1977, Mariah et al., 2006).
- Static pressure measurement (Abdulagatov and Azizov, 2003a, Salavera et al., 2005, Shiah and Tseng, 1996);

4.1.1 Isopiestic methods

This technique is based on the fact that two different solutions when connected through the vapour space, will approach equilibrium by transferring the solvent mass though distillation. Figure 4-1 shows the isopiestic apparatus consisting of a multi-legged glass manifold which is connected to round bottomed flasks through taper male/female joints. Some of the flasks are charged with the reference solution and the remainder are charged with the solution whose vapour pressure is investigated.

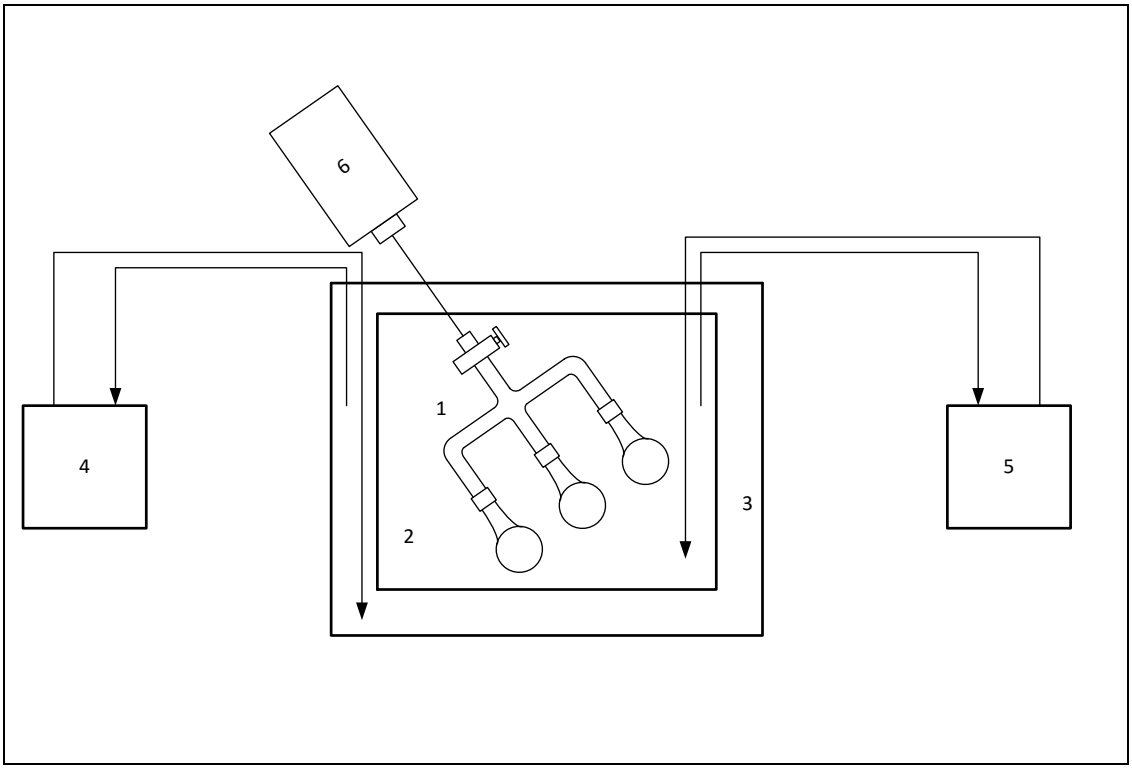

Figure 4-1: Schematic of the Isopiestic apparatus

(1) Sample cell; (2) Inner tank; (3) Outer tank; (4 and 5) Temperature controllers; (6) Electric motor.

The manifold is evacuated so that it is filled with water vapour from the solutions. The solvent will transfer from the solution with higher vapour pressure to that of lower vapour pressure, through isothermal distillation. This transfer will continue until the chemical potentials of the solvent in each flask are equal, as proposed in equation (4.1):

$$\mu_{w,1} = \mu_{w,2} = \mu_{w,3} = ...\mu_{w,n} \tag{4.1}$$

where μ_w represents the chemical potential of each solution. Temperature control is attained by submerging the isopiestic apparatus in a water bath and agitation is achieved by slowly turning the apparatus at a tilted angle. The accuracy of this technique depends on the references solutions used, mixing during the experiment, temperature control and the time allowed for equilibrium to be reached (Lin et al., 1996). After equilibration, the solutions are weighed and the osmotic coefficient of the solution is calculated using the equation (3.2):

$$\varphi = \frac{\nu^o \varphi^o m^o}{\nu m} \tag{4.2}$$

Where ϕ represents the osmotic coefficient; ν represents the stoichiometric numbers of the anions and cations; m represents the molarity; subscripts ° denotes the properties of the reference solution. °This technique is very simple and is regarded as the most accurate method of determining the vapour pressures of aqueous solutions. The error in the activities of water is reported to be within 0.01 % (Lin et al., 1996). However the greatest disadvantage with this technique is that it requires very long equilibration periods (days long) and the temperature should be maintained within ±0.005°C during this period. This makes the system sensitive to temperature fluctuations. Although this method provides accurate measurements, this method was not selected for measuring vapour pressure of urine because of the long equilibration times.

4.1.2 Vapour pressure lowering

These methods are also referred to as static differential methods. Figure 4-2 shows vapour pressure lowering apparatus in which the aqueous solution investigated is connected to the reference solution using a differential manometer. The flasks containing the aqueous solutions and the manometer are submerged in a temperature-controlled water bath. The vapour pressure data is calculated from the difference in the manometer levels.

The method is very simple and the equilibration periods are very short (about 2 h). A source of error within the method is in reading the menisci levels of the manometer. The measurements must be corrected by taking into account the thermal expansion coefficient of the manometric fluid (Patil et al., 1992). The technique also requires that the investigated fluid, the reference fluid, as well as the

manometric fluid, be degassed before the experimental runs. This was regarded as being very tedious work considering that several vapour pressure measurements (approximately 110) had to be performed for the urine solution and its concentrates.

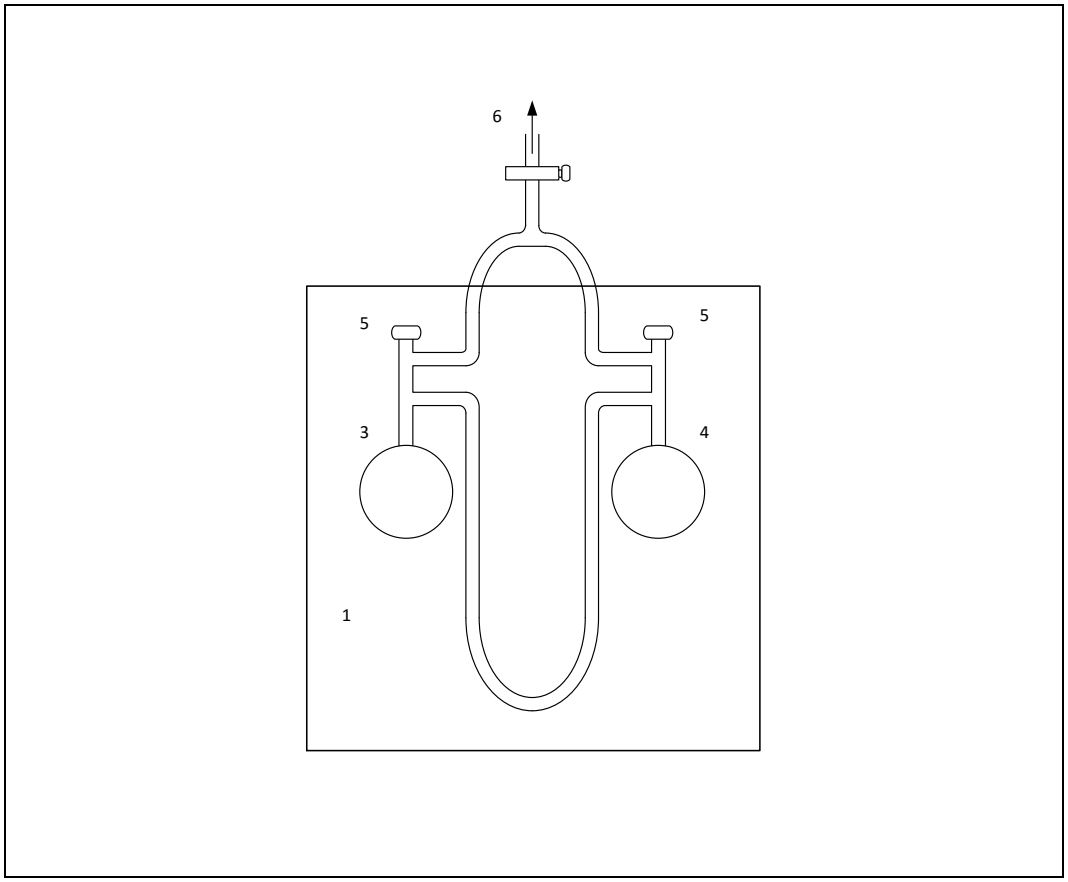

Figure 4-2: Vapour pressure apparatus

(1) Water bath, (2) mercury manometer, (3) solution cell, (4) water cell, (5) Teflon stopcock, (6) leads to vacuum pump.

4.1.3 Ebulliometry

Ebulliometry is a widely used dynamic method which has gone through significant developments to give accuracies close to static methods (Raal et al., 2006). (Mariah et al., 2006) used this method to measure the vapour pressure of concentrated brines. Figure 4-3 shows the ebulliometer apparatus. In dynamic methods, the sample liquid is brought to boil in a boiling chamber. Slugs of flow are transported from the boiler via the Cottrell to the equilibrium chamber where the temperature is measured. In the equilibrium chamber, contact and disengagement of phases occurs and the equilibrium temperature is measured. Vapours are condensed and returned into the still where the condensate mixes with the boiling liquid. In some methods, there is direct circulation of the vapour phase. Dynamic stills can either be operated isobarically or isothermally.

The advantages of this method are that data can be determined more quickly, degassing is not required, and simple apparatus and straightforward procedures are used (Olson, 1989). Problems associated with accurate measurement using an ebulliometer include bumping of liquid at very low pressures that can flash the liquid and cause cooling of the equilibrium chamber, and then discharge of superheat from liquid impinging on the thermometer well where the temperature is being measured. To test the applicability of using this method on urine solutions, 0.1 M, 1 M and 5 M NaCl solutions were prepared for vapour pressure tests. The vapour pressure readings were to be compared with literature values for verification. It was observed that for the 1M NaCl solution, the energy required to raise the temperature of the solution to boiling point exceeded the power ratings of the internal and external heaters of the equipment. Since the starting solution of the hydrolysed urine is 0.3 M, the ebulliometer could not be used.

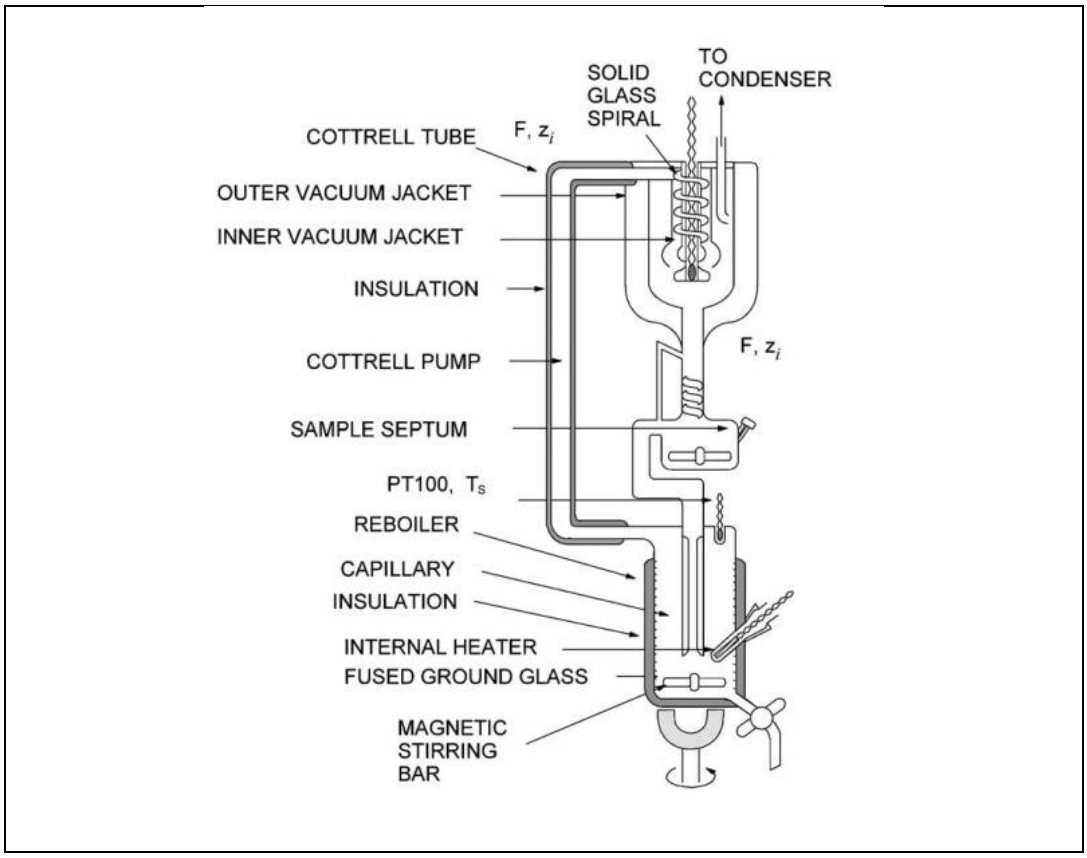

Figure 4-3: Ebulliometer (Raal et al., 2006)

4.1.4 Static pressure measurement

The principle of this technique is to measure the vapour pressure of a solvent in an evacuated equilibrium cell. This makes it sensitive to the presence of air in the enclosed space (Muhlbauer, 1997), therefore the liquid sample is first degassed to eliminate dissolved gases. The cell is connected to a

temperature and pressure control and measuring evacuated system, and once the sample is loaded, the cell is submerged in a thermostated water/oil bath. The liquid solution is constantly agitated using mechanical means until vapour-liquid equilibrium is achieved. At equilibrium, the pressure is measured at the set temperature; hence only isothermal data can be measured using the static method.

Figure 4-4 shows the static apparatus used by (Salavera et al., 2005) to measure the vapour pressure of aqueous ammonia, potassium hydroxide and sodium hydroxide solutions. The advantage of this technique is that it allows for the direct measurement of vapour pressure hence the user can choose instruments with a very high degree of accuracy and wide range of measurement. This allows for the calibration and accurate determination of temperature and pressure depending on the choice of the instruments. The pressure can be measured within a range of 0.001-10 MPa and the temperature can be measured to an accuracy of ±0.002°C. This method was therefore chosen for measuring the vapour pressure solutions of hydrolysed urine because it is simple, accurate and data is quickly determined.

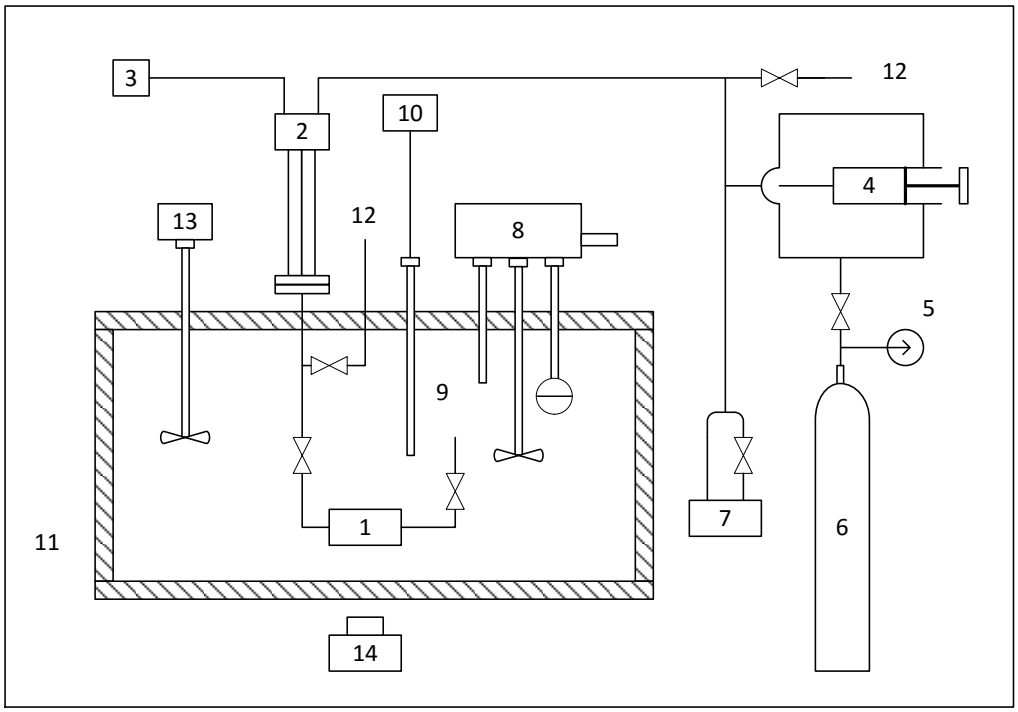

Figure 4-4: Schematic of the static vapour pressure apparatus:

(1) stainless steel cell; (2) diaphragm type differential pressure transducer; (3) differential pressure null indicator; (4) pressure controller; (5) pressure gauge (Bourdon type); (6) nitrogen cylinder; (7) digital pressure gauge; (8) thermoregulator; (9) platinum resistance thermometer (Anton Paar); (10) temperature indicator; (11) thermostat bath (12) to vacuum pump; (13) bath stirrer; (14) magnetic driver of the cell stirrer.

4.2 OSMOTIC PRESSURE

The osmotic pressure of a solution can be measured using

- Membrane osmometry (MO) (Grattoni et al., 2008, Money, 1989, Moon et al., 2000, Wells, 1973, Wu and Prausnitz, 1999),
- Vapour pressure osmometry (VPO) (Apelblat et al., 1973, González et al., 2008, Grattoni et al., 2008, Maali and Sadeghi, 2015)
- Freezing point osmometry (FPO) (Grattoni et al., 2008, Lord, 1999, MacNeil et al., 2011, Wang et al., 2002)
- Vapour pressure measurements (Grattoni et al., 2007, Ksayer et al., 2012, Putnam, 1971, Robinson and Stokes, 2002)

Membrane osmometry is a direct method of determining osmotic pressure, while vapour pressure and freezing point osmometry rely on thermodynamic principles and hence their applicability is constrained by the characteristics of the solutions being measured (Sweeney and Beuchat, 1993).

4.2.1 Membrane Osmometry

Membrane osmometry is a technique to directly measure the osmotic pressure of a solution. The osmotic pressure is determined by measuring the liquid pressure after the solution has reached equilibrium with no net water flux across a membrane. This technique does not need to be calibrated and is not limited by the concentration of the solution. Figure 4-5 shows membrane Osmometer developed by (Grattoni et al., 2008).

Membrane osmometry is affected by the filterability of the solution, hence it cannot measure the osmotic pressure of a solution with very small molecules such a salts and alcohols. The range of molecular weights in the solution that membrane osmometry measurement are reliable, is from $5x10^3$ to $5x10^5$ μm (Slade, 1975). Ballooning of the membrane can be another problem that is caused by the pressure difference. This is due to the viscoelastic nature of the membrane. Large sample volumes and lengthier measurement times are required compared to vapour pressure osmometry and freezing point osmometry. Dissolved air in the liquid affects pressure measurements and hence the liquids need to be degassed. As a result, this technique was considered impractical for measuring the osmotic pressure of urine solutions.

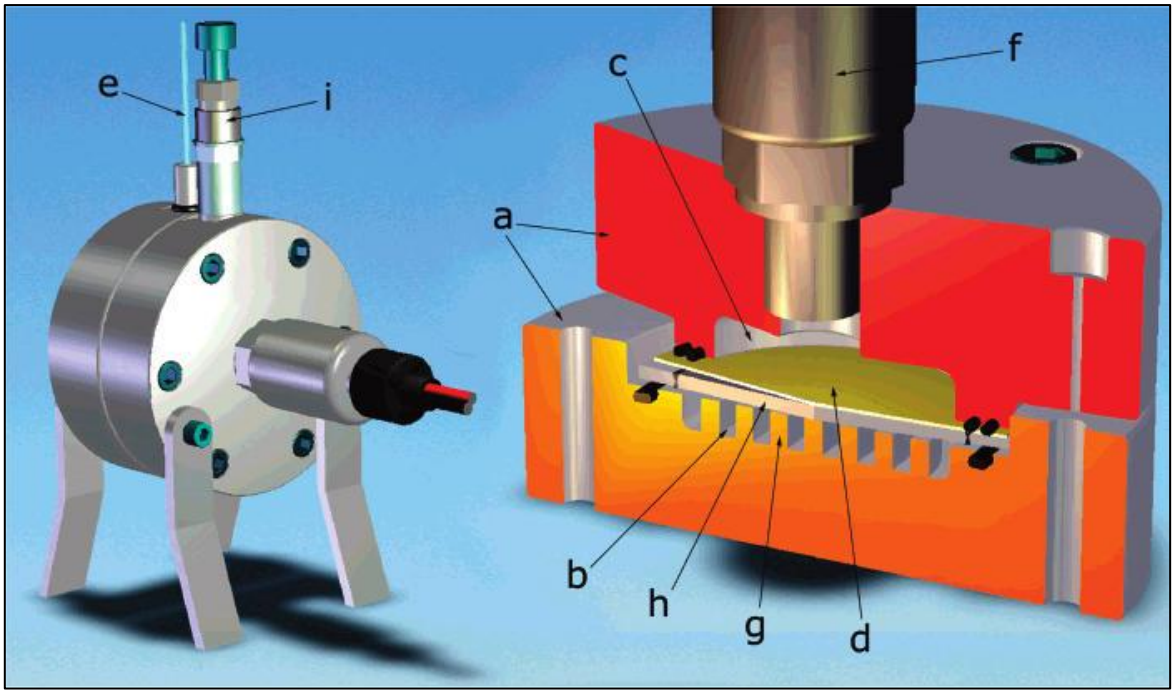

Figure 4-5: Membrane Osmometer module (Grattoni et al., 2008)

(a) stainless steel shells, (b) solvent chamber, (c) solution chamber, (d) membrane, (e) Capillary tube connected to the solvent chamber, (f) pressure transducer, (g) support ribs, (h) support porous disk (i) solution chamber cap

4.2.2 Freezing Point Osmometry

The presence of soluble or mixable substances in water lowers its freezing point. In freezing point osmometry, the osmolality is determined by measuring the freezing point depression. Osmolality is a measure of osmotic concentration expressed in osmoles of solute particles per kilogram of water (Osmol/kg).

The liquid sample is supercooled below the freezing point, and the crystallisation is initiated by a rapid vibration or stir mechanism. The release of the heat of crystallisation will cause the temperature of the solid to rise until an equilibrium plateau which is the freezing point of the solution. The temperature at which a pure solvent freezes at standard conditions is definite and characteristic of that solvent, and the addition of a solute will change the original change of state temperature.

When a pure liquid freezes, the molecules of the solvent group together to form a crystalline structure held by intermolecular forces. The presence of solutes in the liquid makes it more 'difficult' for the molecules of the solvent to align one with each other to form a pure crystal (difficult implies that there are restrictions caused by attractions with the solute that hinder the movement of the solvent molecules from the liquid to the crystalline structure). Therefore, the solidification process will start when the liquid temperature is colder than the temperature required to freeze the pure solvent.

The freezing point depression of a solution is used to estimate the osmolality of a solution using Bladgen's law which states that the freezing point depression is directly proportional to the concentration of the solute, as expressed in equation (4.1):

$$C_{osm} = \frac{\Delta T}{K_f} \tag{4.1}$$

where C_{osm} is the osmolality (Osmol/kg) ; ΔT is the freezing point depression (°C)and is defined as $T_{F(pure\,solvent)} - T_{F(solution)}$; K_f is the freezing point constant which is equal to 1.858 K kg mol^{-1}.

The osmotic pressure of the solution is then calculated using Van't Hoff equation:

$$\pi = iC_{osm}RT \tag{4.2}$$

The disadvantage of this method is that both Bladgen's law and the Van't Hoff's equation are valid for concentrations up to 0.5 M which is not suitable for measuring the osmotic pressure at high concentrations.

4.2.3 Vapour Pressure Osmometry

Vapour Pressure Osmometry is a modified isopiestic method used to determine the vapour pressure of a solution. The vapour pressure is not measured directly due to difficulties in sensitivity. Vapour pressure is determined by measuring the steady-state temperature difference that occurs when a drop of solution and a drop of pure solvent are exposed to an atmosphere saturated with the pure solvent vapour in a chamber. Temperature is measured using thermistors covered with platinum. In the chamber with the solution, the solvent vapour will condense on the thermistor and this process will warm up it. Condensation on the thermistor will continue until the vapour pressure of the solvent is equal to that of the pure solvent in the surrounding chamber. The differential temperature of the two thermistors is measured and correlated to pressure.

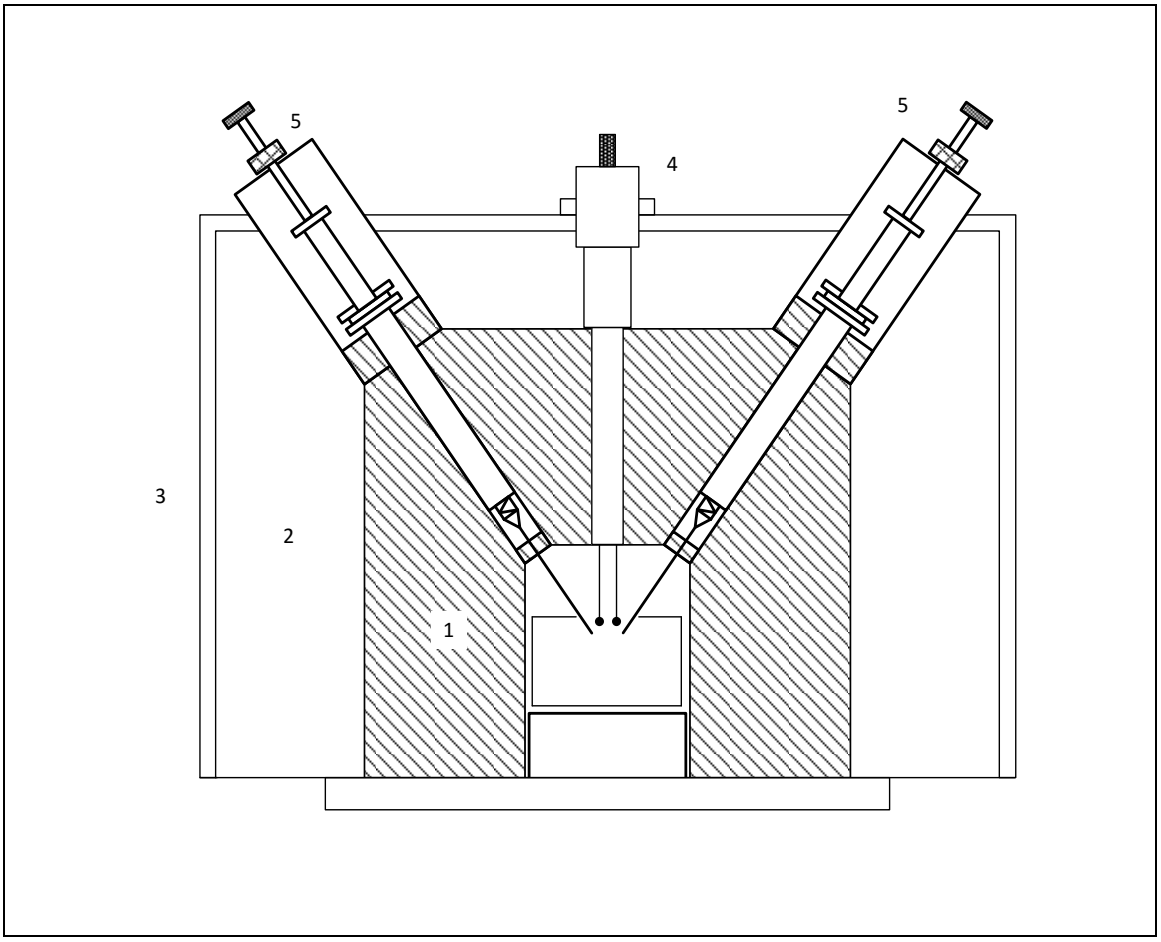

Figure 4-6: Schematic diagram of a Vapour pressure Osmometer

(1) Aluminium block, (2) Polyurethane insulation, (3) Steel case, (4) Temperature sensors, (5) Hypodermic syringes

The difference of the temperatures between the two drops of the solution are used to estimate the osmolality of a solution using the equation:

$$C_{osm} = \frac{\Delta T_b}{K_b} \tag{4.3}$$

where C_{osm} is the osmolality (Osmol/kg) ; ΔT_b is the difference in temperature of the two solutions (K); K_b is the evaporation constant which is equal to 1.858 K kg mol^{-1}..

The advantage of using VPO is that it is not affected by the viscosity of the sample or the presence of suspended particulates. It can be performed over a wide range of temperatures and the solution does not go through a change of state when it is performed. Commercially available instruments for vapour pressure osmometry cannot measure concentrations greater than 3.2 M. The concentration of the urine solutions ranges from 0.3 to 8.0 M, hence the instrument cannot be used at high concentrations.

4.2.4 Vapour Pressure Measurements

The osmotic pressure of electrolyte solutions can be calculated from the vapour pressure of the solution and water using Raoult's law:

$$\pi = -\frac{RT}{v}\ln\left(\frac{P}{P_{H_2O}}\right) \tag{4.3}$$

This law implies that the osmotic pressure can be calculated from data measured using any vapour pressure equipment described in **section 4.1**. Unlike vapour pressure osmometry and freezing point osmometry, this method is not limited by concentration. Additionally, this method provides two sets of data (vapour pressure and osmotic pressure) are obtained from a single measurement.

4.3 DENSITY

The density of fluids can be determined using several types of densimeters which include bellows volumetry, piezometers, isochoric methods, vibrating bodies, and buoyancy densimeters (Goodwin, 2003). Densimeters widely used in literature for electrolyte solutions include:

- Pycometers (Dunn, 1966, Fabuss et al., 1966, Tang and Munkelwitz, 1994)
- Piezometers (Abdulagatov and Azizov, 2003a, Abdulagatov and Azizov, 2004, Abdulagatov and Azizov, 2003b, Abdulagatov and Azizov, 2005, Abdulagatov and Azizov, 2006, Hogenboom et al., 1995)
- Magnetic float densimeters (Blanco and Vargas, 2004, Chen et al., 1980, Lo Surdo and Millero, 1980, Obšil et al., 1997, Simonson and Ryther, 1989)
- Vibrating tube densimeter (Al Ghafri et al., 2012, Gates and Wood, 1989, Holcomb and Outcalt, 1998, Krumgalz and Millero, 1982)

The review will be limited to two densimeters; magnetic float densimeters and vibrating tube densimeters. (Wagner and Kleinrahm, 2004) classifies these densimeters as accurate (uncertainties less than 0.05%) over large ranges of temperatures and pressures. This statement however does not imply that some versions of the piezometer and the pycnometer instruments do not have uncertainties less than 0.05%. Piezometers and pycnometers have been used in the past (up to 1975) because of their simplicity and high accuracy when used with care (Tropea et al., 2007). (Abdulagatov and Azizov, 2006) has used modified piezometers with uncertainties in density clearly less than 0.05%. However, densimeters using magnetic-float and vibrating-bodies now provide densities with low uncertainties rapidly and more conveniently (Tropea et al., 2007).

4.3.1 Magnetic float densimeters

Magnetic float densimeters are buoyancy densimeters that function based on Archimedes principle. All buoyancy densimeters have a sinker with a known weight which is totally submerged in the liquid whose density is being measured. The weight of the fluid that is displaced is equal to the apparent loss in weight of the sinker. The density of the fluid of interest is then determined by the relation:

$$\rho = \frac{W_S - W_S^*}{gV_S} \tag{4.4}$$

where W_s is the true weight of the sinker ; W_s^* is the apparent mass of the sinker submerged in the liquid sample; g is the acceleration due to gravity ;V_s is the volume of the sinker.

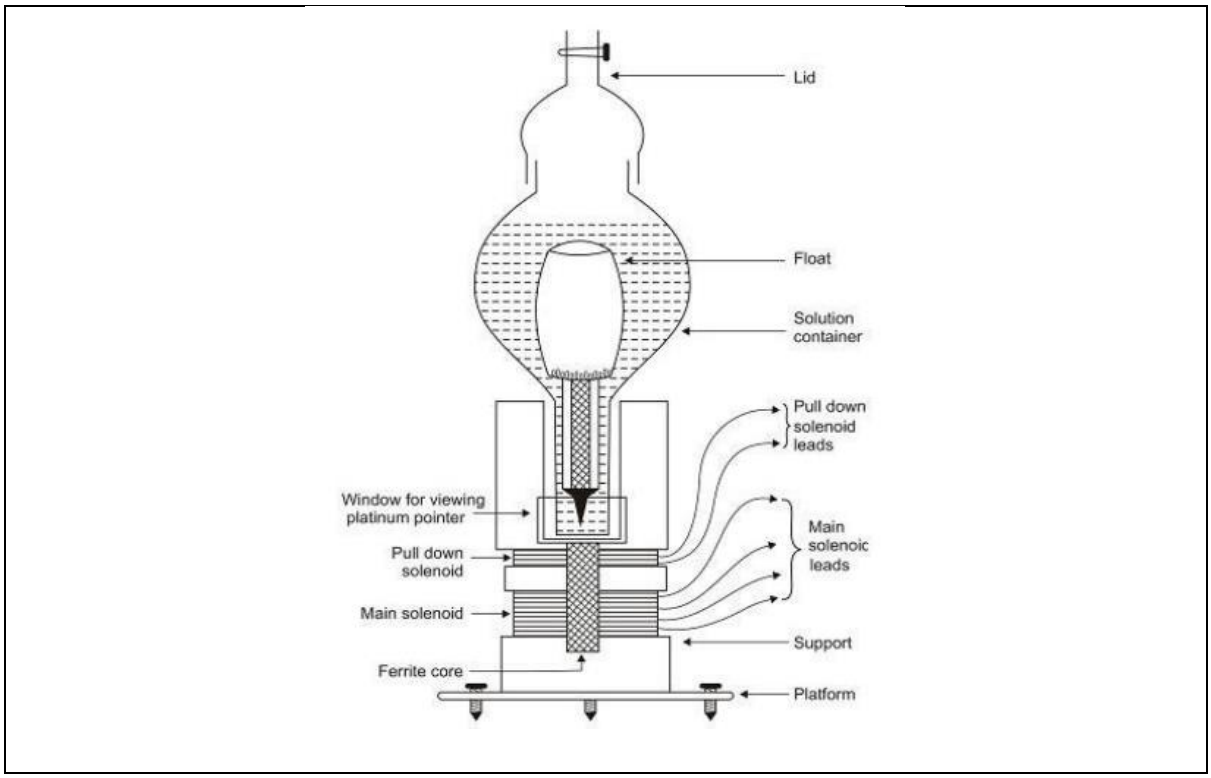

Figure 4-7: Magnetic float densimeter used by (Pathak, 2013)

Magnetic float densimeters use a weighted float (buoy) whose core contains either a magnet or soft iron. The buoy is then kept in equilibrium at any position within the liquid sample using an electromagnetic field usually provided by a solenoid. The density of the solution is calculated from the magnetic force required to hold the float in place in the sample liquid. These densimeters can perform measurements over a temperature range of 90 K to 300 K, pressures up to 5 MPa and can achieve uncertainties of 10^{-7} kg m^{-3}. Calibration is done by using liquids with known densities.

4.3.2 Densimeters with vibrating bodies

The density measured in vibrating densimeters is deduced from the resonant frequency of vibrating bodies that can be related to the density of the fluid samples. The vibrating bodies are usually hollow wires, forks, cylinders and tubes. Densimeters with vibrating hollows and vibrating forks are predominantly used to measure the density of natural gases in pipelines, while vibrating wires and tubes are used for determining the density of liquids.

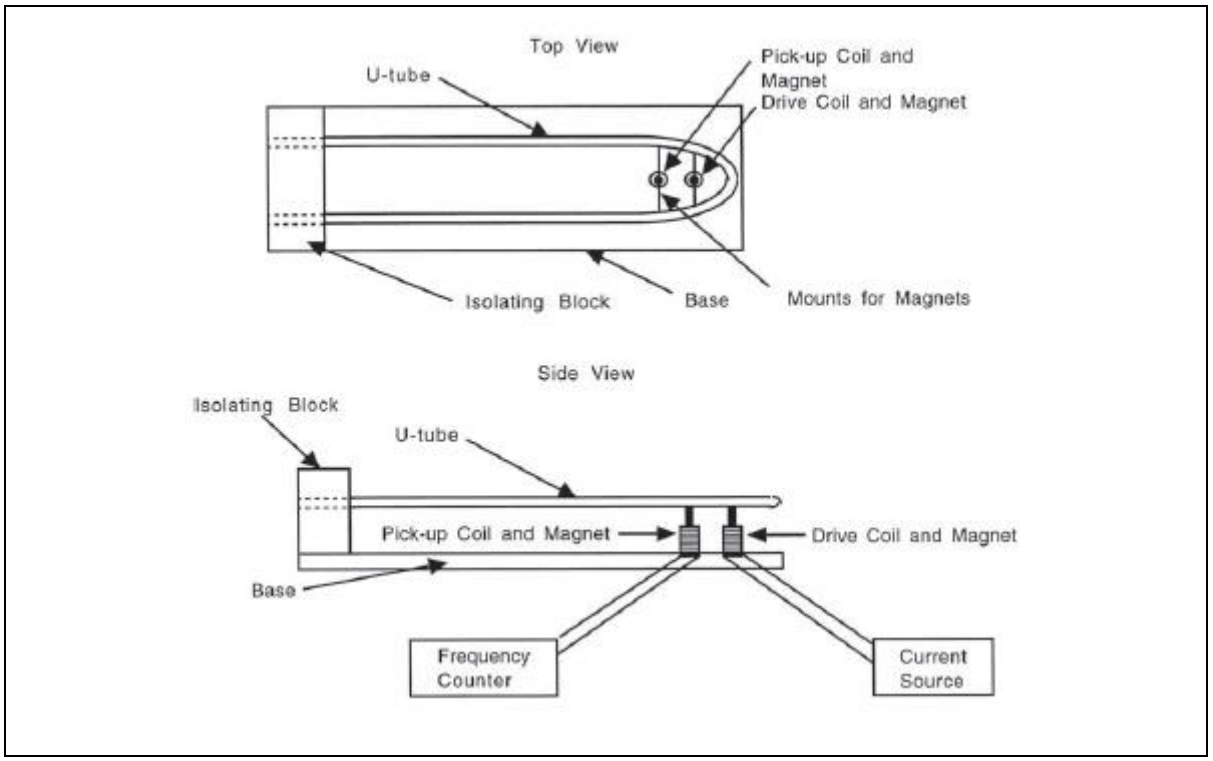

Figure 4-8: Vibrating-tube densimeter (Holcomb and Outcalt, 1998)

Vibrating tube densimeters can make relatively quick and precise measurements over a wide range of temperature (263 to 353 K) and pressure (up to 15Pa) (Holcomb and Outcalt, 1998). Uncertainties from the instrument are less than 0.1% (Wagner and Kleinrahm, 2004). Vibrating tube densimeters have a U-shaped glass or metallic tube placed in a thermo-regulated cell. The tube is filled with the sample liquid and then mechanically agitated. The resonant frequency of the tube filled with the liquid is used to calculate the density of the liquid using the formula:

$$\rho = A\tau^2 - B \tag{4.5}$$

where τ is the period of the vibrating tube, A and B are calibration parameter of the densimeter, which are functions of temperature and pressure.

The magnetic float and vibrating-tube densimeters are both accurate instruments. 243 density measurements of hydrolysed urine were required, and as a result, the vibrating-tube densimeter was selected because it can make rapid and precise measurements.

4.4 ELECTRICAL CONDUCTIVITY

When an electrical potential difference applied to a solution, the resistance of the solution to the flow of charge can be described by Ohm's law shown in equation (4.4)

$$E = IR \tag{4.4}$$

where E is the electrical potential (V); I is the current (A); R is the resistance (Ω). Miller et al. (1988), postulates that the resistance arises from the drag experienced by a migrating ion as it distorts the sphere of oppositely charged ions and water molecules surrounding it. The reciprocal of the electrical resistance of the solution is defined as the conductance, presented in equation (4.5)

$$G = \frac{1}{R} \tag{4.5}$$

When the potential is applied using electrodes with a cross section surface of A (cm^2) and are a distance of $\int$ (cm) apart, then the resistance to conduction can be expressed by equation (4.6).

$$R = \rho \frac{\int}{A} \tag{4.6}$$

where ρ represents the specific resistance or resistivity (Ω /cm). The electrical conductivity or specific conductance (κ) in S/cm, is defined as the reciprocal of the resistivity and it is represented by equation (4.7)

$$\kappa = \frac{1}{\rho} = \frac{\int}{RA} \tag{4.7}$$

The ratio of the length to the area $\int/A$ is fixed for a given cell, and is also defined as the cell constant, K_{cell}. The expression for the specific conductance becomes in the form (4.8).

$$\kappa = K_{cell} G \tag{4.8}$$

4.4.1 Inductive (Toroidal) method

This method employs two wired coils (toroids) which are coupled next to each other and encased in a corrosion resistant plastic casing. The first coil, also termed the drive coil, is supplied with high voltage which induces a magnetic field. This results in a flow of ions (ionic current) of the liquid to pass through the second coil. A magnetic field is created in the second coil and this induces a current which is measured by an analyser. The induced current is proportional to the conductance of the solution and it is converted to specific conductivity by the sensor. This method is suitable for very highly concentrated solutions and is generally used for industrial applications (Ramos et al., 2008), (Gençer and Tek, 1999) and (Karbeyaz and Gençer, 2003).

4.4.2 Amperometric (2 electrodes) method

The electrical conductivity is measured using a probe with two electrodes with a known spacing between them. A known voltage is applied to the pair of electrodes and the current is measured. The resistance offered by the solution is calculated using Ohm's law. The conductance of the solution is the reciprocal of the resistance. These electrodes are commonly used to measure the electrical conductivity of highly diluted aqueous solutions from 0.04 μS/cm to 25 000 μS/cm where deposits on the electrodes are not expected, such as soil salinity (Scoggins and van Iersel, 2006). Solutions with conductivities exceeding 50 000 μS/cm result in polarization effects and deposition of the salts on the electrodes. These polarization effects of the electrodes maybe result in capacitive impedance and give rise to errors in measurement (Bronzino, 1999).

4.4.3 Potentiometric (4-electrode) method

This method employs the use of 4 electrodes which are arranged concentrically. The outer pair of electrodes induces an alternating current which induces a current loop in the solution. The inner pair of electrodes then measures the voltage induced by the current loop. This method of measurement is directly reliant on the conductivity of the solution. As a result the potentiometric method is not affected by polarisation effects for wide range of conductivities, hence it was selected for measuring the conductivity of hydrolysed urine. These electrodes are used to measure electrical conductivities of municipal and industrial sewage waste, water quality (Ramos et al., 2008), cooling water. Electrodes are usually made of platinum because it can withstand high temperatures and provides more stable readings.

4.5 SUMMARY

The equipment used for measuring vapour pressure, osmotic pressure, density and electrical conductivity is reviewed in detail. Knowledge of the principle of measurement for an equipment is important in understanding the uncertainties associated with its measurement. There is no published research on the characterization of the thermophysical properties of hydrolysed urine. As a result, much focus was placed on equipment used for measuring properties of multicomponent solutions such as seawater, natural waters and industrial brines, which are similar to urine. The advantages and limitations of each method is discussed.

The static pressure equipment was selected for vapour pressure because it allows very accurate temperature and pressure measuring devices to be attached to the equilibrium cell. Osmotic pressure can be accurately calculated from vapour pressure measurements. The vibrating tube densimeter was selected for measuring density, because it allows for rapid and accurate measurements. The 4 electrode potentiometric method was chosen for measuring the electrical conductivity of hydrolysed urine. This method was selected because it is quick, simple and accurate method which is not affected by polarisation effects.

5 EXPERIMENTAL METHODS

5.1 INTRODUCTION

The experimental equipment used for measuring the properties of urine was installed in the Thermodynamics Research Group laboratory, which is not certified to handle biohazardous materials such as human waste. As a result, synthetic urine based on the chemical composition of hydrolysed urine presented in **Chapter 2** was prepared. A detailed account of the gravimetric preparation of the synthetic urine and its concentrates is given. The apparatuses for each of the measurements from the previous chapter, the experimental apparatuses and procedures used for the measurements of the physical properties of urine are here described.

5.2 SYNTHETIC URINE SOLUTIONS

The synthetic urine solution for the hydrolysed urine was based on the of Udert (2003). However to prepare a synthetic urine solution which was stabilised with sulphuric acid, the ammonia and the carbonates were replaced with ammonium sulphate. Table 5-1 shows the nine synthetic urine solutions that were prepared. The concentrations of the salt components in the synthetic urine solution prepared were within the functional ranges of human urine reported in literature. Nine urine solutions were prepared with concentrations ranging from 4.5 wt% to 32.2 wt %. This translates to a 10 times increase in concentrations and 90% removal of water.

All salts used were analytical grade reagents from Merck with a purity greater than 99%. The salts were dried in an oven at 105°C for several hours until there was no appreciable change in the weight. Ammonium sulphate $(NH_4)_2SO_4$ and ammonium chloride NH_4Cl were dried at 80°C to avoid decomposition of the salts. Ammonium bicarbonate, which decomposes above 35°C, was used from a recently opened bottle. Distilled water used for preparing the solutions was previously purified using a PURELAB Option-Q Lab Water Purification System where the resistivity and conductivity were reduced to 18.4MΩ/cm and 4.95 μS/cm respectively.

Table 5-1: Composition of the synthetic urine solutions

	Concentration ($g \cdot L^{-1}$)								
	4.5 wt%	**7.7 wt%**	**10.4 wt%**	**14.5 wt%**	**18.4 wt%**	**21.3 wt%**	**25.4 wt%**	**29.2 wt%**	**32.2 wt%**
pH	4.49	4.36	4.27	4.16	4.06	3.99	3.88	3.77	3.69
NaCl	3.00	5.26	7.32	10.73	14.29	17.14	21.54	26.09	30.00
Na_2SO_4	2.30	4.04	5.61	8.23	10.95	13.14	16.51	20.00	23.00
KCl	3.40	5.96	8.29	12.16	16.19	19.43	24.41	29.57	34.00
NH_4Cl	3.90	6.84	9.51	13.95	18.57	22.29	28.00	33.91	39.00
$(NH_4)_2SO_4$	32.82	57.58	80.05	117.38	156.29	187.54	235.65	285.39	328.20
NaH_2PO_4	2.00	3.51	4.88	7.15	9.52	11.43	14.36	17.39	20.00

5.2.1 Vapour Pressure and Osmotic Pressure

The vapour pressure of the 9 urine solutions, as provided in Table 5-1, was measured, using a simple static apparatus based on the method of Salavera et al. (2005). It consisted of the following main components, which will each be described in more detail:

- A stainless steel equilibrium cell,
- Temperature and pressure measuring devices,
- Equipment for mixing the equilibrium cell content which consisted of a mechanical stirrer and a magnet,
- Temperature control equipment which consisted of a double walled bath and an immersion type heater fitted to a circulation pump,
- Evacuation equipment which consisted of a vacuum pump, a heavy walled filter flask.

Figure 5-1 provides a schematic diagram of the experimental vapour pressure apparatus that was constructed and modified in a thermodynamics measurement laboratory.

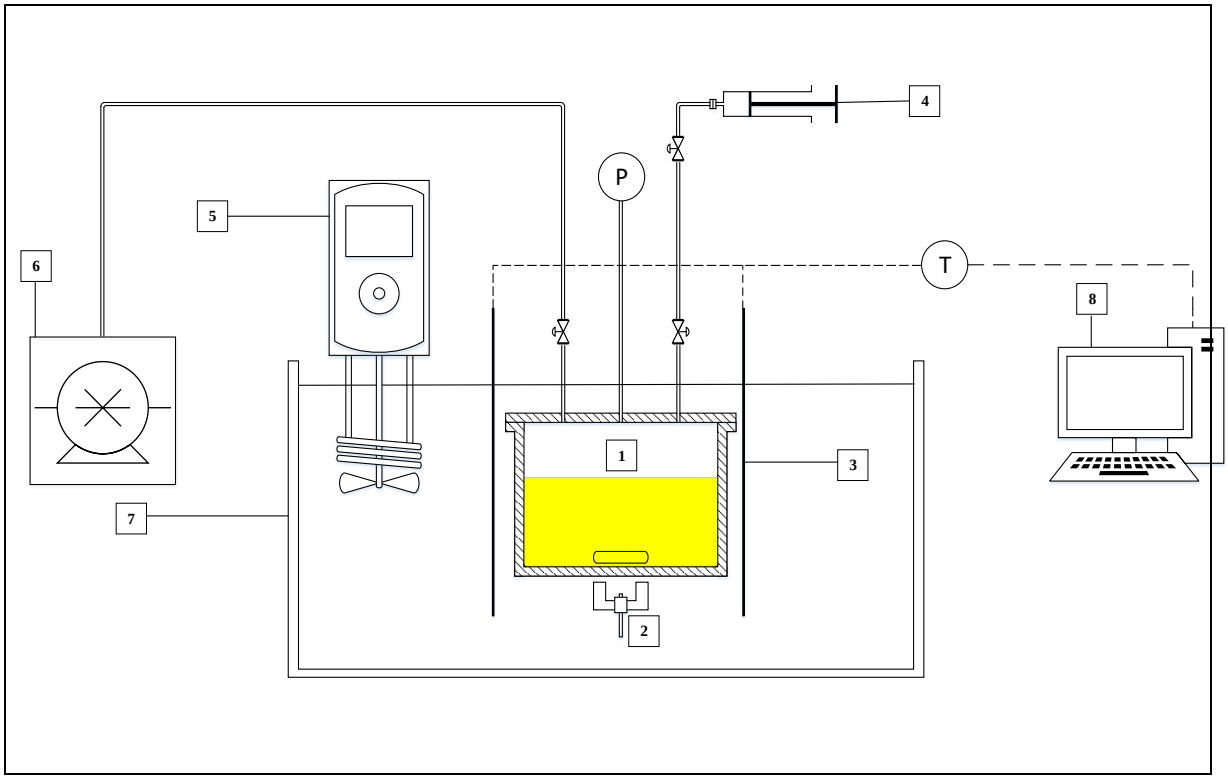

Figure 5-1: Schematic diagram of the experimental vapour pressure apparatus

(1) Equilibrium cell (2) Magnetic stirrer, (3) Temperature sensor (4) Piston pump (5) Heater Stirrer (6) vacuum pump (7) Water bath (8) Computer

Equilibrium Cell

The equilibrium cell was where the urine solution to be investigated is charged and allowed to reach thermodynamic equilibrium. The cell was machined from 316 stainless steel. It was cylindrical in shape and had a round bottom contour to eliminate stagnant zones. The lid of the cell had three valve fittings for connecting the pressure transducer, the vacuum system and the steel piston pump for charging the sample solution.

Pressure and Temperature measuring devices

The pressure in the equilibrium cell was measured using a WIKA transmitter model D-100-P. The transducer had a measuring up to 100 kPa absolute and an accuracy of less than 0.1kPa. The output signal from the transducer was transmitted to a PC via a RS232 port.

The temperature of the system was measured using two platinum resistance thermometers (Pt - 100). The accuracy of the measured temperature was estimated to be within 0.005 K (Reddy, 2006). The equilibrium temperature was measured by monitoring the temperature of the oil bath in which the equilibrium cell was immersed, by placing the probes in closed vicinity to the cell.

Agitating equipment

The content in the equilibrium cell was continuously agitated using a magnetic stirrer. A 12 mm stirring bar was placed inside the equilibrium cell and stirring was achieved by rotating the external magnetic stirrer, placed about 20 mm beneath the equilibrium cell, which caused the bar to rotate due to induced magnetic coupling. The magnetic stirrer was coupled to a mechanical stirrer (Heidolph RZR 2041 model) using a sprocket and a roller chain.

Thermostatic oil bath

The temperature of the system was controlled using a thermostated water bath which consisted of a double walled liquid bath, and an immersion type water heater (FMH instrument-model TRE) fitted with a circulation pump. The inner chamber was made of stainless steel and the outer body made of mild steel. The investigation temperature ranged between 60 ˚C to 100 ˚C and silicone oil was used as the liquid bath. Polystyrene material was used to cover the top of the bath to reduce thermal gradients between the top and bottom of the bath temperatures.

Evacuating Equipment

A vacuum pump was used to evacuate the cell prior to charging the sample solutions. The vacuum pump was also used for degassing the aqueous solutions before measurements. A heavy-walled filter flask was connected to the inlet of the vacuum pump to ensure no fluids were carried over to the pump.

5.2.2 Density

The density of the solutions were measured using an Anton Parr DMA 5000 densimeter that uses the vibration principle. Density measurements were given at an accuracy of 0.000005 g/cm^3 and a repeatability of 0.00001 g/cm^3. The temperature was measured using a high precision platinum thermometer with an accuracy of 0.01 °C. Figure 5-2 shows the vibrating-tube Anton Parr densimeter.

The vibrating tube densimeter consisted of a U-shaped, hollow, glass-walled tube. The tube was filled with the sample liquid and was agitated by an electromagnetic field created by an assembly of electromagnets and a wire coil. The tube vibrated perpendicular to its plane in the electromagnetic field at a characteristic frequency that was inversely proportional to the density of the filled-in sample.

Figure 5-2: Anton Parr DMA 5000 densimeter.

The vibrating tube was placed in a temperature-controlled environment to allow measurements to be made at stable temperature conditions. Uncertainties in the measurement of densities using vibrating tubes were in the order of 0.01%; and they could measure densities at temperatures up to 773 K and pressures up to 50MPa.

5.2.3 Electrical Conductivity

Figure 5-3 is a schematic of the apparatus used for measuring the conductivity of the urine solutions at varying temperatures: a YSI 3200 conductivity meter with an optimal range of up to 500mS. Measurement readings from this equipment are based on ratiometric resistance measurements where an unknown conductance and a known conductance were placed in series with an AC voltage source. The voltage across each conductance was measured and the unknown conductance was computed.

A YSI 3253 dipstyle conductivity cell with a wide conductivity range of 0.5 to 1000 $mS.cm^{-1}$ was used. The probe had a cell constant of 1.0 cm^{-1}, and an internal chamber diameter and depth of 10 mm and 20 mm, respectively. The cell had an inbuilt temperature sensor made of sintered metallic oxide whose resistance varied with temperature. Temperature calculation from resistance and compensation functions to the reference temperature was performed by the built in software in the 3200 model.

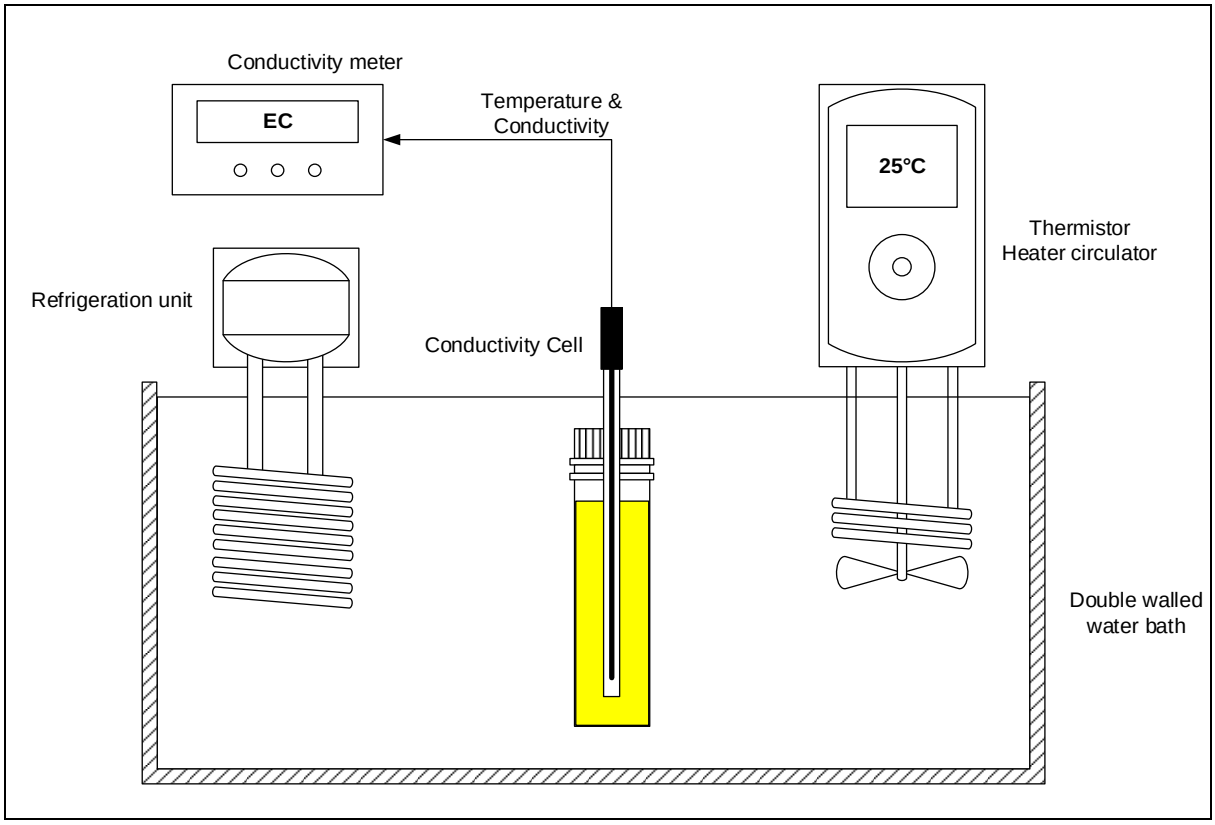

Figure 5-3: Apparatus for measuring the Electrical conductivity

The platinum, black coating on the cell was resistant to contamination and therefore ensured a more effective surface area for conductivity measurements. The temperature of the urine solutions was controlled using a thermostatic water bath that consisted of a double walled water bath, a refrigeration unit and an immersion type water heater (FMH instrument-model TRE) fitted with a circulation pump. The inner chamber was made of stainless steel and the outer body made of mild steel.

5.3 PROCEDURES

5.3.1 Vapour Pressure

Accurate vapour pressure measurements required the correct preparation and operation of the experimental apparatus. Preparation of the apparatus involved performing leak tests, cleaning the equilibrium cell, and calibrating the temperature and pressure sensors.

5.3.1.1 Leak Test

The equilibrium cell was tested for leaks by pressurizing the cell with nitrogen gas to approximately 15 bars. The pressure reading was monitored for any drop and a soap solution (Snoop ®) was apply on the joints and fittings to detect any leaks. Leaks were identified by the bubbling of the soap solution.

In order to identify leaks on the entire apparatus, all valves were shut, the system was evacuated and the valves were systematically opened moving away from the cell. A loss in pressure after opening a specific valve indicated a leak in the line after it. The leak was located by applying acetone onto the suspect joints, which would produce a sudden decrease and rise in pressure within the cell. The leaks were removed by either tightening the fittings or replacing them where they were damaged.

5.3.1.2 Cleaning the Equilibrium Cell

Before cleaning, the cell was detached from the assembly, and the content was drained using the evacuation valve on the lid. The cell was then flushed with acetone several times before fitting it back on to the apparatus, and lowered it into the oil bath. Acetone was charged into the cell and heated to approximately 60 ˚C under a vacuum, in order to clean entirely the lines and fittings from the cell to the vacuum pump. The cell was removed from the oil bath and allowed to cool. After cleaning, the cell was evacuated and isolated for a few hours while monitoring the pressure to ensure that all the acetone was removed.

5.3.1.3 Pressure and Temperature calibration

The pressure transmitter was calibrated from a standard pressure transducer (model CPC 3000, WIKA) with certified accuracy of less than 0.025 %. A vacuum pump was used to vary the pressure between 0 – 100 kPa in increments of 5 units, and the pressure readings from the transmitters were noted. This process was performed four times in order to ascertain the accuracy and repeatability of the calibration procedure.

The Pt-100 temperature sensors were calibrated using a standard reference probe (Pt-100 resistance thermometer type) with a certified accuracy of ± 0.03 K connected to a handheld WIKA CTH 6500 unit. The sensors were immersed into a stirred WIKA 9100 micro calibration bath. The temperature of the oil bath was systematically increased by 10 units within a temperature range of 20 – 110 °C. Similarly, the process was repeated four times to ascertain accuracy and reproducibility.

Figure 5-4 shows the calibration plot for the temperature probes, and Figure 5-5 shows the calibration probes for the pressure transducers. The equations were obtained by performing a linear regression of the values measured by the experimental instruments and the standard instruments.

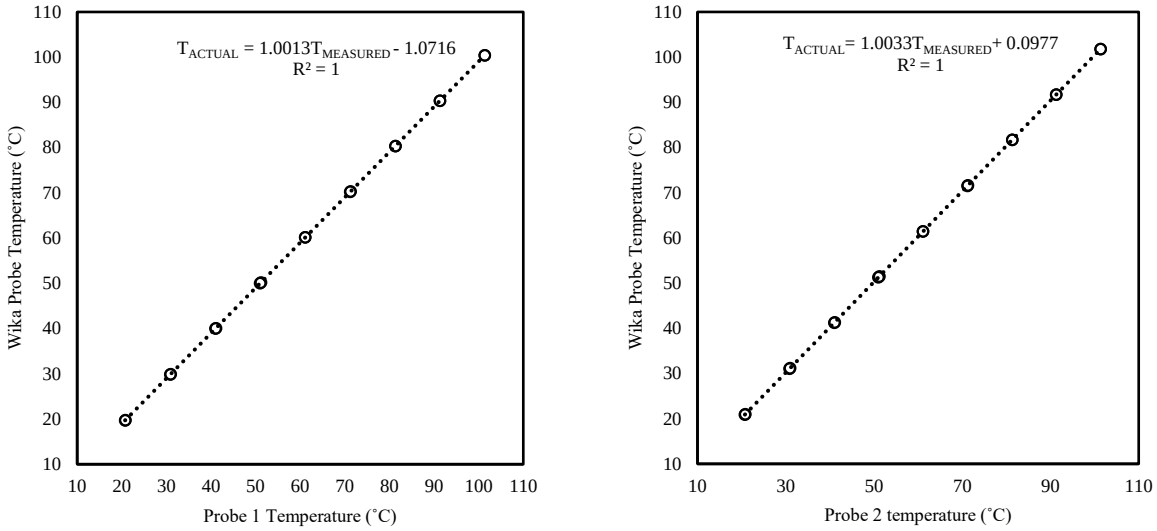

Figure 5-4: Calibration of the temperature probes

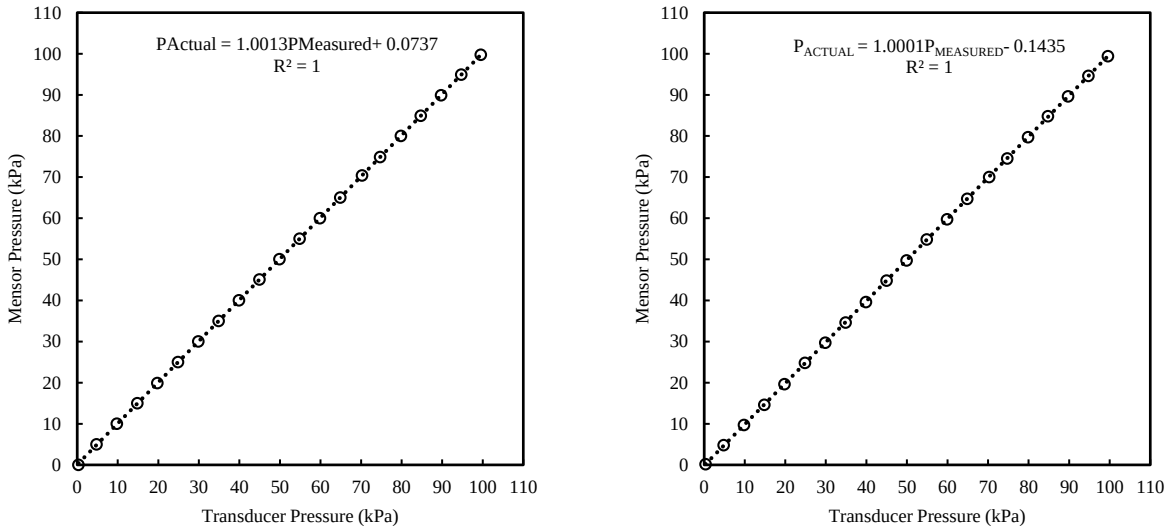

Figure 5-5: Calibration curve for the pressure transmitter 1

The uncertainty in the temperature measurements was calculated to be between ±0.04 ˚C and ±0.05 ˚C for sensors 1 and 2, respectively. The accuracy of the pressure measurements was estimated to be within ± 0.54 kPa and ±0 .55 kPa for transducers 1 and 2, respectively.

5.3.1.4 Degassing Procedure

Degassing of the aqueous solutions is essential for accurate measurements when using static methods. The aqueous solutions were degassed using a freeze and thaw method. The aqueous solutions were transferred into degassing bulbs and freezing was done by dipping the bulbs into liquid nitrogen. The gas was evacuated from the headspace of the frozen solution using a vacuum pump for 10 minutes. The solution was isolated and allowed to thaw. This procedure was repeated four times.

5.3.1.5 Vapour Pressure –Temperature measurements

Before loading the solution, the equilibrium cell was evacuated and isolated. The solution was loaded into the cell using a piston pump. The cell was then submerged into the oil bath and the required temperature was set. The mechanical stirrer was switched on in order to commence stirring of the cell content. Pressure readings were taken after temperature equilibration was obtained. The vapour pressure of the urine solutions was measured between 323 and 373 K.

5.3.2 Density

The accuracy of the vibrating tube densimeters is limited by the calibration procedure and the selection of calibrating fluids. This problem can be resolved by using reference liquids with a wide density range (Wagner and Kleinrahm, 2004). The instrument was calibrated using distilled water and air at 25 °C, whose densities were 0.999044 g/cm^3 and 0.001185 g/cm^3, respectively. The values were extracted from CRC tables.

Firstly, the U tube was flushed using distilled water, and cleaned with acetone. The tube was then dried by pumping air through it for 2 minutes. Using a syringe, the tube was filled with the sample liquid; and there could not be bubbles in the tube. The temperature was set to the required value and the densimeter had an allowed time to equilibrate before density measurements could be taken. To ensure reproducibility, the same procedure was undertaken three times for the same liquid sample.

5.3.3 Electrical Conductivity

5.3.3.1 Calibration

The YSI 3200 electrical conductivity meter can be calibrated using two methods, which include:

1. Directly entering either the manufacturer's stated or a manually calculated cell constant;
2. Allowing the conductivity meter to calculate the cell constant using standard conductivity solutions.

The YSI 3200 conductivity model was calibrated using the second method, at 5 points using potassium chloride (KCl) standard solutions. The calculated cell constants were stored in a non-volatile memory in the YSI 3200 conductivity model. Table 5-2 shows the certified potassium chloride solutions used to calibrate the cell.

Table 5-2: KCl solutions used for calibrating the conductivity meter extracted from Covington (1986)

Concentration (mol/kg)	Conductivity (mS/cm)
0.010	1.413
0.100	12.90
1.000	111.8
2.337	197.8
4.415	299.6

Prior to calibration, A YSI 3253 dipstyle conductivity cell was cleaned by placing it in acetone for 30 minutes, and allowing it to stand in distilled water overnight. Drying was done using compressed air. The cell and the container for the sample were first rinsed 2 times with the standard solution before calibration was undertaken. After rinsing, the cell was immersed carefully into the KCl standard solution in order to avoid trapping air bubbles in the probe. Any trapped air was removed by gently tapping the cell. The KCl solution was then submerged in the water bath thermostated at 298 K, and time was allowed for it to equilibrate before storing the calculated cell constant in the conductivity meter. This procedure was repeated using the KCl standard solutions in Table 5-2.

5.3.3.2 Procedure

Prior to measurements, the sample container and the YSI 3253 cell were cleaned as described in the procedure above and then rinsed with the sample solution to be measured. The sample container was completely filled with the urine solution and care was taken not to allow any vapour space above the liquid surface. The temperature of the water bath was set to the desired temperature and the reference temperature on the conductivity meter was adjusted accordingly. Temperatures investigated for

conductivity measurements were from 293 – 333 Kin increments of 5 K. The urine solution was given time to thermally equilibrate before the conductivity reading was measured. To check for reproducibility, the conductivity measurements were repeated three times.

5.4 UNCERTAINTIES AND ERROR ANALYSIS

5.4.1 Error Analysis

Error is different from uncertainty in that it is defined as the difference between the measured value and the 'true value' of the property being measured (Bell, 1999). For the purposes of this project, the difference between the measured value and the calculated value will be referred to as the relative error/deviation.

The following equations were used for the error analysis in calculating the relative deviation, absolute average deviation, and bias:

$$\Delta(\%) = \frac{\chi_{exp} - \chi_{calc}}{\chi_{exp}} \times 100\% \tag{5.1}$$

$$AAD(\%) = \frac{100}{N}\sum_{i=1}^{N}|\Delta| \tag{5.2}$$

$$Bias(\%) = \frac{100}{N}\sum_{i=1}^{N}(\Delta) \tag{5.3}$$

where Δ is the relative deviation; AAD is the absolute average deviation; and χ is the measured property.

5.4.2 Uncertainty in measurement

Uncertainty is defined as the magnitude of doubt that exists as a result of any measurement (Bell, 1999). In order to quantify the overall uncertainty in any measurement, all the individual contributing sources have to be identified. Sources of uncertainty include; bias, wear, aging and drift in the measuring instrument, operator skill, calibration of the instrument and environmental conditions, such as, temperature, pressure humidity etc. The combined standard uncertainty (u_c) is calculated by taking the square root of the sum of the squared uncertainties (u_i):

$$u_c = \pm\sqrt{\sum_i u_i^2} \tag{5.4}$$

The quantifiable sources considered in this work include uncertainties in

- Calibration
- Resolution (size of the divisions on the instrument) and
- Manufacturer's specifications

The maximum calibration uncertainty is assumed to be 0.1% of the reading. The uncertainty is randomly distribution and hence the uncertainty is divided by 2 as shown by equation (5.5)

$$u_{calibration} = \frac{1}{2} \times 0.1\% \times measurement \tag{5.5}$$

The resolution uncertainty is considered to be uniformly distributed between the upper and the lower limit of the smallest division on the instrument. The uncertainty is calculated using equation (5.6)

$$u_{resolution} = \frac{1}{2} \times \frac{smallest\ interval}{\sqrt{3}} \tag{5.6}$$

5.5 CHAPTER SUMMARY

The preparation procedure of the synthetic urine and its concentrates, based on the hydrolysed urine composition in **Chapter 2** is outlined. Nine urine solutions were prepared with concentrations ranging from 4.5 to 32.2 wt%. The specific equipment used, shown in Table 5-3 and the operating procedures is described in detail. In conclusion, the equations for calculating uncertainty and errors are given.

Table 5-3: Equipment used measuring the thermophysical properties of hydrolysed urine

Property	Equipment
Vapour Pressure and Osmotic pressure	Static apparatus based on (Salavera et al., 2005) with D-100-P pressure transducer and Pt-100 platinum resistance thermometers
Density	Anton Parr DMA 5000 densimeter a high precision platinum thermometer
Electrical Conductivity	YSI 3200 conductivity meter with a YSI 3253 dipstyle conductivity cell

6 . EXPERIMENTAL RESULTS

The results for all experimental work are presented in this chapter. The measured properties include vapour pressure, density and electrical conductivity. Osmotic pressure was calculated from the vapour pressure data using equation (3.19).

But, prior to gathering experimental data on urine solutions, the accuracy and suitability of experimental procedures and equipment were verified by performing measurements on test solutions. Sodium chloride (NaCl) was selected as a test solution, based on the extensive availability of data in literature, at a wide range of temperatures and concentrations.

After verifying the measurement methods, the physical properties of urine solutions were measured at varying temperatures and concentrations.

6.1 SODIUM CHLORIDE TEST SOLUTIONS

Vapour pressure, density and electrical conductivity measurements of NaCl solutions were performed and compared to literature data in order to test the suitability and accuracy of the experimental procedure and equipment. Figure 6-1 to Figure 6-3 show the comparison between the experimental and literature data.

The vapour pressure of the sodium chloride solution was measured for temperatures between 333 K and 373 K for the following concentrations 0.1, 0.5 and 2.0 wt%. The experimental data was compared to data presented by Clarke and Glew (1985). Since the experimental and the literature data were not presented at precisely the same temperature values, to evaluate and compare them at the exact temperature values recorded in the experiments, the literature data was fitted into the Antoine equation. The regression constants (A, B and C) for the Antoine's equation, and the error analysis for the literature data are presented in Appendix G. Comparison of the experimental and literature data were in good agreement with an percentage average error of 0.66% for the 1 wt% solution, 0.72% for the 5 wt% solution and 0.71% for the 20 wt% solution. Table 6-1 shows the statistical error analysis of the experimental and literature data where the maximum deviations recorded were 1.08%, 1.24% and 1.36%. These large discrepancies in the error were obtained at high vapour pressures. The range between the minimum and maximum errors for each solution was less than 1.09%. Based on the above results, the technique and equipment were deemed to be suitable for the accurate and reliable measurement of vapour pressure.

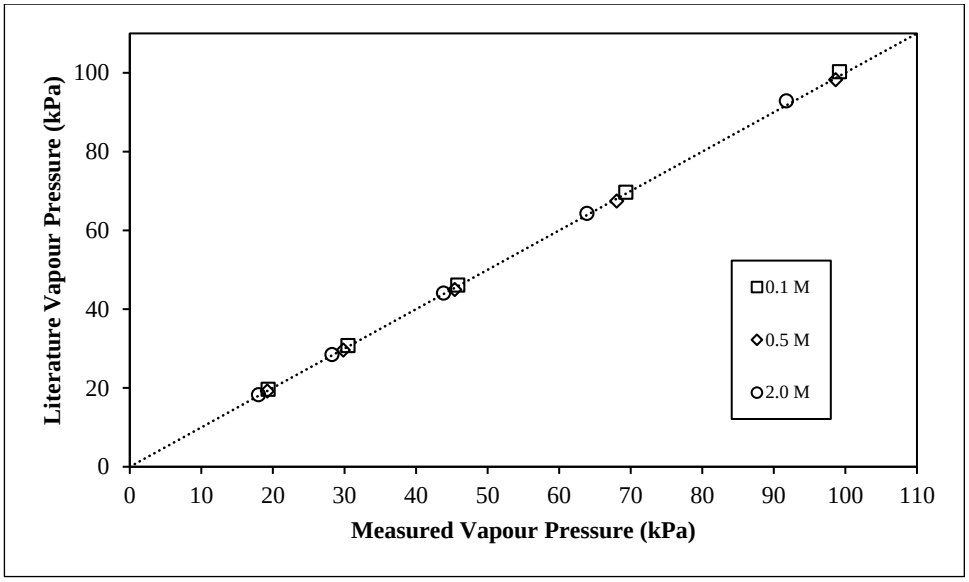

Figure 6-1: Comparison between the measured and literature vapour pressures for NaCl solutions

The density of the sodium chloride solution was measured for a temperature range of 293 – 333 K for the following concentrations. 2 wt%, 6 wt% and 12wt %. Figure 6-2 shows the comparison between experimental and literature densities. Data for the density of sodium chloride solutions at varying concentrations and temperature were extracted from Zaytsev et al (1992). Comparison between the measured and the published data showed excellent agreement. The average absolute error for the 2 wt %, 6 wt %, and 12 wt % solutions were 0.003%. 0.004% and 0.007%. This is mainly because density measurement is relatively easy and repeatable. The maximum deviation obtained in the density measurements was ±0.006%. This confirmed the ability of the Anton Parr DMA 5000 to make high precision measurements at temperatures controlled to ±0.01°C.

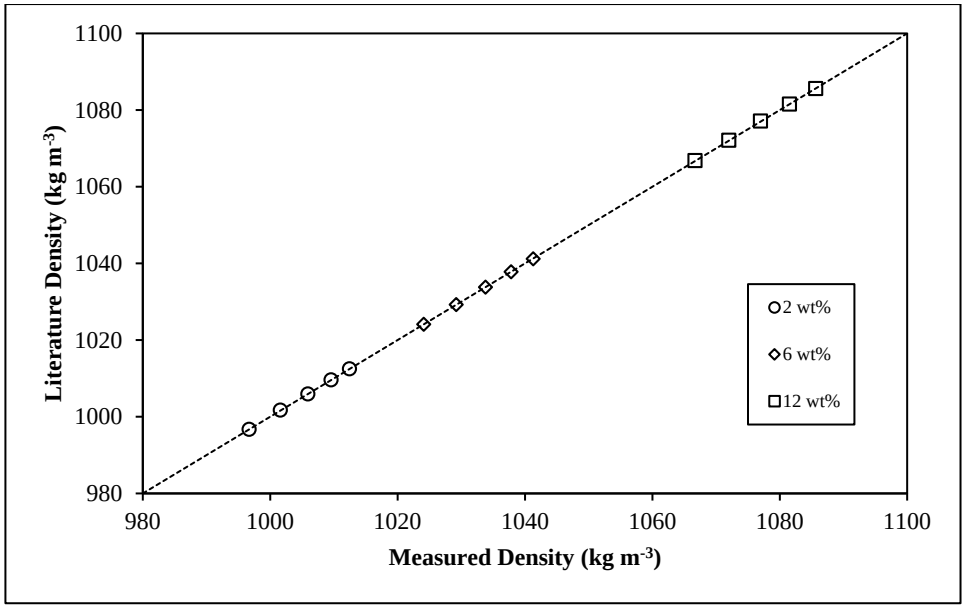

Figure 6-2: Comparison between the measured and literature density data for NaCl solutions

The measured electrical conductivity of 0.1, 1.0 and 5.0 wt% aqueous NaCl solutions were compared to conductivities correlated by McCleskey (2011) for temperatures ranging from 293 to 333 K. The empirical equations expressed the electrical conductivity as a function of temperature and molality using an equation in a form suggested by Lattey (1927). A comparison between the conductivities predicted by the Lattey equation and the measured values showed reasonable accuracy with a maximum percent error of 1.70% for all measurements. Table 6-3 shows the difference between the experimental and literature data. Large discrepancies were observed for low concentrations of sodium chloride solutions.

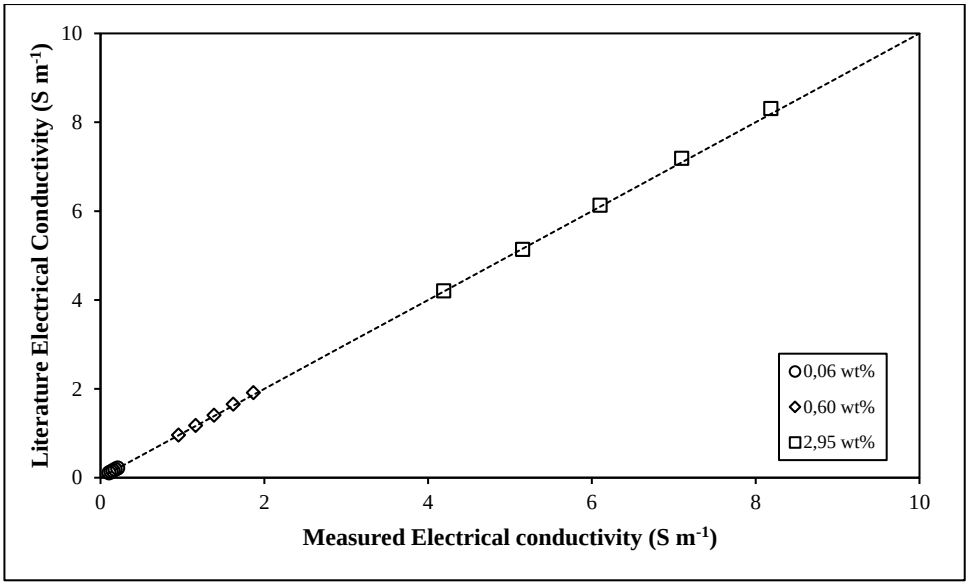

Figure 6-3: Comparison between the measured and literature conductivity data for NaCl solutions

Tables 6.1 to 6.4 summarises the comparison of the measured data and the data in literature. The tables outline the average, maximum, standard deviation of the error as well as the root mean square of the data. The experimental data obtained for the NaCl solutions were comparable with the data in literature. Hence the equipment was deemed suitable for measuring the thermophysical properties of hydrolysed urine.

Table 6-1: Analysis of the error between the experimental and literature vapour pressure data

Concentration, (wt %)	Average (%)	Std.Dev (%)	Maximum, (%)	RMS (kg m^{-3})
0.1	0.652	0.357	1.221	0.607
0.5	0.720	0.344	1.083	0.299
2.0	0.712	0.424	1.357	0.624

Table 6-2: Analysis of the error between the experimental and literature density data

Concentration, (wt %)	Average (%)	Std.Dev (%)	Maximum, (%)	RMS (kg m^{-3})
2	0.003	0.003	0.008	0.038
6	0.004	0.003	0.009	0.048
12	0.007	0.007	0.006	0.017

Table 6-3: Analysis of the error between the experimental and literature conductivity data

Concentration, wt %	Average (%)	Std.Dev (%)	Maximum, (%)	RMS ($S\ m^{-1}$)
0.1	1.627	1.138	3.057	0.003
1.0	1.685	0.741	2.672	0.030
5.0	0.767	0.553	1.466	0.069

6.2 URINE SOLUTIONS

The vapour pressure, osmotic pressure, density and electrical conductivity of the urine solutions were measured for a concentration range of 4.5 wt% to 32.2 wt %. The tabulated data for the urine properties is presented in Appendix D.

6.2.1 Vapour Pressure and Osmotic Pressure

The vapour pressure of the urine solutions was measured at 333 K - 373 K. Osmotic pressure data was calculated from vapour pressure using equation (3.19) Figure 6-4 shows the vapour pressure data for the urine solutions at varying temperatures. The vapour pressure ranged from 14.5 kPa to 99.5 kPa. The vapour pressure increased with temperature but decreased with concentration. The drop in vapour pressure with concentration is a result of boiling point elevation. During the experiment, it was noted that the equilibration time taken to get a vapour pressure reading decreased with increasing concentrations. It took approximately 2 h to get a vapour pressure value for the 32.2 wt% solution and it took about 4 h for the 4.5 wt% solution. The experimental data are reported with a calculated standard error of 0.01 kPa for vapour pressure and 0.02 MPa for osmotic pressure. Temperature was controlled at an accuracy of 0.02 K.

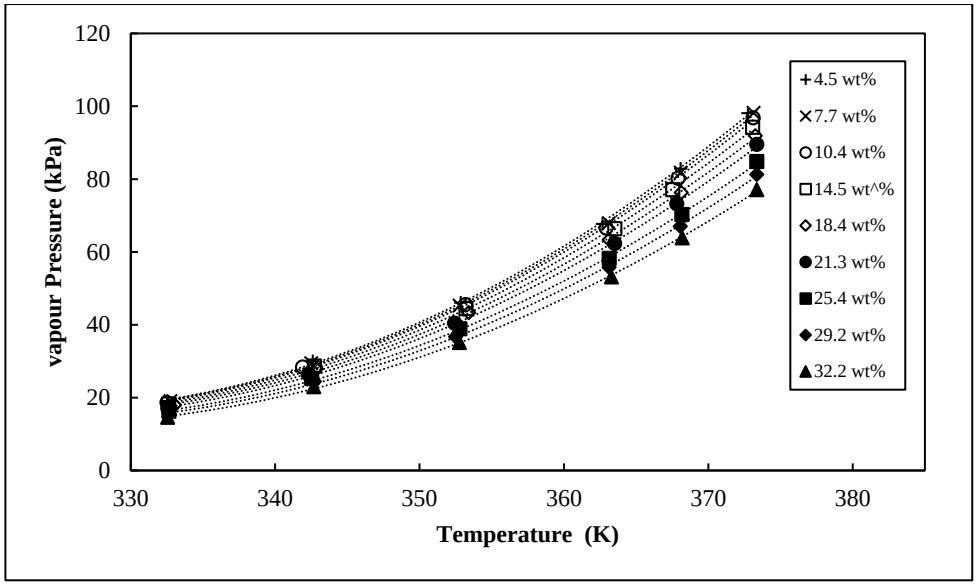

Figure 6-4: Variations in urine vapour pressure with temperature and concentration

Figure 6-5 shows the variation of the osmotic pressure with concentration and temperature which ranged from 2.50 MPa to 46.30 MPa. The osmotic pressure data showed a trend opposite to that of vapour pressure. The osmotic pressure increases with concentration and a decrease with temperature. The osmotic pressure increases with both concentration and temperature. Osmotic pressure is a colligative property which relies on the number of particles in the solution, and this explains the linear relation between osmotic pressure and concentration.

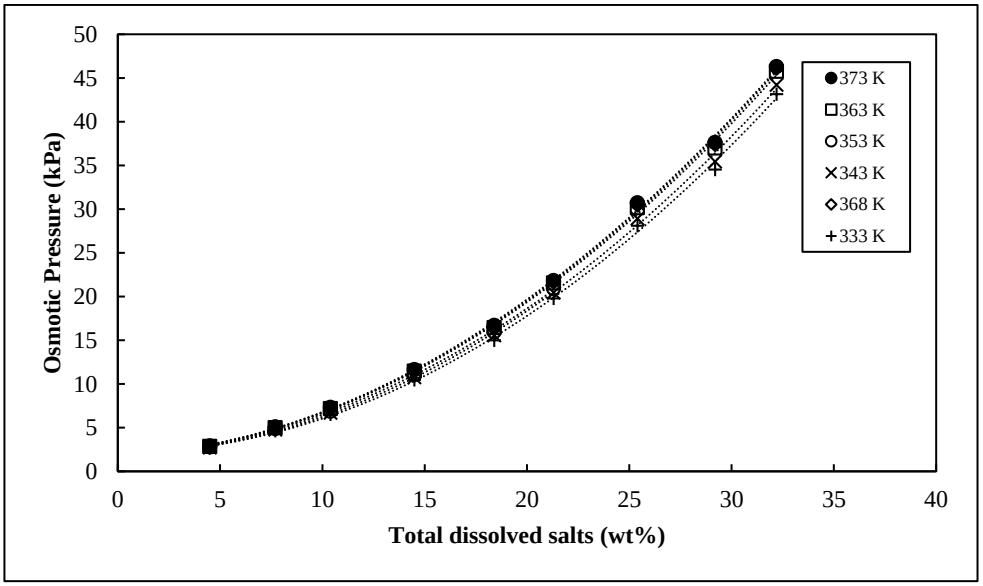

Figure 6-5: Variations in urine osmotic pressure with temperature and concentration

6.2.2 Density

Density measurements for the urine solutions were performed for a temperature of 293.15 K – 333.15 K in 5 K increments. Temperatures during measurement were controlled at ±0.01K. Figure 6-6 shows the variation of the density with temperature and concentration. The experimental data ranged from 1025.5 – 1173.7 kg m^{-3}. The trend in the experimental data shows that the density of the hydrolysed urine, typically increases with concentration and decreased with temperature. The effect of temperature can be explained from the view of the molecular packing structures in liquids. When the temperature is increased, particle mobility and particle excitations is increased and this reduces the packing of molecules in a given structure and hence lowers the density

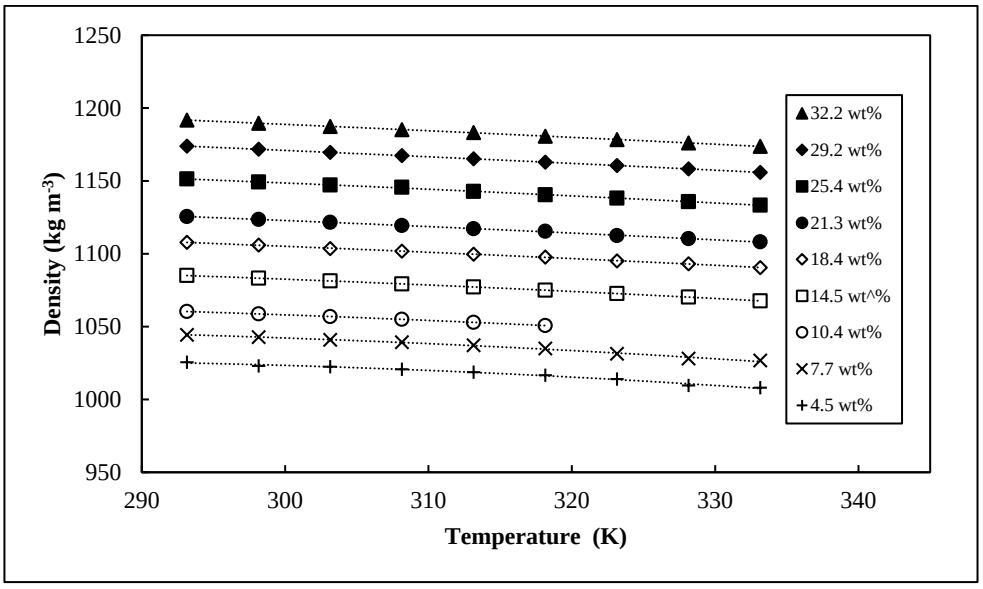

Figure 6-6: Variations in urine density with temperature and concentration

6.2.3 Electrical Conductivity

Figure 6-7 shows the variation of the electrical conductivity with concentration and temperature. Electrical conductivity measurements were made in increments of 5 K for temperature ranging from 293.15 – 333.15 K. Temperatures were maintained within ±0.01K during measurements. The electrical conductivity shows a linear relationship with both temperature and concentration, with values ranging between 5.40 – 41.01 S m^{-1}.

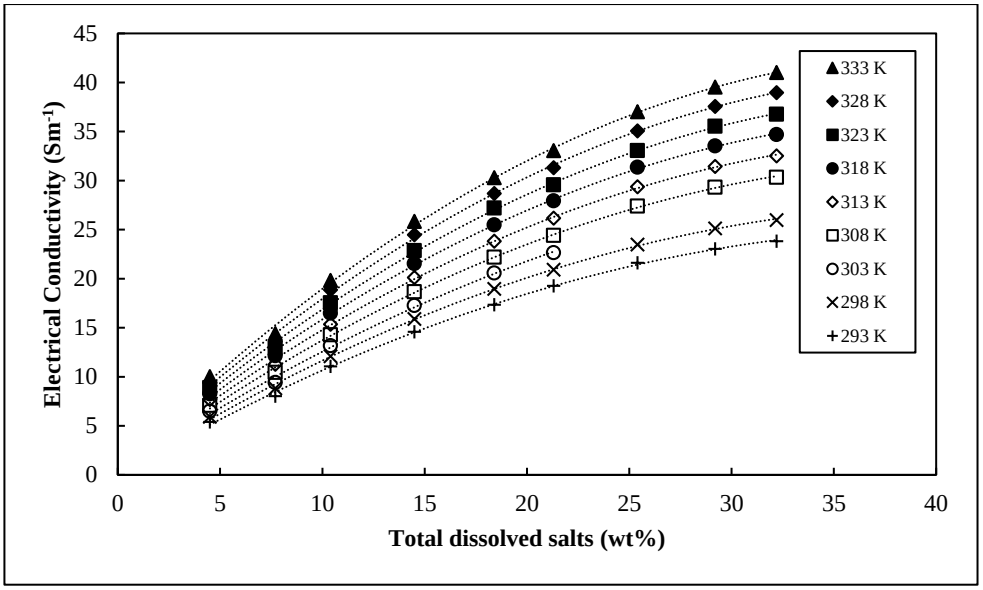

Figure 6-7: Variations in urine electrical conductivity with temperature and concentration

6.3 CHAPTER SUMMARY

In order to test the accuracy of the equipment prior to measuring the properties of hydrolysed urine, measurements for vapour pressure, density and electrical conductivity were performed. The measurements compared well with the data in literature as shown in Table 6-4

Table 6-4: Comparison between experimental and literature data for NaCl solutions

Property	Concentration range (wt%)	Temperature range (K)	Average error (%)	Standard Deviation (%)	Maximum error (%)	References
Vapour Pressure	0.1 - 2.0	333 - 373	0.695	0.375	1.220	(Clarke and Glew, 1985)
Density	2.0 – 12.0	293 - 333	0.005	0.005	0.007	(Zaytsev and Aseyev, 1992)
Electrical Conductivity	0.1 - 5.0	293 - 333	1.360	0.810	0.034	(McCleskey, 2011)

After the verification of the equipment and methodology, vapour pressure, osmotic pressure, density and electrical conductivity measurements were performed on synthetic hydrolysed urine solutions ranging in concentration from 4.5 to 32.2 wt%. The temperature range for vapour pressure and osmotic pressure measurements was 333 – 373 K while that for density and electrical conductivity was 293 – 333 K.

The thermophysical properties of hydrolysed urine sowed trends similar to multicomponent solutions like seawater and brines. Vapour Pressure increased with temperature but decreased concentration. Conversely, osmotic pressure decreased with temperature and increased with concentration. Density data increased with concentration but decreased with temperature. Electrical conductivity increased with both concentration and temperature.

7 DISCUSSION

This chapter applies the models selected in **Chapter 3** to the experimental results in Chapter 6. The first section discusses the correlative models while the second section discusses the thermodynamic models. The accuracy and the validity of both modeling techniques in calculating the thermophysical properties of urine, are presented and reviewed in both sections. The last section demonstrates how the experimental data and models are used to solve engineering problems which include the design of a multiple effect evaporator, mechanical vapour pressure compression evaporator and forward osmosis and reverse osmosis processes.

7.1 CORRELATIVE MODELS

The experimental data for the thermophysical properties of urine in Chapter 6 were fitted into correlative models as functions of temperature and concentration using the method of least squares. The equations are valid for a temperature range of 333K to 373K for vapour pressure and osmotic pressure and 293K to 333K for density and electrical conductivity. The concentration of the urine solutions was based on the total dissolved solids (TDS) and it ranged from 4.5 – 32.2 wt% for all properties.

7.1.1 Equations

Table 7-1 shows the correlative models used to fit the thermophysical properties of hydrolysed urine. These models were based on polynomial functions, as they are computationally easy to use with good accuracy. Various orders of the polynomials were tested by evaluating objectively the error between the experimental data and the calculated results, and it was observed that suitable accuracy was achieved without exceeding 3rd order polynomials. Vapour pressure data was correlated using an extended form of the Antoine equation (7.1) and osmotic pressure data was fitted into a second order polynomial (7.2). The density for pure water used with the urine density equation (7.3) was calculated using equation (7.4) which has a maximum deviation of ± 0.01 % from the IAPWS-95. In order to improve the accuracy of the electrical conductivity equation, an intercept of zero was chosen, resulting in a truncated polynomial.

Table 7-1 shows the correlative equations, with their respective regression coefficients, for the thermophysical properties. The detailed regression calculations for the correlation equations are presented in **Appendix E.**

Table 7-1: Correlative models for calculating the properties of urine

Correlation	Eqn
Vapour Pressure (kPa)	
$log_{10} P = A - \frac{B}{T} + \frac{C}{T^2}$	(7.1)
Validity Range: 333 K < T < 373 K; 0.045≤ X≤ 0.322	
$A = 6.998 - 0.0013X - 3.682 \times 10^{-5} X^2 - 5.03 \times 10^{6} X^3$	
$B = -573.68 + 0.6706X - 0.0709X^2 - 0.00263X^3$	
$C = -108438 - 142.8X + 19.12X^2 - 0.246X^3$	
Osmotic Pressure (MPa)	
$\pi = A + BX + CX^2$	(7.2)
Validity Range: 333 K < T < 373 K; 0.045≤ X≤ 0.322	
$A = -220.39 + 1.1908T - 0.0054T^2 - 5.03 \times 10^{-6} T^3$	
$B = 7973.5 - 68.189T + 0.1935T^2 - 0.0002T^3$	
$C = -25080 + 213.8T - 0.5978T^2 + 0.0006T^3$	
Density (kg m^{-3})	
$\rho - \rho_{H_2O} = A - BT - CT^2$	(7.3)
Validity Range:293 K < T < 333 K; 0.045≤ X≤ 0.322	
$A = 3.943 - 0.431X - 0.0100X^2 - 2.179^4 X^3$	
$B = 2.503 + X + 0.213X - 0.009X^2 1.09X^3$	
$C = -108438 - 0.006X + 2.604X^2 - 3.185X^3$	
$\rho_{H_2O} = \sum_{i=0}^{4} a_i T^i$,	(7.4)
Validity Range:273 K < T < 453 K;	
where $a_0 = 999.9$, $a_1 = 0.2034$, $a_2 = -0.006162$, $a_3 = 0.00002261$, $a_4 = -0.00000004657$	
Electrical Conductivity (S m^{-1})	
$\kappa = AX - BX^2 - CX^3$	(7.5)
Validity Range: 293 K < T < 333 K; 0.045≤ X≤ 0.322	
$A = 641.2 + 28.3T$	
$B = 95.3 - 74.6T$	
$C = 1903 + 87.8T$	

7.1.2 Comparison with experimental data

The thermophysical properties calculated by the equations (7.1) to (7.5) were compared with the experimental data. Table 7-3 outlines the analysis of the percent error for each property which includes; the average error, standard deviation and maximum error. The variation of the percent error with temperature and concentration for each property is show in Figures 7-1 to 7- 5.

Figure 7-1 shows that the vapour pressure data calculated by the Antoine equation (7.1) are in good agreement with experimental data with the percent error varying within ±0.60%. This is because a plot of log P against 1/T for the urine solutions produced linear curves, as shown in Figure 7-2, which could be correlated by the second order polynomial form of the Antoine equation.

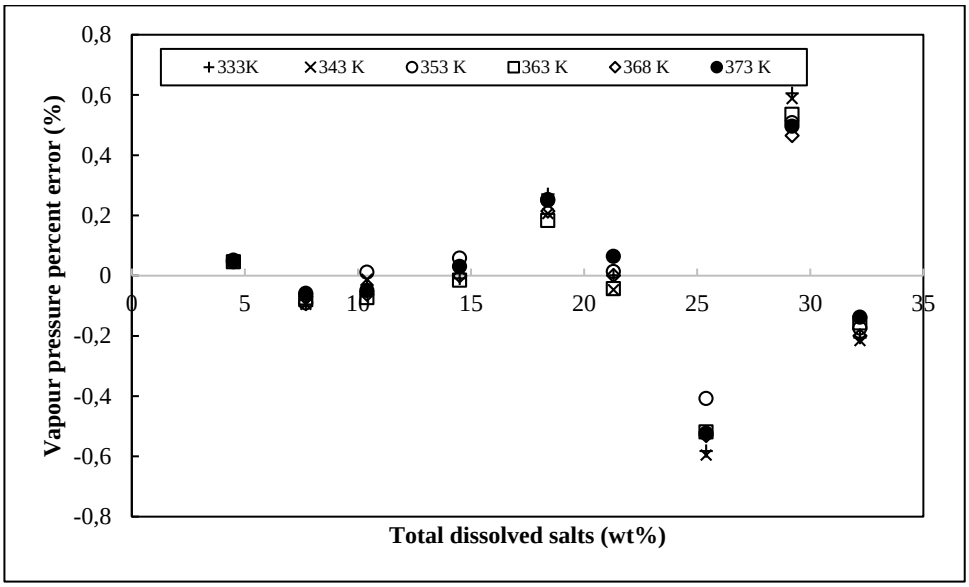

Figure 7-1: Variation of the vapour pressure error (%) with temperature and concentration

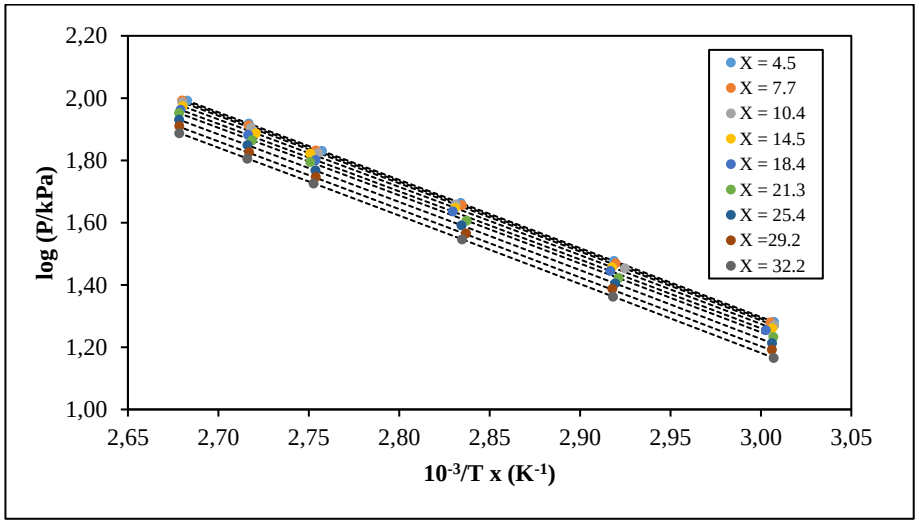

Figure 7-2: Plot of log P against 1/T for the hydrolysed urine

Since osmotic pressure was calculated from vapour pressure data, the data was adequately correlated using a second order polynomial with good accuracy, where the maximum deviation was less than 1.0% as shown in Figure 7-3.

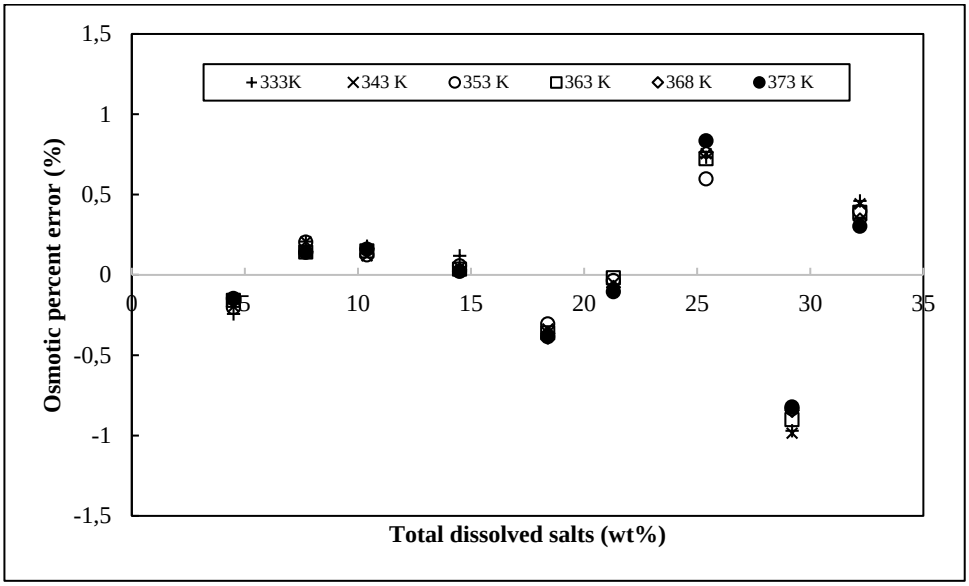

Figure 7-3 Variation of the osmotic pressure error (%) with temperature and concentration

As expected, the density data was excellently correlated using equation (7.3) and (7.4) because it is an easy parameter to measure repeatedly with sufficient accuracy. The percent error for density calculations were within ±0.15%, as shown in Figure 7-4.

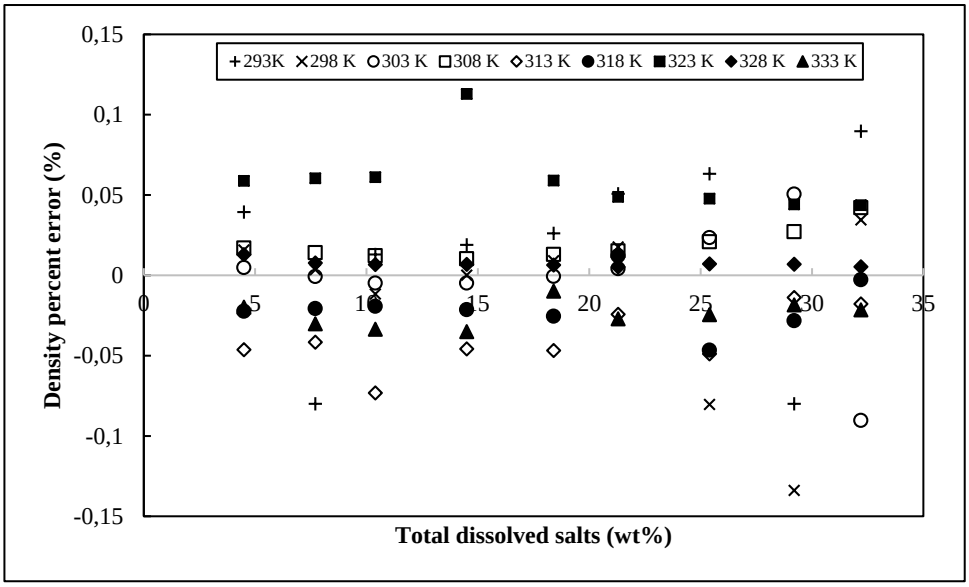

Figure 7-4 Variation of the density error (%) with temperature and concentration

Equation (7.5) calculates the electrical conductivity with reasonably accuracy. Deviations were within ±1.80% with a reported average of 0.43% with a standard deviation of 0.38%. A graphical plot of the percent error in Figure 7-5, shows larger deviations at low concentrations which decrease as the concentration decreases.

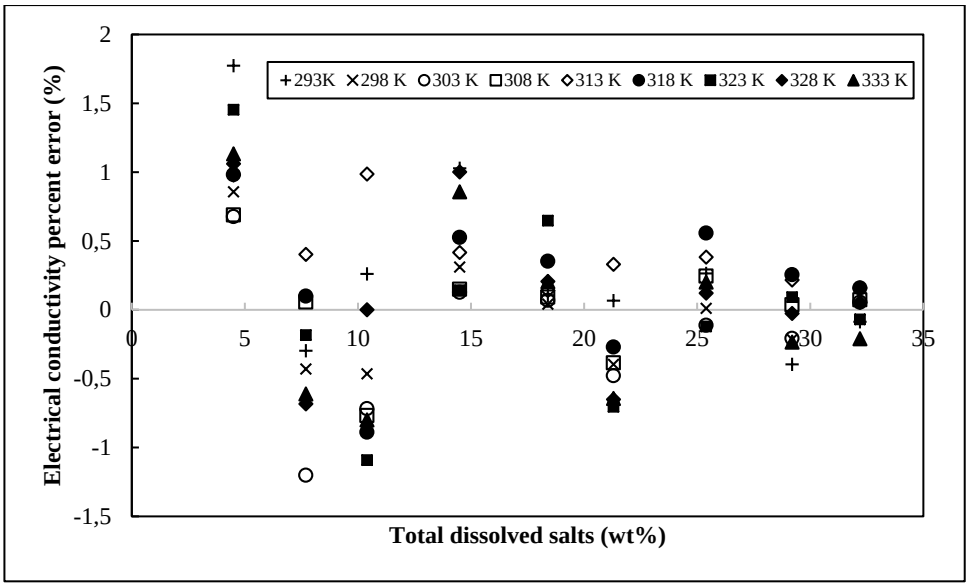

Figure 7-5 Variation of the electrical conductivity error (%) with temperature and concentration

7.2 THERMODYNAMIC MODELS

The results for the chemical speciation model and the thermodynamic models are discussed in detail.

7.2.1 Speciation of the urine solutions

The B-dot equation (extended Debye-Hückel model) was used to calculate the distribution and concentration of the species in the urine solutions for concentrations ranging from 4.5 to 32.2 wt% and at temperatures ranging from 293 to 333 K. PHREEQC 2.0 was used for the speciation calculations. The *PhreeqC.dat* database was selected for the simulation as it contains the required ion pairing reactions, thermodynamics data for calculating the activity coefficients and the parameters for the temperature dependence of the equilibrium constants. A sample speciation calculation is presented in **Appendix A.**

Figure 7-6 and Figure 7-7 shows the theoretical distribution and concentration of the species simulated by PHREEQC 2.0 for the urine solution and its concentrates. Model calculations show that the species exist as individual ions, ion pairs and neutral molecules. The dominant species in the urine solutions included the NH_4+, Cl-, $SO_4$2- and the $NH_4SO_4^-$. Generally the concentration of most ions increased with the total ionic strength of the urine solution, except for species like $NH_4SO_4^-$ and NH_3 whose concentration passes through a maximum. The thermodynamic calculations also show that the urine can be concentrated 10 times without any precipitation of the salts.

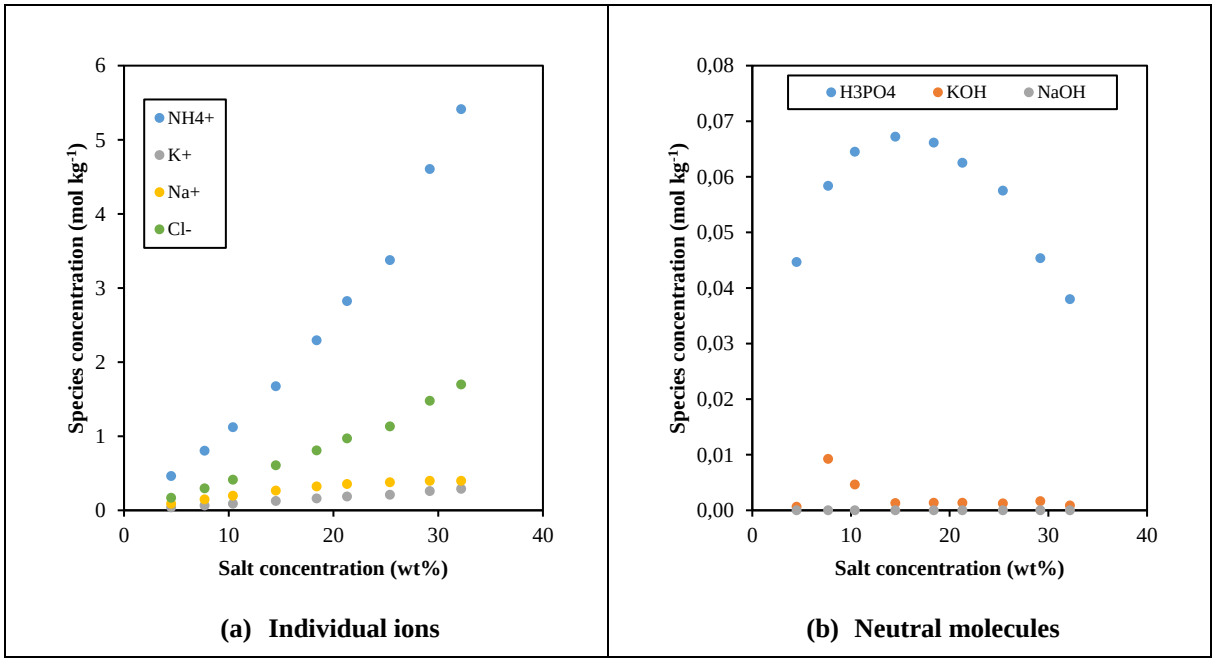

Figure 7-6: Speciation of individual ions and neutral molecules

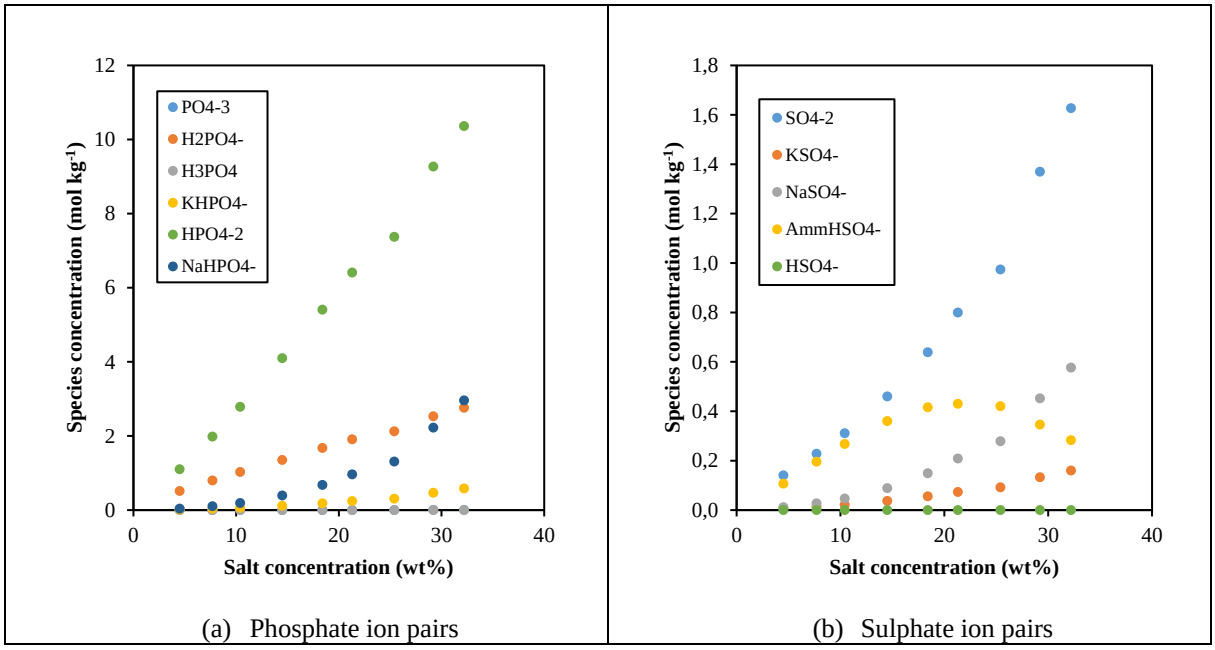

(a) Phosphate ion pairs (b) Sulphate ion pairs

Figure 7-7: Speciation of the ion pairs of phosphate and sulphate ions

7.2.2 Vapour Pressure and Osmotic Pressure

The vapour pressure and osmotic pressure were both calculated from the activity of water using equations (3.18) and (3.19) respectively. The activity of water was predicted using the expression developed by Brouckaert (1995) using the speciated data obtained from PHREEQC 2.0. Figure 7-8 and Figure 7-9 shows the variation of the error for the vapour pressure and osmotic pressure predicted by the thermodynamic equations. The calculations reveal that the prediction equation underestimates vapour pressure and overestimate osmotic pressure.

Graphical comparison of the experimental and calculated values shows two trends in the prediction of both vapour pressures and osmotic pressures. Very good predictions are observed at low concentrations up to 18 wt% salt concentration but beyond that the model predictions become increasingly inaccurate. Below 18 wt%, the average error was 0.30% and 0.46% for vapour pressure and osmotic pressure respectively. Above 18 wt%, the percent error increased progressively with the concentration to maximum deviations of 7.3% and 10.7% for vapour pressure and osmotic pressure predictions respectively.

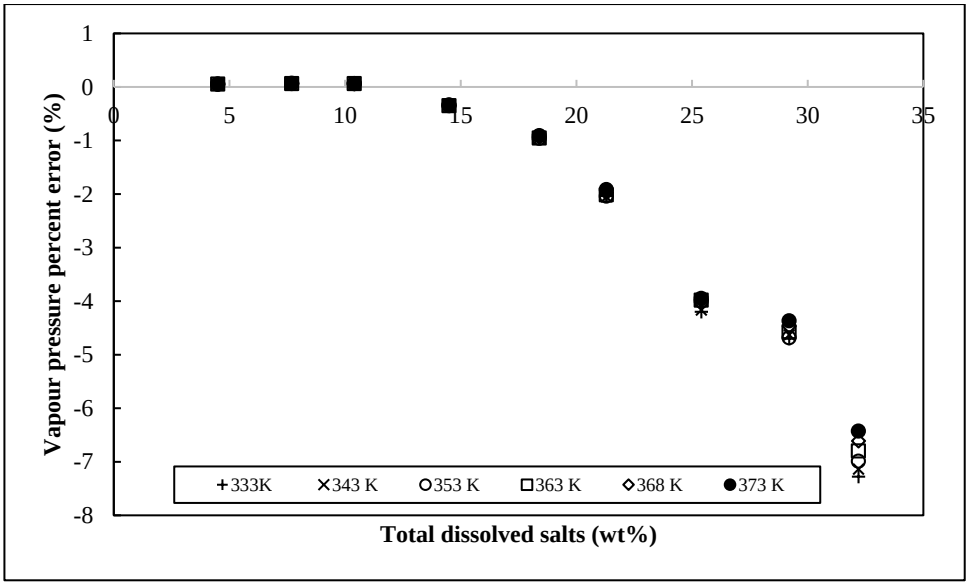

Figure 7-8: Comparison of the vapour pressure equation with the experimental data

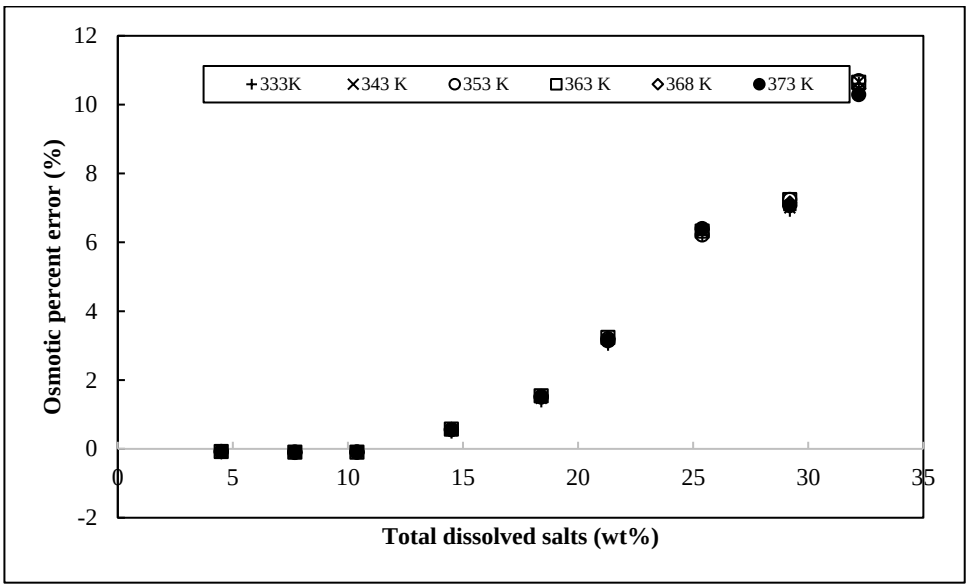

Figure 7-9: Comparison of the osmotic pressure equation with the experimental data

As discussed in **Chapter 3,** the extended Debye-Hückel produces fairly accurate results for low ionic strengths and the model disintegrates as the concentration increases above ionic strengths of 1.5 M. The salt weight of 14 wt% translates to an ionic strength of 3.0 M for urine solutions and this is the maximum concentration accurately predicted by the Davies equation for solutions contain sodium chloride. The model does not take into account the ion-ion interactions and the ion-solvent interactions that occur at very high concentrations.

7.2.3 Density

The initial step in calculating the density of the urine solutions was to calculate the molar volume of the single salts in urine from their density values. The densities of the single salts (NaCl, Na_2SO_4, NH_4Cl, $(NH_4)_2SO_4$, NaH_2PO_4) at varying temperatures and concentrations were extracted from Zaytsev (1992). Calculated molar volumes were fitted into the equation developed by Millero (1970). The constants for the equations are shown in **Appendix G** as well as the statistical analysis calculations which include the average percent error, standard deviation, and the maximum deviation. The analysis shows that the densities calculated using Millero's expression are in good agreement with the densities reported in literature. The maximum deviations for all salts were less than 1.0%. The density of the urine solutions was calculated using the additive rule, equation (3.25), by summing up the molar volumes of the salts.

Figure 7-10 shows the variation of the relative deviation of the densities with temperature and concentration.

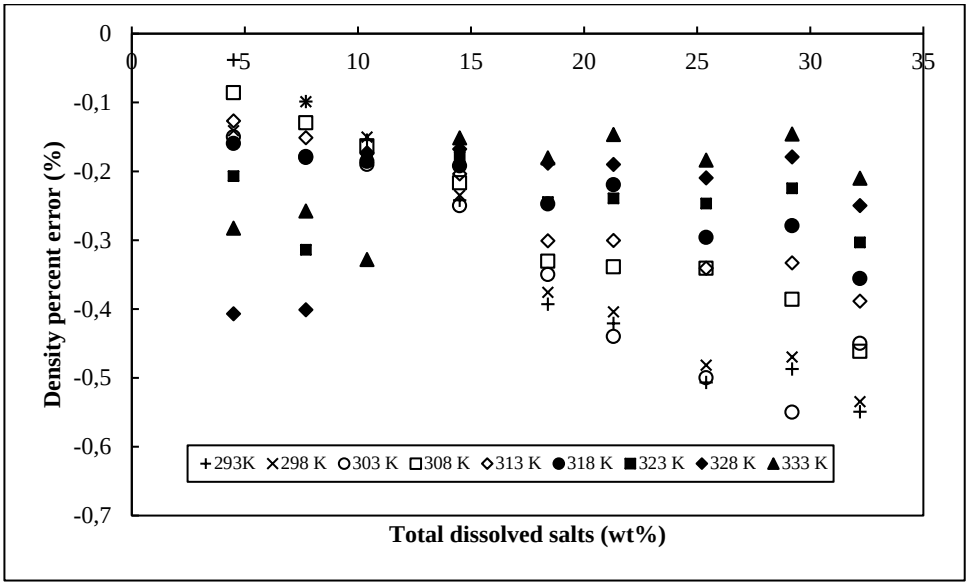

Figure 7-10: Comparison of the density equation with the experimental data

The ionic strength of the urine solutions was calculated using the speciation program PHREEQC 2.0 Excellent predictions were obtained with the average percent error being less than 0.60% for the entire concentration and temperature range. This is in agreement with Millero's theory that the molar volume of ions in solution are additive. The good predictions are a result of two main reasons, firstly because density is a relatively easy property to measure in a repeatable manner, and secondly because Millero's expression for predicting the molar volumes of single salts was a good fit for all the salts.

7.2.4 Electrical Conductivity

The electrical conductivity of the urine solutions was calculated from the speciated ionic composition using a model proposed by Brouckaert (1995). The method involved adding up the conductivities of each ionic species at infinite dilution and then correcting for the conductivity using an empirical term for ionic strength. The limiting conductivities for ion-pairs which were not available in literature were calculated using the equation proposed by Anderko and Lencka (1997) and these are presented in Table 7-2.

Table 7-2: Calculated Limiting Conductivities of selected complex ions at 298 K

Complex	Predicted λ° (10^{-4} S.m^2.mol^{-1})
$NH_4SO_4^-$	71.1
$KHPO_4^-$	76.8
KSO_4^-	75.2
$NaHPO_4^-$	49.8
$NaSO_4^-$	49.6
$NaCO_3^-$	49.3

The regression coefficients for the conductivity equation (3.46) were 0.253, -47.255 and -26.735. Since the limiting specific conductivities of the ions and complexes provided in literature were evaluated at 25 ˚C, the conductivity of the urine solutions for other temperatures were calculated using a viscosity-temperature relation equation. The viscosity of pure water was calculated using the correlation proposed by Laliberte (2007) which had an average error of 0.04% and a maximum deviation of 0.08%.

Figure 7-11 shows the comparison between the experimental values and the predicted conductivities. A graphical comparison shows that the predicted conductivities are in good agreement with the experimental data an average percent error of 0.63% standard deviation of 0.38% and a maximum error of 1.78%.

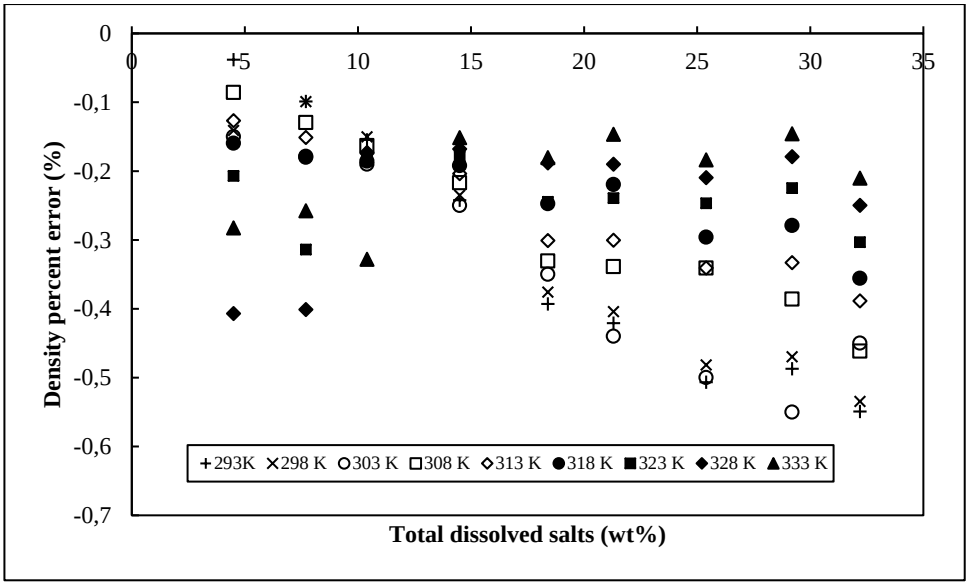

Figure 7-11: Comparison of the electrical conductivity equation with the experimental data

Greater deviations were observed at lower concentrations and the accuracy of the model improved as it was extended to higher concentrations. Another trend is that the calculated error increases as the temperature deviates away from the reference temperature of 25˚C. The viscosity-temperature relation for water corrects for temperature by taking into account the mobility of the ions as the temperature of the solution changes. The increase in error with temperature can be explained by the fact that, the viscosity-temperature relation does not consider the temperature dependency of the speciation in the urine solutions.

7.3 APPLICATION OF THE DATA MODELS FOR HYDROLYSED URINE

The objective of this section is to demonstrate the engineering applications for the measured data and the developed models. The application of experimental data are demonstrated in the following case studies;

- design of a multiple effect evaporator, using vapour pressure and density data
- design of a mechanical vapour compression evaporator, using vapour pressure data
- design of membrane separation (Forward Osmosis and Reverse Osmosis) processes using osmotic pressure data and
- monitoring the performance of a urine evaporator using electrical conductivity data and vapour pressure data

7.3.1 Design of a Multiple Effect Evaporator

Evaporation is energy intensive process and the use of multiple-effect evaporators can significantly reduce the amount of steam required per unit mass of urine. In multiple effect evaporators, the vapour produced from the first evaporator is used to heat the second evaporator unit. The reuse of vapour generated to heat the next effect therefore reduces the total energy required by the overall system. In order to allow for optimum heat transfer, the boiling temperature in the second effect is lowered by reducing the pressure. Further energy savings can be improved by adding several effects to the system. The energy saving in steam is defined as the steam economy, which is expressed as the ratio of the mass of water vaporised to the mass of steam fed to the system.

In designing the multiple effect evaporator, the design engineer needs to establish the optimum boiling temperatures as well as the boiling point elevation of the urine solution in each effect. As the concentration of the dissolved solids increases in the urine solution, the boiling point elevation of urine rises to levels which cannot be ignored. Jayes (2004) developed an algorithm for calculating the optimum distribution of the heating surface area for a multiple effect evaporator train which is detailed in **Appendix H.** A spreadsheet model using the algorithm was constructed for a plant processing 12 m^3/d of urine with a supply of saturated steam at 200 kPa. The initial and final concentrations of the urine solutions were the limit values studied in this work, i.e. 4.7 and 32.2wt%. The vapour pressure data were used to calculate the boiling temperatures as well as the boiling point elevations of the urine solutions in each effect .The overall heat transfer coefficient (OHTC) of each effect were assumed to have the following fixed values 2 600, 1 600, 1 200, 850 and 450 W/m^2 K

The calculations in **Appendix H** show that the total heating surface area required to concentrate 12 m^3/d of urine from 4.5 to 32 wt% is 26 538 m^2. Without the boiling point elevation of urine, the calculated heating surface area would be 23 688 m^2. This implies that without including the boiling point elevation

in the design calculation, the heating surface area would be undersized by 10%. Figure 7-12 shows the distribution of the calculated heating surface areas and the boiling point elevation in each effect. It is interesting to note that the distribution of the heating surface areas has a typical U-shape observed in the process design of multiple effect evaporators. This is largely because of low temperature, high viscosity of the solution, low OHTC and very high boiling point elevation. Figure 7-12 shows that there is a large increase in the boiling point elevation in the last effect which is a result of the increase in the concentration of the urine solution. As a result, the required driving force temperature difference is high resulting in a larger heating surface area.

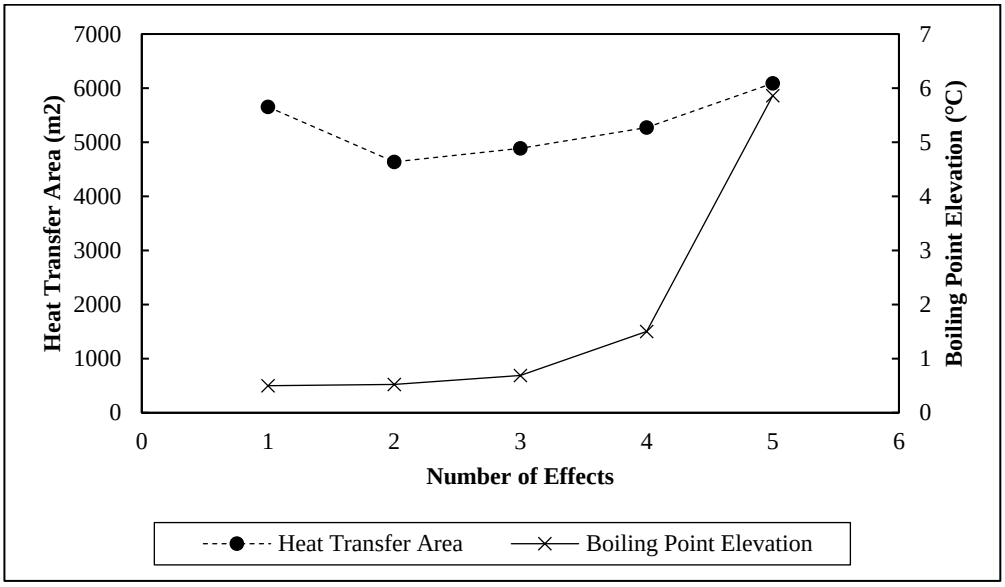

Figure 7-12: Heating surface areas and boiling point elevation in each effect

The design calculations show that 166 tonnes of steam is required to evaporate 437 tonnes of water from the urine which translates to a steam economy of 2.62. For a single effect evaporator, the steam requirement at the same pressure would have been 473 tonnes to evaporate same amount of water from urine.

7.3.2 Design of Mechanical Vapour Recompression Evaporator

Mechanical vapour recompression evaporators have been widely used in the desalination (Al-Juwayhel et al., 1997, Aly and El-Figi, 2003), in process industry (Palacios-Bereche et al., 2014, Reid and Rein, 1983) and as well as in wastewater treatment (Colin et al., 2005, GAO et al., 2012, Jiangcai, 2012). In the VUNA project, (Etter et al., 2014) and (Fumasoli et al., 2016) used a commercially available mechanical vapour recompression evaporator supplied by KMU-Loft Cleanwater, Hausen, Germany to concentrate. The vapour produced from the evaporator is compressed using a mechanically driven compressor to a higher pressure. This raises the temperature of the vapour produced and this allows it to be used for heating the solution from which it was evolved. The advantages of vapour recompression

are that, the evaporation efficiency is improved and there is no need for external steam heat the evaporator.

(Ettouney, 2006) gives a detailed model for the design of a mechanical vapour compression evaporator based on fundamental mass and heat balances, thermodynamics properties of the vapour and liquid streams, and the power requirements of the compressor. Most of the input parameters required for the model were not included in the scope of this work. However, an important parameter that can be deduced from this work is the pressure ratio of the system. It is given as the ratio the vapour pressure at X = 0 to that at concentration X.

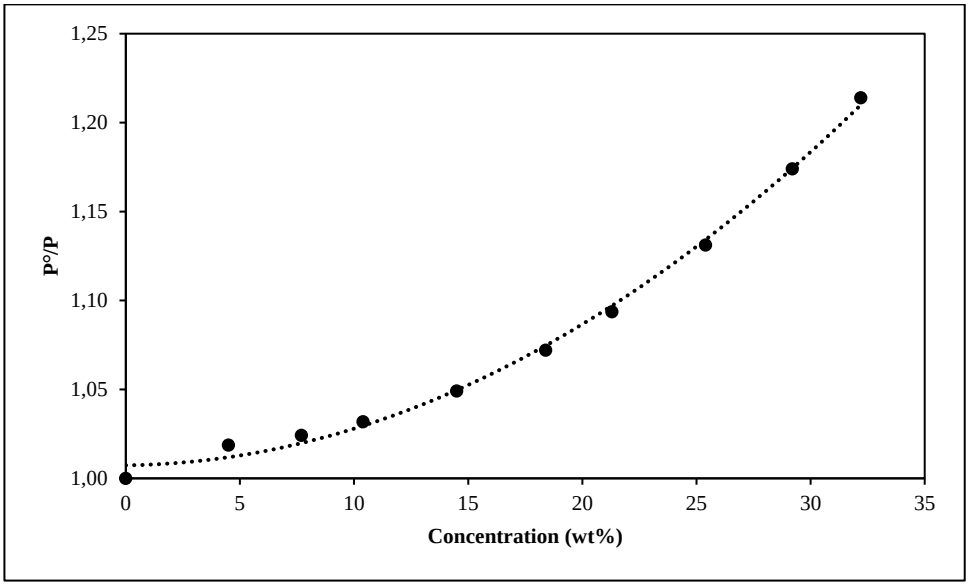

Figure 7-13: Pressure ratio of urine at 333 K

The compressed vapour must always be at a higher pressure than the evolved vapour, in order to create the temperature driving force required for heat transfer. The pressure ratio is the magnitude by which the pressure of the evolved vapour needs to be raised so that its temperature is greater than that of the boiling urine solution. The experimental data shows that the vapour pressure decreases as the concentration of the urine solution increases and that the boiling point elevation increases with the concentration of urine. This means that as the urine is fed and contained in the evaporator, the pressure ratio gradually increases as the concentration of the urine increases. Figure 7-13 therefore assists the designer in calculating the point where it is no longer beneficial to raise the pressure ratio for the sake of increasing water recoveries. Without the boiling point elevation data, which can be calculated from the vapour pressure of urine, the pressure ratio cannot be calculated.

7.3.3 Reverse Osmosis

The experimental data plotted in Figure 6-5 shows that as water is extracted from the urine, the osmotic pressure increases. In order to extract water from a reverse osmosis (RO) process, the applied pressure should be greater than the osmotic pressure of the urine. The generation of the required pressure requires energy and has a cost component. Approximately 50 -75 % of the energy consumed by reverse osmosis processes in desalination is used to generate the pressures required for the reverse osmotic flow (Gude, 2011). Excessive pressures lead to high equipment costs and also results in high maintenance costs and downtime due to the failure of the membranes. The designer needs to know how the osmotic pressure of the urine varies with concentration not only to design a robust system that can handle the applied pressures but also to design a cost effective RO process.

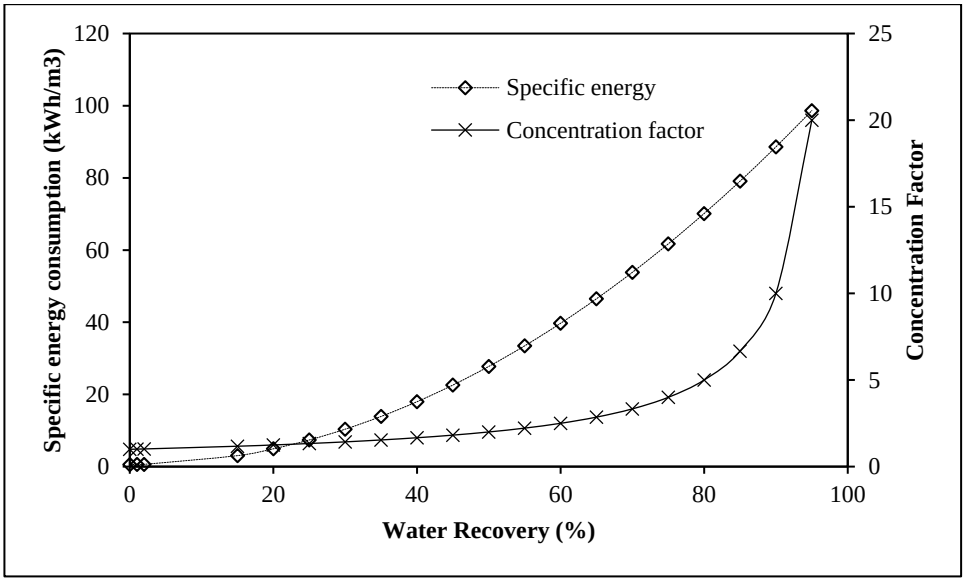

Figure 7-14: Specific energy consumption and concentration factor plotted against water recovery

Figure 7-14 shows the how the specific energy and the concentration vary with the water recovered from the urine. The specific energy consumption is the energy required by the pump to ensure reverse osmotic flow, and this was calculated from the osmotic pressure data of the urine using equation (3.19). The concentration factor is an important parameter in the design of a reverse osmosis system which is related to the water recovery. As water is continually extracted from the urine, the concentration of salts in the retained stream increases and this increases the potential of scaling of the membrane surfaces. Scaling is consequence of the concentration of the salts exceeding the solubility limits resulting in precipitation of the salts on the membrane. Typically, most RO processes are designed with a recovery ranging between 75 – 80 %, hence Figure 7-14 helps the designer in establishing the energy requirements and the resultant concentration factor for a targeted water recovery.

7.3.4 Forward Osmosis

Forward Osmosis (FO) uses the osmotic pressure difference between two solutions separated by a membrane to extract water. The process employs the natural process of osmosis, and hence no additional energy is required to move water across a membrane. The pollution Research Group (PRG) investigated the feasibility of using FO in concentrating urine using ammonium bicarbonate (NH_4HCO_3) as the draw solution. Ammonium bicarbonate was chosen because it is an ammonia based salt which after drawing water can be regenerated from the water using low grade heat.

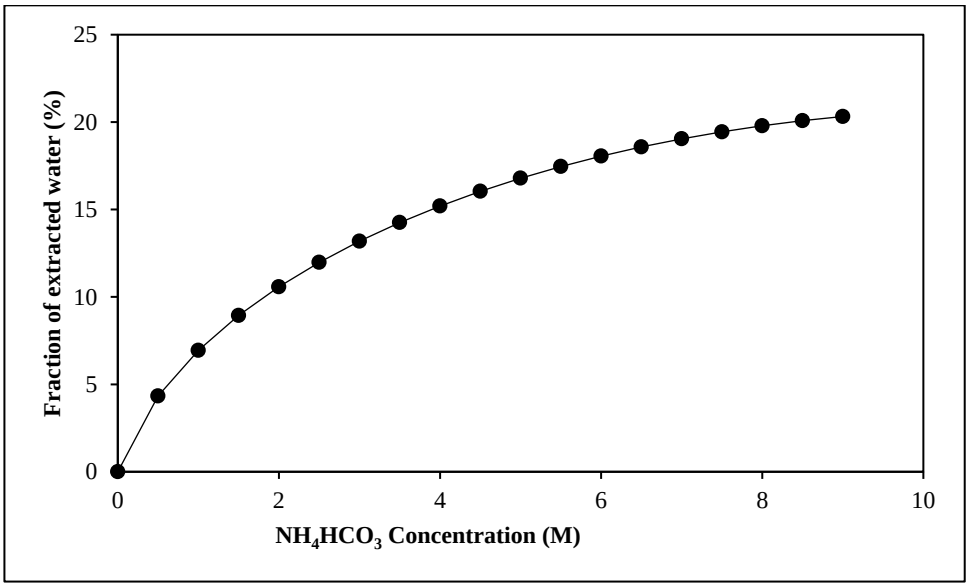

Figure 7-15: Variation of extracted water from urine with the concentration of the ammonium bicarbonate.

Since FO is an osmotically driven process, the total amount of water extracted from urine will depend on the initial concentration of the ammonia bicarbonate solution. The flux of water across the membrane will stop when the osmotic pressures of the urine and the ammonium bicarbonate are equal. Figure 7-15 was generated by combining the osmotic pressure data of urine and the osmotic pressure data of the ammonium bicarbonate. The Pollution Research Group investigated how the water flux and water recovery would be affected by the use 3 ammonium bicarbonate solutions with the following concentrations 1.0M, 2.0M and 2.5M. Figure 7-15 compliments the data obtained by the Pollution Research Group for ammonium concentration greater 2.5M.

7.3.5 Monitoring the performance of a urine evaporator

The Pollution Research Group partnered with EAWAG, a Swiss institute of Aquatic Science and Technology, and eThekwini Water and Sanitation (EWS) in a project called VUNA (Valorization of Urine Nutrients in Africa). This project culminated in the development of a nitrification and distillation process for the complete recovery of nutrients in urine. The nitrification stage stabilises the urine by lowering the pH and converting the ammonia in urine into nitrates which are non-volatile. The evaporation stage then removes about 95% of the water to produce a viscous urine concentrate. The evaporator used was a commercially available mechanical vapour recompression evaporator supplied by KMU-Loft Cleanwater, Hausen, Germany.

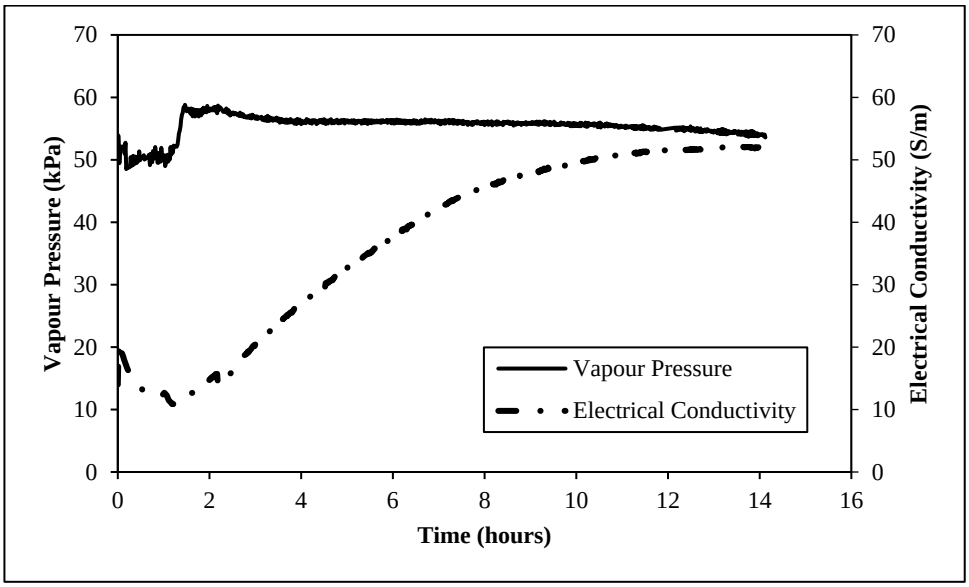

Figure 7-16: Process parameters measured in the urine evaporator in Durban

Figure 7-16 shows the vapour pressure and the electrical conductivity which are the key parameters measured during the evaporation process. The evaporator is operated in a semi batch mode where the urine is continuously fed while the concentrate is retained in the evaporator. The process is stopped when the required concentration factor of 20 is achieved. The electrical conductivity is used as a measure of the urine concentration in the evaporator. When the electrical conductivity of the urine concentrate reaches a conductivity value of the 52 S/m, the controller stops the process and stops the urine feed. The electrical conductivity data from the evaporator shows a similar trend to the experimental data in Figure 6-7. This shows that the electrical conductivity is a simple, accurate and reliable means of monitoring and controlling the evaporation process.

The vapour pressure data is used to monitor the performance of the vacuum pump and check on the progress and smoothness of the evaporation process. Erratic fluctuations in the vapour pressure data could mean failure of the vacuum pump or excessive boiling of the urine liquor which may result in

entrainment of the urine into the condensate. The gradual drop in the vapour pressure shown in Figure 7-16 is a result of the increase in the concentration of the retain urine in the evaporator.

7.4 CHAPTER SUMMARY

In general, the correlative equations for the physical properties of urine were in good agreement with the experimental data for the entire range of concentrations and temperatures under investigation. Table 7-3 summarises the statistical analysis of the variation in percent error for all the thermophysical properties. A limitation with this modeling technique is that it considers the total dissolved solids in the urine solutions and does not account for the ion-ion interactions in the aqueous solution. Hence the regression constants in equations (7.1) to (7.5) are unique for hydrolysed urine used.

Table 7-3: Analysis of the error between the correlative equations and experimental data

	Temperature range (K)	**Concentration range (wt%)**	**Average error (%)**	**Standard Deviation (%)**	**Maximum error (%)**
Vapour Pressure	333 – 373	4.5 – 32.2	0.188	0.199	0.605
Osmotic Pressure	333 – 373	4.5 – 32.2	0.333	0.287	0.985
Density	293 – 333	4.5 – 32.2	0.031	0.028	0.134
Electrical Conductivity	293 – 333	4.5 – 32.2	0.413	0.317	1.201

The speciation model for urine was incorporated into the equations for calculating the vapour pressure, osmotic pressure, density and electrical conductivity properties for urine. Model predictions were compared with the experimental data for a concentration range of 4.5 to 32.2 wt% and temperatures range of 293 to 333 K. The vapour pressure and osmotic pressure can be estimated within a percent error of 0.30% and 0.46% respectively from the activity of water for concentrations up 14 wt%. However caution is required in the use of the model for concentrations greater than 14 wt%, as the accuracy of equation (3.22) decreases with concentration. The equations for density and electrical conductivity showed adequate agreement with the experimental data. Good predictions were obtained for density with error within ±0.60%. Electrical conductivity was estimated within ±1.80% for the entire ranges for concentration and temperature.

Finally, the applicability of the data and models was demonstrated in the design of a multiple effect evaporator, a vapour compression evaporator and membrane separation processes.

8 CONCLUSION & RECOMMENDATIONS

8.1 CONCLUSION

The purpose of this study was to measure and model the thermophysical properties of hydrolysed urine at temperature and concentration ranges required for the design of thermal, membrane and electrochemical treatment processes. The investigated thermophysical properties included; vapour pressure, osmotic pressure, density and electrical conductivity for a concentration range of 4.5 to 32.2 wt%. No published research has been found providing this experimental data for hydrolysed urine and its concentrates.

Experimental data on hydrolysed urine showed trends similar to those of seawater, brines and other multicomponent aqueous solutions, at varying temperatures and concentrations. 110 sets of experimental vapour pressure data for hydrolysed urine were measured for a temperature range of 333 and 373 K, using a static pressure method. Temperatures were controlled within 0.01 K and the uncertainties in the measurements were less than 0.5 %.

The osmotic pressure of the urine solutions was calculated from the vapour pressure data. Density measurements for 245 data points were determined using a vibrating-tube, Anton Parr DMA 5000 densimeter, with reported uncertainties of 0.05%. Similarly, 245 measurements for electrical conductivity were made using a commercially available conductivity meter (YSI model 3200) with a (YSI 3253) dip-style cell. The temperature was controlled within deviations of ±0.01 K and the uncertainties in the conductivity data were in the range of ±1.0 %. The uncertainties reported for the investigated thermophysical properties of hydrolysed urine were well within the values reported in literature for aqueous solutions.

Modeling of the experimental data was undertaken to assist the design engineer to calculate the thermophysical properties from the composition of hydrolysed urine. Two existing techniques for modeling were applied. These included correlative modeling and predictive thermodynamic equations coupled with an ionic speciation model. These models can be incorporated into computer software used in chemical engineering design processes.

By means of correlative modeling, the experimental data was fit into regression equations expressing the thermophysical properties as functions of the total concentration (TDS) and temperature. The experimental data was adequately correlated using polynomial functions over the entire concentration and temperature ranges under investigation, as shown in Table 8-1

Table 8-1: Comparison between the correlative equations and experimental data

	Temperature range (K)	Concentration range (wt%)	Average error (%)	Standard Deviation (%)	Maximum error (%)
Vapour Pressure	333 – 373	4.5 – 32.2	0.188	0.199	0.605
Osmotic Pressure	333 – 373	4.5 – 32.2	0.333	0.287	0.985
Density	293 – 333	4.5 – 32.2	0.031	0.028	0.134
Electrical Conductivity	293 – 333	4.5 – 32.2	0.413	0.317	1.201

By means of thermodynamic modeling, the thermophysical properties were predicted using thermodynamic equations based on the speciated concentration of urine. The activity coefficients of the ionic species in the urine solutions were calculated using the B-dot model, which is an extension of the Debye-Hückel law.

Model predictions for vapour pressure and osmotic pressure were accurately predicted within a percent error of 0.30% for concentrations up 14 wt%. However, beyond 14 wt% caution is required in the use of the model as its accuracy decreases with concentration. Density and electrical conductivity were satisfactorily predicted over the entire temperature and concentration range with maximum errors of 0.60% and.1.80% respectively.

To conclude this work, the application of the measured data and models were demonstrated and presented in **section 7.3.** The vapour pressure data was used to calculate the optimum heating surface area of a quintuple effect and the sizing of a compressor in a mechanical vapour recompression evaporator.

Eawag and EThekwini Water and Sanitation have installed evaporators using the principle of vapour compression for the treatment of urine. The vapour pressure and electrical conductivity data was also used in monitoring the performance of the vapour recompression evaporator. The vapour pressure data can also be applied in low cost concentration applications such as solar evaporation.

Finally, osmotic pressure data were used in the design of reverse and forward osmosis processes. The Pollution Research Group is investigating the forward osmosis concentration of hydrolysed urine using an ammonium bicarbonate draw solution. The osmotic pressure data from this work was successfully used to determine the maximum water recoveries achievable by various concentrations of the ammonium bicarbonate.

8.2 FUTURE WORK

This work investigated four thermophysical properties of urine, namely, vapour pressure, osmotic pressure, density and electrical conductivity. Thereafter, case studies were presented to demonstrate simple designs using evaporation and membrane technology, applying the experimental data obtained from hydrolysed urine. However, the detailed design of urine treatment units requires the knowledge of a wide range of physical properties, in addition to the properties mentioned above, which include: viscosity, specific heat capacity, thermal conductivity and heat of vaporization.

The thermodynamic model based on the Davies equation failed to accurately predict the vapour pressure of the urine at concentrations greater than 14 wt%. This is because the assumptions made in the development of the Davies approximation do not hold at high ionic concentrations.

The literature review on thermodynamic models revealed that the Pitzer model, which is applicable for ionic strengths up to 6M, could not be applied to urine because the specific ionic interaction parameters for the ammonia and phosphate ions were not available in literature. Ammonium and phosphate ions are key constituents in urine and, therefore, experimental work needs to be conducted on ammonium- and phosphate-based salts in order to generate the interaction parameters required for modeling at high ionic strengths.

9 REFERENCES

ABDULAGATOV, I. & AZIZOV, N. 2003a. PVTx measurements and partial molar volumes for aqueous Li2SO4 solutions at temperatures from 297 to 573 K and at pressures up to 40 MPa. *International Journal of Thermophysics,* 24**,** 1581-1610.

ABDULAGATOV, I. & AZIZOV, N. 2004. Densities and apparent molar volumes of aqueous LiI solutions at temperatures from (296 to 600) K and at pressures up to 30 MPa. *The Journal of Chemical Thermodynamics,* 36**,** 829-843.

ABDULAGATOV, I. M. & AZIZOV, N. D. 2003b. Densities and apparent molar volumes of aqueous NaNO3 solutions at temperatures from 292 to 573 K and at pressures up to 30 MPa. *Journal of solution chemistry,* 32**,** 573-599.

ABDULAGATOV, I. M. & AZIZOV, N. D. 2005. Densities, apparent molar volumes and viscosities of concentrated aqueous NaNO3 solutions at temperatures from 298 to 607 K and at pressures up to 30 MPa. *Journal of solution chemistry,* 34**,** 645-685.

ABDULAGATOV, I. M. & AZIZOV, N. D. 2006. Densities and apparent molar volumes of concentrated aqueous LiCl solutions at high temperatures and high pressures. *chemical Geology,* 230**,** 22-41.

ADAM, N., MITCHELL, J. L. & PICKERING, K. D. 2012. Development of Low-Toxicity Urine Stabilization for Spacecraft Water Recovery Systems.

AL-JUWAYHEL, F., EL-DESSOUKY, H. & ETTOUNEY, H. 1997. Analysis of single-effect evaporator desalination systems combined with vapor compression heat pumps. *Desalination,* 114**,** 253-275.

AL GHAFRI, S., MAITLAND, G. C. & TRUSLER, J. M. 2012. Densities of Aqueous MgCl2 (aq), CaCl2 (aq), KI (aq), NaCl (aq), KCl (aq), AlCl3 (aq), and (0.964 NaCl+ 0.136 KCl)(aq) at Temperatures Between (283 and 472) K, Pressures up to 68.5 MPa, and Molalities up to 6 mol· kg–1. *Journal of Chemical & Engineering Data,* 57**,** 1288-1304.

ALY, N. H. & EL-FIGI, A. K. 2003. Mechanical vapor compression desalination systems—a case study. *Desalination,* 158**,** 143-150.

ANTOINE, C. 1988. A New Relationship between Vapour Pressure and Temperature. *Compt. Rend,* 107**,** 836.

APELBLAT, A., AZOULAY, D. & SAHAR, A. 1973. Properties of aqueous thorium nitrate solutions. Part 2.—Water activities and osmotic and activity coefficients of thorium nitrate at 25, 35 and 45° C. *Journal of the Chemical Society, Faraday Transactions 1: Physical Chemistry in Condensed Phases,* 69**,** 1624-1627.

APELBLAT, A. & KORIN, E. 1998. Vapour pressures of saturated aqueous solutions of ammonium iodide, potassium iodide, potassium nitrate, strontium chloride, lithium sulphate, sodium thiosulphate, magnesium nitrate, and uranyl nitrate fromT=(278 to 323) K. *The Journal of Chemical Thermodynamics,* 30**,** 459-471.

APELBLAT, A. & KORIN, E. 2009. Temperature Dependence of Vapor Pressures over Saturated Aqueous Solutions at Invariant Points of the NaCl+ KCl+ H2O, NaCl+ NaNO3+ H2O, KCl+ KBr+ H2O, KCl+ KI+ H2O, KCl+ KNO3+ H2O, and KCl+ K2SO4+ H2O Systems†. *Journal of Chemical & Engineering Data,* 54**,** 1619-1624.

APELBLAT, A. & KORIN, E. 2011. Temperature Dependence of Vapor Pressures over Saturated Aqueous Solutions at Invariant Points of the NaCl+ KNO3+ H2O, NaCl+ Na2CO3+ H2O, and NaCl+ Na2SO4+ H2O Systems. *Journal of Chemical & Engineering Data,* 56**,** 988-994.

APPELO, C., PARKHURST, D. & POST, V. 2014. Equations for calculating hydrogeochemical reactions of minerals and gases such as CO 2 at high pressures and temperatures. *Geochimica et Cosmochimica Acta,* 125**,** 49-67.

APPELO, C. A. J. 2010. *Specific conductance: how to calculate,to use, and the pitfalls* [Online]. Available: http://www.hydrochemistry.eu/exmpls/sc.html [Accessed 21/04/2016 2016].

BLACK, R. E., COUSENS, S., JOHNSON, H. L., LAWN, J. E., RUDAN, I., BASSANI, D. G., JHA, P., CAMPBELL, H., WALKER, C. F. & CIBULSKIS, R. 2010. Global, regional, and national causes of child mortality in 2008: a systematic analysis. *The lancet,* 375**,** 1969-1987.

BLANCO, L. H. & VARGAS, E. F. 2004. An improved magnetic float densimeter. *Instrumentation Science & Technology,* 32**,** 13-20.

BMFG. 2011. *Water, Sanitation and Hygiene, Strategy Review* [Online]. Seattle, USA: Bill and Melinda Gates Foundation. Available: http://www.susana.org/en/resources/library/details/1663 [Accessed 26/09/2015 2015].

BOTHEJU, D., SVALHEIM, O. & BAKKE, R. 2010. Digestate nitrification for nutrient recovery. *The Open Waste Management Journal,* 3.

BRONZINO, J. D. 1999. *Biomedical engineering handbook*, CRC press.

BROUCKAERT, B. M. 1995. **Prediction of Conductivity from Equilibrium Ionic Speciation**.

CHEN, C.-T. A., CHEN, J. H. & MILLERO, F. J. 1980. Densities of sodium chloride, magnesium chloride, sodium sulfate, and magnesium sulfate aqueous solutions at 1 atm from 0 to 50. degree. C and from 0.001 to 1.5 m. *Journal of Chemical and Engineering Data,* 25**,** 307-310.

CHUTIPONGTANATE, S. & THONGBOONKERD, V. 2010. Systematic comparisons of artificial urine formulas for in vitro cellular study. *Analytical biochemistry,* 402**,** 110-112.

CIBA-GEIGY, DIEM, K. & LENTNER, C. 1970. *Scientific Tables: Excerpts from the 7th Ed*, Ciba-Geigy.

CLARKE, E. C. W. & GLEW, D. N. 1985. Evaluation of the thermodynamic functions for aqueous sodium chloride from equilibrium and calorimetric measurements below 154 C. *Journal of Physical and Chemical Reference Data,* 14**,** 489-610.

COLIN, T., BORIES, A., SIRE, Y. & PERRIN, R. 2005. Treatment and valorisation of winery wastewater by a new biophysical process (ECCF®). *Water Science and Technology,* 51**,** 99-106.

COVINGTON, A. 1986. Handbook of Aqueous Electrolyte Solutions. Physical Properties, Estimation and Correlation methods. Pergamon.

CROCKER, L. & ALGINA, J. 1986. *Introduction to classical and modern test theory*, ERIC.

CROWE, A. & LONGSTAFFE, F. Extension of geochemical modelling techniques to brines: coupling of the Pitzer equations to PHREEQE. Proc. of the National Water Well Conf. on Solving Groundwater Problems with Models, National Water Well Association, Dublin, OH, 1987. 110-129.

DAVIES, C. 1962. *Ion Association,* London, Butterworths.

DE AZEVEDO, F. G. & DE OLIVEIRA, W. A. 1984. Ebulliometric study of the decomposition of urea in aqueous media. *International journal of chemical kinetics*, 16**,** 793-799.

DE DIEGO, A., MADARIAGA, J. & CHAPELA, E. 1997. Empirical model of general application to fit (k, c, T) experimental data from concentrated aqueous electrolyte solutions. *Electrochimica acta,* 42**,** 1449-1456.

DE DIEGO, A., USOBIAGA, A., FERNÁNDEZ, L. A. & MADARIAGA, J. M. 2001. Application of the electrical conductivity of concentrated electrolyte solutions to industrial process control and design: from experimental measurement towards prediction through modelling. *TrAc trends in analytical chemistry,* 20**,** 65-78.

DE OLIVEIRA, W. A. & MEITES, L. 1977. Precise twin ebulliometry. *Analytica Chimica Acta,* 93**,** 3-18.

DUNN, L. 1966. Apparent molar volumes of electrolytes. Part 1.—Some 1—1, 1—2, 2—1, 3—1 electrolytes in aqueous solution at 25° C. *Transactions of the Faraday Society,* 62**,** 2348-2354.

EK M, B. R., BJURHEM J, BJORLENIUS B AND HELLSTROM D 2006. Concentration of nutrients from urine and reject water from anaerobically digested sludge. *Water Science & Technology,* **54,** 437-444.

ELLIOTT, J., PRICKETT, R., ELMOAZZEN, H., PORTER, K. & MCGANN, L. 2007. A multisolute osmotic virial equation for solutions of interest in biology. *The Journal of Physical Chemistry B,* 111**,** 1775-1785.

ELLIS, A. 1968. Partial molal volumes in high-temperature water. Part III. Halide and oxyanion salts. *Journal of the Chemical Society A: Inorganic, Physical, Theoretical***,** 1138-1143.

EMBARGO, U. S. 2014. INVESTING IN WATER AND SANITATION: INCREASING ACCESS, REDUCING INEQUALITIES.

ETTER, B., UDERT, K. & GOUNDEN, T. VUNA–Scaling Up Nutrient Recovery from Urine. to be submitted for the Tech4Dev conference (EPFL, 2014.

ETTOUNEY, H. 2006. Design of single-effect mechanical vapor compression. *Desalination,* 190**,** 1-15.

FABUSS, B. M. & KOROSI, A. 1968. Properties of sea water and solutions containing sodium chloride, potassium chloride, sodium sulfate and magnesium sulfate.

FABUSS, B. M., KOROSI, A. & HUG, A. S. 1966. Densities of Binary and Ternary Aqueous Solutions of NaCl, Na2SO4 and MgSO4 of Sea Waters, and Sea Water Concentrates. *Journal of Chemical and Engineering Data,* 11**,** 325-331.

FIREMAN, M. & REEVE, R. Some characteristics of saline and alkali soils in Gem County, Idaho. Soil Science Society of America Proceedings, 1948. 494-498.

FOFONOFF, N. 1985. Physical properties of seawater: A new salinity scale and equation of state for seawater. *J. geophys. Res,* 90**,** 3332-3342.

FUMASOLI, A., ETTER, B., STERKELE, B., MORGENROTH, E. & UDERT, K. M. 2016. Operating a pilot-scale nitrification/distillation plant for complete nutrient recovery from urine. *Water Science and Technology,* 73**,** 215-222.

GAO, L.-L., ZHANG, L. & DU, M.-Z. 2012. Energy efficiency comparative analysis on MVR and multi-effect evaporation technology [J]. *Modern Chemical Industry,* 10**,** 031.

GATES, J. A. & WOOD, R. H. 1989. Density and apparent molar volume of aqueous calcium chloride at 323-600 K. *Journal of Chemical and Engineering Data,* 34**,** 53-56.

GENÇER, N. G. & TEK, M. N. 1999. Electrical conductivity imaging via contactless measurements. *Medical Imaging, IEEE Transactions on,* 18**,** 617-627.

GONZÁLEZ, B., CALVAR, N., DOMÍNGUEZ, Á. & MACEDO, E. A. 2008. Osmotic coefficients of aqueous solutions of four ionic liquids at T=(313.15 and 333.15) K. *The Journal of Chemical Thermodynamics,* 40**,** 1346-1351.

GOODWIN, A., MARSH, K. & WAKEHAM, W. 2003. *Measurement of the thermodynamic properties of single phases, Elsevier,* CHEMISTRY International.

GRATTONI, A., CANAVESE, G., MONTEVECCHI, F. M. & FERRARI, M. 2008. Fast membrane osmometer as alternative to freezing point and vapor pressure osmometry. *Analytical chemistry,* 80**,** 2617-2622.

GRATTONI, A., MERLO, M. & FERRARI, M. 2007. Osmotic pressure beyond concentration restrictions. *The Journal of Physical Chemistry B,* 111**,** 11770-11775.

GRIFFITH 1976. Urease. The primary cause of infection-induced urinary stones. *Investigative urology,* 13**,** 346-350.

GUDE, V. G. 2011. Energy consumption and recovery in reverse osmosis. *Desalination and water treatment,* 36**,** 239-260.

GUGGENHEIM, E. & TURGEON, J. 1955. Specific interaction of ions. *Transactions of the Faraday Society,* 51**,** 747-761.

HEFTER, G., MAY, P. M., MARSHALL, S. L., CORNISH, J. & KRON, I. 1997. Improved apparatus and procedures for isopiestic studies at elevated temperatures. *Review of scientific instruments,* 68**,** 2558-2567.

HELGESON, H. C., GARRELS, R. M. & MACKENZIE, F. T. 1969. Evaluation of irreversible reactions in geochemical processes involving minerals and aqueous solutions—II. Applications. *Geochimica et Cosmochimica Acta,* 33**,** 455-481.

HELGESON, H. C. & KIRKHAM, D. H. 1976. Theoretical prediction of thermodynamic properties of aqueous electrolytes at high pressures and temperatures. III. Equation of state for aqueous species at infinite dilution. *Am. J. Sci.;(United States),* 276.

HELGESON, H. C., KIRKHAM, D. H. & FLOWERS, G. C. 1981. Theoretical prediction of the thermodynamic behavior of aqueous electrolytes by high pressures and temperatures; IV, Calculation of activity coefficients, osmotic coefficients, and apparent molal and standard and relative partial molal properties to 600 degrees C and 5kb. *American Journal of Science,* 281**,** 1249-1516.

HELLSTRÖM, D., JOHANSSON, E. & GRENNBERG, K. 1999. Storage of human urine: acidification as a method to inhibit decomposition of urea. *Ecological Engineering,* 12**,** 253-269.

HOGENBOOM, D., KARGEL, J., GANASAN, J. & LEE, L. 1995. Magnesium sulfate-water to 400 MPa using a novel piezometer: Densities, phase equilibria, and planetological implications. *Icarus,* 115**,** 258-277.

HÖGLUND, C., STENSTRÖM, T., JÖNSSON, H. & SUNDIN, A. 1998. Evaluation of faecal contamination and microbial die-off in urine separating sewage systems. *Water Science and Technology,* 38**,** 17-25.

HOLCOMB, C. & OUTCALT, S. 1998. A theoretically-based calibration and evaluation procedure for vibrating-tube densimeters. *Fluid phase equilibria,* 150**,** 815-827.

HUTTON, G., RODRIGUEZ, U.-P. E., NAPITUPULU, L., THANG, P. N. & KOV, P. 2007. Economic Impacts of Sanitation in Southeast Asia: A Four-Country Study Conducted in Cambodia, Indonesia, the Philippines and Vietnam under the Economics of Sanitation Initiative (ESI). *East Asia and the Pacific*.

JAYES, W. 2004. Optimum distribution of heating surface in a multiple effect evaporator train. *International sugar journal,* 106**,** 612-619.

JIANGCAI, F. 2012. Application and Economic Analysis of NH4Cl Wastewater Treatment by MVR Evaporation Craft [J]. *Guangdong Chemical Industry,* 8**,** 053.

JONES, G. & DOLE, M. 1930. The electrical conductance of aqueous solutions of barium chloride as a function of the concentration. *Journal of the American Chemical Society,* 52**,** 2245-2256.

KAGHAZCHI, T., MEHRI, M., RAVANCHI, M. T. & KARGARI, A. 2010. A mathematical modeling of two industrial seawater desalination plants in the Persian Gulf region. *Desalination,* 252**,** 135-142.

KAPAŁKA, A., KATSAOUNIS, A., MICHELS, N.-L., LEONIDOVA, A., SOUENTIE, S., COMNINELLIS, C. & UDERT, K. M. 2010. Ammonia oxidation to nitrogen mediated by electrogenerated active chlorine on Ti/PtO x-IrO 2. *Electrochemistry Communications,* 12**,** 1203-1205.

KARAK, T. & BHATTACHARYYA, P. 2011. Human urine as a source of alternative natural fertilizer in agriculture: A flight of fancy or an achievable reality. *Resources, conservation and recycling,* **55,** 400-408.

KARBEYAZ, B. Ü. & GENÇER, N. G. 2003. Electrical conductivity imaging via contactless measurements: an experimental study. *Medical Imaging, IEEE Transactions on,* 22**,** 627-635.

KIMBERLIN, C. L. & WINTERSTEIN, A. G. 2008. Validity and reliability of measurement instruments used in research. *Am J Health Syst Pharm,* 65**,** 2276-84.

KIRCHMANN, H. & PETTERSSON, S. 1994. Human urine-chemical composition and fertilizer use efficiency. *Fertilizer research,* **40,** 149-154.

KOT, A. & NAMIESŃIK, J. 2000. The role of speciation in analytical chemistry. *TrAC Trends in Analytical Chemistry,* 19**,** 69-79.

KRUMGALZ, B. S. & MILLERO, F. J. 1982. Physico-chemical study of Dead Sea waters: II. Density measurements and equation of state of Dead Sea waters at 1 atm. *Marine Chemistry,* 11**,** 477-492.

KSAYER, E. B. L., YOUNES, M. & CLODIC, D. 2012. Concentration of brine solution used for low-temperature air cooling. *international journal of refrigeration,* 35**,** 418-423.

KVARNSTRÖM, E., EMILSSON, K., STINTZING, A. R., JOHANSSON, M., JÖNSSON, H., AF PETERSENS, E., SCHÖNNING, C., CHRISTENSEN, J., HELLSTRÖM, D. & QVARNSTRÖM, L. 2006. *Urine diversion: one step towards sustainable sanitation,* EcoSanRes Programme.

LALIBERTE, M. & COOPER, W. E. 2004. Model for calculating the density of aqueous electrolyte solutions. *Journal of Chemical & Engineering Data,* 49**,** 1141-1151.

LARSEN, T. & MAURER, M. 2011. Source separation and decentralization. *Treatise on Water Sciences, Academic Press, Oxford,* 4**,** 203-229.

LARSEN, T. A. & GUJER, W. 1996. Separate management of anthropogenic nutrient solutions (human urine). *Water Science and Technology,* 34**,** 87-94.

LIDE, D. R. 1999. CRC Handbook of Chemistry and Physics-1999-2000.

LIN, D.-Q., MEI, L.-H., ZHU, Z.-Q. & HAN, Z.-X. 1996. An improved isopiestic method for measurement of water activities in aqueous polymer and salt solutions. *Fluid Phase Equilibria,* 118**,** 241-248.

LIND, B.-B., BAN, Z. & BYDÉN, S. 2000. Nutrient recovery from human urine by struvite crystallization with ammonia adsorption on zeolite and wollastonite. *Bioresource Technology,* **73,** 169-174.

LIU, H., RAMNARAYANAN, R. & LOGAN, B. E. 2004. Production of electricity during wastewater treatment using a single chamber microbial fuel cell. *Environmental science & technology,* 38**,** 2281-2285.

LO SURDO, A. & MILLERO, F. J. 1980. Apparent molal volumes and adiabatic compressibilities of aqueous transition metal chlorides at 25. degree. C. *The Journal of Physical Chemistry,* 84**,** 710-715.

LOGAN, B. E. 2008. *Microbial fuel cells*, John Wiley & Sons.

LOGAN, B. E., HAMELERS, B., ROZENDAL, R., SCHRÖDER, U., KELLER, J., FREGUIA, S., AELTERMAN, P., VERSTRAETE, W. & RABAEY, K. 2006. Microbial fuel cells: methodology and technology. *Environmental science & technology,* 40**,** 5181-5192.

LOGAN, B. E. & REGAN, J. M. 2006. Electricity-producing bacterial communities in microbial fuel cells. *TRENDS in Microbiology,* 14**,** 512-518.

LORD, R. 1999. Osmosis, osmometry, and osmoregulation. *Postgraduate medical journal,* 75**,** 67-73.

MAALI, M. & SADEGHI, R. 2015. Vapour pressure osmometry determination of water activity of binary and ternary aqueous (polymer+ polymer) solutions. *The Journal of Chemical Thermodynamics,* 84**,** 41-49.

MACNEIL, J. A., RAY, G. B. & LEAIST, D. G. 2011. Activity coefficients and free energies of nonionic mixed surfactant solutions from vapor-pressure and freezing-point osmometry. *The Journal of Physical Chemistry B,* 115**,** 5947-5957.

MARIAH, L., BUCKLEY, C. A., BROUCKAERT, C. J., CURCIO, E., DRIOLI, E., JAGANYI, D. & RAMJUGERNATH, D. 2006. Membrane distillation of concentrated brines—Role of water activities in the evaluation of driving force. *Journal of membrane science,* 280**,** 937-947.

MASSON, D. O. 1929. XXVIII. Solute molecular volumes in relation to solvation and ionization. *The London, Edinburgh, and Dublin Philosophical Magazine and Journal of Science,* 8**,** 218-235.

MATHERS, C., FAT, D. M. & BOERMA, J. T. 2008. *The global burden of disease: 2004 update*, World Health Organization.

MAURER, M., PRONK, W. & LARSEN, T. 2006a. Treatment processes for source-separated urine. *Water Research,* 40**,** 3151-3166.

MAURER, M., PRONK, W. & LARSEN, T. A. 2006b. Treatment processes for source-separated urine. *Water Research,* **40,** 3151-3166.

MCCLESKEY, R. B. 2011. Electrical conductivity of electrolytes found in natural waters from (5 to 90) C. *Journal of Chemical & Engineering Data,* 56**,** 317-327.

MCCLESKEY, R. B., NORDSTROM, D. K. & RYAN, J. N. 2012a. Comparison of electrical conductivity calculation methods for natural waters. *Limnology and Oceanography: Methods,* 10**,** 952-967.

MCCLESKEY, R. B., NORDSTROM, D. K., RYAN, J. N. & BALL, J. W. 2012b. A new method of calculating electrical conductivity with applications to natural waters. *Geochimica et Cosmochimica Acta,* 77**,** 369-382.

MCNEAL, B. L., OSTER, J. & HATCHER, J. 1970. Calculation of electrical conductivity from solution composition data as an aid to in-situ estimation of soil salinity. *Soil Science,* 110**,** 405-414.

MILADINOVIĆ, J., NINKOVIĆ, R., TODOROVIĆ, M. & RARD, J. A. 2008. Isopiestic Investigation of the Osmotic and Activity Coefficients of {yMgCl2+ (1− y) MgSO4}(aq) and the Osmotic Coefficients of Na2SO4· MgSO4 (aq) at 298.15 K. *Journal of Solution Chemistry,* 37**,** 307-329.

MILLER, R. L., BRADFORD, W. L. & PETERS, N. E. 1988. *Specific conductance: theoretical considerations and application to analytical quality control,* US Government Printing Office.

MILLERO, F. J. 1970. The apparent and partial molal volume of aqueous sodium chloride solutions at various temperatures. *The Journal of Physical Chemistry,* 74**,** 356-362.

MILLERO, F. J. 1971. Molal volumes of electrolytes. *Chemical Reviews,* 71**,** 147-176.

MILLERO, F. J. 1972. *The partial molal volumes of electrolytes in aqueous solutions,* University of Miami, Rosenstiel School of Marine and Atmospheric Sciences.

MILLERO, F. J. 1973. Theoretical estimates of the isothermal compressibility of sea water. *Deep Sea Research and Oceanographic Abstracts,* 20**,** 101-105.

MILLERO, F. J. 1985. The physical chemistry of natural waters. *Pure and applied chemistry,* 57**,** 1015-1024.

MILLERO, F. J. 2000. The equation of state of lakes. *Aquatic Geochemistry,* 6**,** 1-17.

MILLERO, F. J. & HUANG, F. 2009. The density of seawater as a function of salinity (5 to 70 g kg− 1) and temperature (273.15 to 363.15 K). *Ocean Science,* 5**,** 91-100.

MILLERO, F. J., LAWSON, D. & GONZALEZ, A. 1976. The density of artificial river and estuarine waters. *Journal of Geophysical Research,* 81**,** 1177-1179.

MOBLEY, H. & HAUSINGER, R. 1989. Microbial ureases: significance, regulation, and molecular characterization. *Microbiological reviews,* 53**,** 85-108.

MONEY, N. P. 1989. Osmotic pressure of aqueous polyethylene glycols relationship between molecular weight and vapor pressure deficit. *Plant physiology,* 91**,** 766-769.

MONNIN, C. 1999. A thermodynamic model for the solubility of barite and celestite in electrolyte solutions and seawater to 200 C and to 1 kbar. *Chemical Geology,* 153**,** 187-209.

MONTANGERO, A. S., MARTIN 2004. Eawag, Swiss Federal Institute of Aquatic Science & Technology Sandec, Dept. of Water & Sanitation in Developing Countries.

MOON, Y., ANDERSON, C., BLANCH, H. & PRAUSNITZ, J. 2000. Osmotic pressures and second virial coefficients for aqueous saline solutions of lysozyme. *Fluid Phase Equilibria,* 168**,** 229-239.

MUHLBAUER, A. 1997. *Phase Equilibria: Measurement & Computation*, CRC Press.

NATIONS, U. 2015. *SUSTAINABLE DEVELOPMENT GOAL 6: Ensure availability and sustainable management of water and sanitation for all* [Online]. UN - Department of Economic and Social Affairs. Available: https://sustainabledevelopment.un.org/sdg6 [Accessed 10/10/2016 2016].

NOVOTNY, P. & SOHNEL, O. 1988. Densities of binary aqueous solutions of 306 inorganic substances. *Journal of Chemical and Engineering Data,* 33**,** 49-55.

OBŠIL, M., MAJER, V., HEFTER, G. T. & HYNEK, V. 1997. Densities and Apparent Molar Volumes of Na2SO4 (aq) and K2SO4 (aq) at Temperatures from 298 K to 573 K and at Pressures up to 30 MPa. *Journal of Chemical & Engineering Data,* 42**,** 137-142.

OTTERPOHL, R., ALBOLD, A. & OLDENBURG, M. 1999. Source control in urban sanitation and waste management: ten systems with reuse of resources. *Water Science and Technology,* 39**,** 153-160.

PALACIOS-BERECHE, R., ENSINAS, A. V., MODESTO, M. & NEBRA, S. A. 2014. Mechanical vapour recompression incorporated to the ethanol production from sugarcane and thermal integration to the overall process applying pinch analysis. *CHEMICAL ENGINEERING,* 39.

PANG, F. M. 2007. Measurement And Prediction Of Densities And Viscosities Of Aqueous Binary And Ternary Solutions At Temparatures From 20 To 60 C.

PARKHURST, D. L. 1995. User's guide to PHREEQC: A computer program for speciation, reaction-path, advective-transport, and inverse geochemical calculations.

PATHAK, R., N,; SAXENA, I, MISHRA; A, K, KUMAR; R, SINGH 2013. Introduction of an Auto-circuit in Magnetic Float Densitometer using Semiconductor Devices. *International Journal of Chemical and Physical Sciences,* 2.

PATIL, K. R., CHAUDHARI, S. K. & KATTI, S. S. 1992. Thermodynamic properties of aqueous electrolyte solutions. 3. Vapor pressure of aqueous solutions of lithium nitrate, lithium chloride+ lithium nitrate and lithium bromide+ lithium nitrate. *Journal of Chemical and Engineering Data,* 37**,** 136-138.

PATIL, K. R., TRIPATHI, A. D., PATHAK, G. & KATTI, S. S. 1990. Thermodynamic properties of aqueous electrolyte solutions. 1. Vapor pressure of aqueous solutions of

lithium chloride, lithium bromide, and lithium iodide. *Journal of Chemical and Engineering Data,* 35**,** 166-168.

PATIL, K. R., TRIPATHI, A. D., PATHAK, G. & KATTI, S. S. 1991. Thermodynamic properties of aqueous electrolyte solutions. 2. Vapor pressure of aqueous solutions of sodium bromide, sodium iodide, potassium chloride, potassium bromide, potassium iodide, rubidium chloride, cesium chloride, cesium bromide, cesium iodide, magnesium chloride, calcium chloride, calcium bromide, calcium iodide, strontium chloride, strontium bromide, strontium iodide, barium chloride, and barium bromide. *Journal of chemical and engineering data,* 36**,** 225-230.

PAWLOWICZ, R. 2008. Calculating the conductivity of natural waters. *Limnology and Oceanography: Methods,* 6**,** 489-501.

PAWLOWICZ, R. 2010. A model for predicting changes in the electrical conductivity, practical salinity, and absolute salinity of seawater due to variations in relative chemical composition. *Ocean Science,* 6**,** 361-378.

PITZER, K. S. 1973. Thermodynamics of electrolytes. I. Theoretical basis and general equations. *The Journal of Physical Chemistry,* 77**,** 268-277.

PITZER, K. S. 1975. Thermodynamics of electrolytes. V. Effects of higher-order electrostatic terms. *Journal of Solution Chemistry,* 4**,** 249-265.

PITZER, K. S. & KIM, J. J. 1974. Thermodynamics of electrolytes. IV. Activity and osmotic coefficients for mixed electrolytes. *Journal of the American Chemical Society,* 96**,** 5701-5707.

PITZER, K. S. & MAYORGA, G. 1973. Thermodynamics of electrolytes. II. Activity and osmotic coefficients for strong electrolytes with one or both ions univalent. *The Journal of Physical Chemistry,* 77**,** 2300-2308.

PLUMMER, L. N., PARKHURST, D., FLEMING, G. & DUNKLE, S. 1988. A computer program incorporating Pitzer's equations for calculation of geochemical reactions in brines.

PRG. 2014. *Reinvent the toilet challenge Phase I (2011 - 2012)* [Online]. Pollution Research Group. Available: http://prg.ukzn.ac.za/projects/completed-projects [Accessed].

PRONK, W. & KONE, D. 2009. Options for urine treatment in developing countries. *Desalination,* 248**,** 360-368.

PRÜSS-ÜSTÜN, A., BOS, R., GORE, F. & BARTRAM, J. 2008. *Safer water, better health: costs, benefits and sustainability of interventions to protect and promote health*, World Health Organization.

PUTNAM 1971. COMPOSITION AND CONCENTRATIVE PROPERTIES OF HUMAN URINE.

RAAL, J. D., GADODIA, V., RAMJUGERNATH, D. & JALARI, R. 2006. New developments in differential ebulliometry: Experimental and theoretical. *Journal of molecular liquids,* 125**,** 45-57.

RABAEY, K., LISSENS, G., SICILIANO, S. D. & VERSTRAETE, W. 2003. A microbial fuel cell capable of converting glucose to electricity at high rate and efficiency. *Biotechnology letters,* 25**,** 1531-1535.

RAMOS, P. M., PEREIRA, J. D., RAMOS, H. M. G. & RIBEIRO, A. L. 2008. A four-terminal water-quality-monitoring conductivity sensor. *Instrumentation and Measurement, IEEE Transactions on,* 57**,** 577-583.

REDLICH, O. 1940. Molal Volumes of Solute. IV. *The Journal of Physical Chemistry,* 44**,** 619-629.

REDLICH, O. & MEYER, D. M. 1964. The molal volumes of electrolytes. *Chemical Reviews,* 64**,** 221-227.

REID, M. & REIN, P. Steam balance for the new Felixton II mill. Proc S Afr Sug Technol Ass, 1983. 85-91.

REYNOLDS, J. G. & CARTER, R. 2008. Reconciliation of solute concentration data with water contents and densities of multi-component electrolyte solutions. *Journal of Solution Chemistry,* 37**,** 1113-1125.

RICHARDS, L. A. 1954. Diagnosis and improvement of saline and alkali soils. *Soil Science,* 78**,** 154.

ROBINSON, R. A. & STOKES, R. H. 2002. *Electrolyte solutions,* Courier Corporation.

RODRIGUEZ, C. & MILLERO, F. J. 2013. Modeling the density and isentropic compressibility of seawater. *Journal of Solution Chemistry,* 42**,** 303-316.

RONTELTAP, M., MAURER, M. & GUJER, W. 2007. Struvite precipitation thermodynamics in source-separated urine. *Water Research,* 41**,** 977-984.

ROSE, C., PARKER, A., JEFFERSON, B. & CARTMELL, E. 2015. The characterisation of faeces and urine; a review of the literature to inform advanced treatment technology. *Critical Reviews in Environmental Science and Technology***,** 00-00.

RUSH, R. M. & JOHNSON, J. S. 1966. Osmotic Coefficients of Synthetic Sea-Water Solutions at 25° C. *Journal of Chemical and Engineering Data,* 11**,** 590-592.

SAKO, T., HAKUTA, T. & YOSHITOME, H. 1985. Vapor pressures of binary (water-hydrogen chloride,-magnesium chloride, and-calcium chloride) and ternary (water-magnesium chloride-calcium chloride) aqueous solutions. *Journal of Chemical and Engineering Data,* 30**,** 224-228.

SALAVERA, D., CHAUDHARI, S. K., ESTEVE, X. & CORONAS, A. 2005. Vapor-liquid equilibria of ammonia+ water+ potassium hydroxide and ammonia+ water+ sodium hydroxide solutions at temperatures from (293.15 to 353.15) K. *Journal of Chemical & Engineering Data,* 50**,** 471-476.

SAMSONOV, N., BOBE, L., NOVIKOV, V., FARAFONOV, N., PINSKY, B. J., RAKOV, V. & KOMOLOV, V. 1999. Development and Testing of a Vacuum Distillation Subsystem for Water Reclamation From Urine. *Training,* 2014**,** 01-29.

SCOGGINS, H. L. & VAN IERSEL, M. W. 2006. In situ probes for measurement of electrical conductivity of soilless substrates: Effects of temperature and substrate moisture content. *HortScience,* 41**,** 210-214.

SHARQAWY, M. H., LIENHARD, J. H. & ZUBAIR, S. M. 2010. Thermophysical properties of seawater: a review of existing correlations and data. *Desalination and Water Treatment,* 16**,** 354-380.

SHIAH, I.-M. & TSENG, H.-C. 1996. Experimental and theoretical determination of vapor pressures of NaCl · KCl, NaBr · KBr and NaCl · CaCl 2 aqueous solutions at 298 to 343 K. *Fluid phase equilibria,* 124**,** 235-249.

SHOCK, E. L., OELKERS, E. H., JOHNSON, J. W., SVERJENSKY, D. A. & HELGESON, H. C. 1992. Calculation of the thermodynamic properties of aqueous species at high pressures and temperatures. Effective electrostatic radii, dissociation constants and standard partial molal properties to 1000 C and 5 kbar. *J. Chem. Soc., Faraday Trans.,* 88**,** 803-826.

SILVESTER, L. F. & PITZER, K. S. 1977. Thermodynamics of electrolytes. 8. High-temperature properties, including enthalpy and heat capacity, with application to sodium chloride. *The Journal of Physical Chemistry,* 81**,** 1822-1828.

SILVESTER, L. F. & PITZER, K. S. 1978. Thermodynamics of electrolytes. X. Enthalpy and the effect of temperature on the activity coefficients. *Journal of Solution Chemistry,* 7**,** 327-337.

SIMONSON, J. M. & RYTHER, R. J. 1989. Volumetric properties of aqueous sodium hydroxide from 273.15 to 348.15 K. *Journal of Chemical and Engineering Data,* 34**,** 57-63.

SLADE, P. E. 1975. *Polymer Molecular Weights,(2 Part),* CRC Press.

SORENSEN, J. A. & GLASS, G. E. 1987. Ion and temperature dependence of electrical conductance for natural waters. *Analytical Chemistry,* 59**,** 1594-1597.

SPARROW, B. S. 2003. Empirical equations for the thermodynamic properties of aqueous sodium chloride. *Desalination,* 159**,** 161-170.

STIGTER, D. & HILL, T. L. 1959. Theory of the Donnan membrane equilibrium. II. Calculation of the osmotic pressure and of the salt distribution in a Donnan system with highly charged colloid particles. *The Journal of Physical Chemistry,* 63**,** 551-555.

STUMM, W. & MORGAN, J. J. 1996. Aquatic chemistry: chemical equilibria and rates in natural waters. *A Wiley-Interscience publication*.

SUN, F., DONG, W., SHAO, M., LI, J. & PENG, L. 2012. Stabilization of source-separated urine by biological n itrification process: treatment performance and nitrite accumulation. *Water Science & Technology,* 66.

SUN, H., FEISTEL, R., KOCH, M. & MARKOE, A. 2008. New equations for density, entropy, heat capacity, and potential temperature of a saline thermal fluid. *Deep Sea Research Part I: Oceanographic Research Papers,* 55**,** 1304-1310.

SWEENEY, T. E. & BEUCHAT, C. A. 1993. Limitations of methods of osmometry: measuring the osmolality of biological fluids. *American Journal of Physiology,* 264**,** R469-R469.

TALBOT, J. D., HOUSE, W. A. & PETHYBRIDGE, A. D. 1990. Prediction of the temperature dependence of electrical conductance for river waters. *Water Research,* 24**,** 1295-1304.

TAMPONNET, C., SAVAGE, C., AMBLARD, P., LASSERRE, J., PERSONNE, J. & GERMAIN, J. 1999. Water recovery in space. *ESA bulletin***,** 56-60.

TANG, I. & MUNKELWITZ, H. 1994. Water activities, densities, and refractive indices of aqueous sulfates and sodium nitrate droplets of atmospheric importance. *Journal of Geophysical Research,* 99**,** 18801-18808.

TETTENBORN, F., BEHRENDT, J., OTTERPOHL, R. & PROTECTION, W. 2007. Resource recovery and removal of pharmaceutical residues-Treatment of separate collected urine. *Final report for task,* 7.

TILLEY, E., ATWATER, J. & MAVINIC, D. 2008. Effects of storage on phosphorus recovery from urine. *Environmental technology,* **29,** 807-816.

TROPEA, C., YARIN, A. L. & FOSS, J. F. 2007. *Springer handbook of experimental fluid mechanics*, Springer Science & Business Media.

UDERT, K., FUX, C., MNSTER, M., LARSEN, T., SIEGRIST, H. & GUJER, W. 2003a. Nitrification and autotrophic denitrification of source-separated urine. *Water Science & Technology,* **48,** 119-130.

UDERT, K., LARSEN, T. & GUJER, W. 2006. Fate of major compounds in source-separated urine. *Water Science & Technology,* **54,** 413-420.

UDERT, K. & WÄCHTER, M. 2012. Complete nutrient recovery from source-separated urine by nitrification and distillation. *Water research,* **46,** 453-464.

UDERT, K. M. 2003. Electrodialysis of Source-Separated Urine. *Internal Report, Eawag, Dubendorf, Switzerland.*

UDERT, K. M., BUCKLEY, C. A., WÄCHTER, M., MCARDELL, C. S., KOHN, T., STRANDE, L., ZÖLLIG, H., FUMASOLI, A., OBERSON, A. & ETTER, B. 2015. Technologies for the treatment of source-separated urine in the eThekwini Municipality. *Water SA,* 41**,** 212-221.

UDERT, K. M., LARSEN, T. A., BIEBOW, M. & GUJER, W. 2003b. Urea hydrolysis and precipitation dynamics in a urine-collecting system. *Water Research,* **37,** 2571-2582.

UNICEF 2015. Progress on Sanitation and Drinking-Water: 2015 Update and MDG Assessment. *World Health Organization: Geneva, Switzerland*.

VINNERÅS, B., BJÖRKLUND, A. & JÖNSSON, H. 2003. Thermal composting of faecal matter as treatment and possible disinfection method—laboratory-scale and pilot-scale studies. *Bioresource Technology,* 88**,** 47-54.

VISCONTI, F., DE PAZ, J. & RUBIO, J. L. 2010. An empirical equation to calculate soil solution electrical conductivity at 25 C from major ion concentrations. *European journal of soil science,* 61**,** 980-993.

WAGNER, W. & KLEINRAHM, R. 2004. Densimeters for very accurate density measurements of fluids over large ranges of temperature, pressure, and density. *Metrologia,* 41**,** S24.

WAGNER, W. & PRUß, A. 1995. The IAPWS formulation 1995 for the thermodynamic properties of ordinary water substance for general and scientific use. *Journal of Physical and Chemical Reference Data,* 31**,** 387-535.

WANG, S.-C., WANG, C.-K., CHANG, F.-M. & TSAO, H.-K. 2002. Second virial coefficients of poly (ethylene glycol) in aqueous solutions at freezing point. *Macromolecules,* 35**,** 9551-9555.

WELLS, J. 1973. Salt activity and osmotic pressure in connective tissue. I. A study of solutions of dextran sulphate as a model system. *Proceedings of the Royal Society of London B: Biological Sciences,* 183**,** 399-419.

WIESENBURG, D. A. & LITTLE, B. J. 1988. A synopsis of the chemical/physical properties of seawater. DTIC Document.

WILSON, A. D. & STEWART, F. F. 2013. Deriving osmotic pressures of draw solutes used in osmotically driven membrane processes. *Journal of membrane science,* 431**,** 205-211.

WU, J. & PRAUSNITZ, J. M. 1999. Osmotic pressures of aqueous bovine serum albumin solutions at high ionic strength. *Fluid Phase Equilibria,* 155**,** 139-154.

YOKOZEKI, A. 2006. Osmotic pressures studied using a simple equation-of-state and its applications. *Applied energy,* 83**,** 15-41.

ZAYTSEV, I. D. & ASEYEV, G. G. 1992. *Properties of aqueous solutions of electrolytes,* CRC press.

APPENDIX A: SPECIATION

This appendix shows the input file for the speciation software, PHREEQC 2.0. The software was downloaded from the website http://wwwbrr.cr.usgs.gov/projects/GWC_coupled/phreeqc/. For modeling of the speciation of hydrolysed urine, the input data required by the program was:

1) major elements and their respective concentration,
2) pH and
3) Temperature.

The tables below typical input and output files from Phreeqc C 2.0 for hydrolysed urine wih a concentration of 4.5 wt% and temperature of 298K

Table A- 1: Output Phreeqc file for hydrolysed urine with a concentration of 4.5 wt%

```
Solution 1: Hydrolysed urine [Concentration =4.5wt%]
        temp    25
         pH     7 charge
        -units mol/kgw
                Na      0.10034
                K       0.04503
                Amm     0.57017
                Cl      0.16921
                H(1)    0.0333
                P       0.01667
                S       0.26483
End
```

Table A- 2: Output Phreeqc file for hydrolysed urine with a concentration of wt%

```
Beginning of initial solution calculations.
-----------------------------------------
Initial solution 1.     # Acidified Urine 4.5 wt%


-----------------------------Solution composition------------------------------
        Elements        Molality        Moles

        Amm         5.702e-01           5.702 e-01
        Cl          1.692 e-01          1.692 e-01
        K           4.503 e-02          4.503 e-02
        Na           1.003 e-01          1.003 e-01
        P           1.667 e-02          1.667 e-02
        S           2.648 e-01          2.64 8e-01
```

----------Description of solution----------

pH	=	4.49
Specific Conductance (uS/cm, 60 ˚C)	=	86279
Density (g/cm3)	=	1.00813 (Millero)
Activity of water	=	0.982
Ionic strength	=	7.469e-01
Mass of water (kg)	=	1.000e+00
Total alkalinity (eq/kg)	=	5.309e-03
Total carbon (mol/kg)	=	0.000e+00
Total CO_2 (mol/kg)	=	0.000e+00
Temperature (deg C)	=	60.000
Electrical balance (eq)	=	-5.309e-03
Percent error, 100*(Cat-|An|)/ (Cat+|An|)	=	-0.44
Iterations	=	9
Total H	=	1.116106e+02
Total O	=	5.663222e+01

----------Distribution of species----------

Species	Molality	Activity	Log Molality	Log Activity	Log Gamma
H+	1.399e-06	1.035e-06	-5.854	-5.985	-0.131
OH-	1.512e-07	8.810e-08	-6.821	-7.055	-0.235
H2O	5.551e+01	9.822e-01	1.744	-0.008	0.000
Amm 5.702e-01					
AmmH+	4.694e-01	2.498e-01	-0.328	-0.602	-0.274
AmmHSO4-	9.976e-02	7.382e-02	-1.001	-1.132	-0.131
Amm	1.048e-03	1.244e-03	-2.980	-2.905	0.075
Cl 1.692e-01					
Cl-	1.692e-01	1.012e-01	-0.772	-0.995	-0.223
H2	5.925e-24	7.037e-24	-23.227	-23.153	0.075
K 4.503e-02					
K+	3.673e-02	2.197e-02	-1.435	-1.658	-0.223
KSO4-	8.263e-03	6.115e-03	-2.083	-2.214	-0.131
KHPO4-	3.201e-05	2.369e-05	-4.495	-4.625	-0.131
KOH	6.087e-11	7.229e-11	-10.216	-10.141	0.075
Na 1.003e-01					
Na+	8.870e-02	6.097e-02	-1.052	-1.215	-0.163
NaSO4-	1.155e-02	8.549e-03	-1.937	-2.068	-0.131
NaHPO4-	8.885e-05	6.575e-05	-4.051	-4.182	-0.131
NaOH	3.219e-10	3.823e-10	-9.492	-9.418	0.075
P 1.667e-02					
H2PO4-	1.240e-02	7.734e-03	-1.907	-2.112	-0.205
HPO4-2	4.149e-03	5.530e-04	-2.382	-3.257	-0.875
NaHPO4-	8.885e-05	6.575e-05	-4.051	-4.182	-0.131
KHPO4-	3.201e-05	2.369e-05	-4.495	-4.625	-0.131
PO4-3	4.195e-08	4.505e-10	-7.377	-9.346	-1.969
S (6) 2.648e-01					
SO4-2	1.452e-01	2.294e-02	-0.838	-1.639	-0.802
AmmHSO4-	9.976e-02	7.382e-02	-1.001	-1.132	-0.131
NaSO4-	1.155e-02	8.549e-03	-1.937	-2.068	-0.131
KSO4-	8.263e-03	6.115e-03	-2.083	-2.214	-0.131
HSO4-	7.343e-06	5.434e-06	-5.134	-5.265	-0.131

----------Saturation indices----------

End of simulation.

APPENDIX B: CALIBRATION OF VAPOUR PRESSURE MEASURING EQUIPMENT

This appendix contains the calibration data of the temperature and pressure probes used with the static pressure equipment.

The Pt-100 temperature sensors were calibrated using a standard reference probe (Pt-100 resistance thermometer type) with a certified accuracy of ± 0.03 K connected to a handheld WIKA CTH 6500 unit. The sensors were immersed into a stirred WIKA 9100 micro calibration bath. The temperature of the oil bath was systematically increased by 10 units within a temperature range of 20 – 110 °C. Similarly, the process was repeated four times to ascertain accuracy and reproducibility. Table B- 1 shows 2 calibration runs performed for the two temperature probes.

Table B- 1: Calibration data for the pressure probes

T_{BATH} [°C]	Probe 1	Probe 2	T_{WIKA} [°C]	T_{BATH} [°C]	Probe 1	Probe 2	T_{WIKA} [°C]
20.000	20.743	20.902	19.700	20.000	20.842	20.987	19.770
30.000	30.870	31.077	29.850	30.000	30.982	31.185	29.920
40.000	40.996	41.228	39.990	40.000	41.113	41.339	40.070
50.000	50.986	51.280	50.030	50.000	51.225	51.492	50.200
60.000	61.125	61.437	60.160	60.000	61.125	61.437	60.160
70.000	71.184	71.514	70.210	80.000	71.311	71.631	70.320
80.000	81.334	81.701	80.350	80.000	81.334	81.701	80.350
90.000	91.307	91.706	90.360	90.000	91.316	91.714	90.360
100.000	101.367	101.792	100.410	100.000	101.367	101.792	100.410

The pressure transmitter was calibrated from a standard pressure transducer (model CPC 3000, WIKA) with certified accuracy of less than 0.025 %. A vacuum pump was used to vary the pressure between 0 – 100 kPa in increments of 1 units, and the pressure readings from the transmitters were noted. This process was performed four times in order to ascertain the accuracy and repeatability of the calibration procedure. Table B- 2 the calibration data for the pressure transducers.

Table B- 2: Calibration data for the temperature probes

Run	Pressure (kPa)			
	Setpoint	Mensor	Transducer 1	Transducer 2
1	0	0.00	0.32	0.15
2	5	5.00	4.78	4.80
3	10	9.99	9.78	9.70
4	15	15.00	14.81	14.60
5	20	19.89	19.76	19.60
6	25	24.98	24.84	24.80
7	30	30.00	29.86	29.70
8	35	35.00	34.86	34.60
9	40	40.00	39.87	39.60
10	45	45.07	44.94	44.80
11	50	50.01	49.88	49.70
12	55	55.00	54.86	54.80
13	60	60.00	59.86	59.70
14	65	65.00	64.85	64.70
15	70	70.40	70.25	70.00
16	75	74.87	74.71	74.50
17	80	80.00	79.84	79.70
18	85	84.90	84.73	84.80
19	90	89.89	89.71	89.60
20	95	94.91	94.72	94.60
21	100	99.73	99.53	99.40

APPENDIX C: SODIUM CHLORIDE DATA

This appendix contains the raw data for the NaCl Test solutions which were compared to the literature data in Chapter 5. Statistical parameters such as the sum of squared errors, absolute average deviation (AAD) and standard deviation were calculated in order to perform an error analysis. The data shown in this appendix is for the following measured properties, vapour pressure, density and electrical conductivity. The tables containing vapour pressure data also include the regressed constants for the Antoine equation.

C.1 VAPOUR PRESSURE

Table C- 1 to Table C- 3 shows the vapour pressure data used to regress the Antoine's constants for the three NaCl solutions.

Table C- 1: Regressed Antoine's constants for vapour pressure data for 0.1M NaCl solution

Constants		**T(K)**	**P_{expt}(kPa)**	**P_{calc}(kPa)**	**ΔP(kPa)**
A	7.0891	313.15	7.36	7.35	0.009
B	1668.25	323.15	12.30	12.30	0.002
C	-45.069	333.15	19.87	19.87	-0.003
		343.15	31.07	31.08	-0.006
Error Analysis		353.15	47.22	47.22	-0.004
Average (%)	0.20	363.15	69.88	69.88	0.002
Std Dev (%)	0.54	373.15	100.98	100.98	0.007
RMS (kPa)	0.005	383.15	142.76	142.77	-0.004

Table C- 2: Regressed Antoine's constants for vapour pressure data for 0.5M NaCl solution

Constants		**T(K)**	**P_{expt}(kPa)**	**P_{calc}(kPa)**	**ΔP(kPa)**
A	7.0846	313.15	7.26	7.25	0.008
B	1669.03	323.15	12.14	12.14	0.002
C	-44.998	333.15	19.60	19.61	-0.003
		343.15	30.66	30.67	-0.006
Error Analysis		353.15	46.59	46.59	-0.004
Average (%)	0.20	363.15	68.96	68.95	0.002
Std Dev (%)	0.52	373.15	99.64	99.64	0.007
RMS (kPa)	0.005	383.15	140.87	140.87	-0.003

Table C- 3: Regressed Antoine's constants for vapour pressure data for 2.0M NaCl solution

Constants		T(K)	P_{expt}(kPa)	P_{calc}(kPa)	ΔP(kPa)
A	7.0755	313.15	6.87	6.86	0.007
B	1678.21	323.15	11.49	11.48	0.002
C	-44.164	333.15	18.54	18.55	-0.003
		343.15	29.00	29.00	-0.005
Error Analysis		353.15	44.07	44.07	-0.003
Average (%)	0.19	363.15	65.22	65.22	0.002
Std Dev (%)	0.43	373.15	94.26	94.26	0.005
RMS (kPa)	0.004	383.15	133.29	133.29	-0.003

Table C- 4 to Table C- 6 shows the comparison between the experimental and calculated values for the vapour pressure data of the three NaCl solutions.

Table C- 4: Comparison between experimental and calculated vapour pressure data for 0.1M NaCl solution

Error Analysis		T(K)	P_{expt}(kPa)	P_{calc}(kPa)	ΔP(kPa)
Average (%)	0.65	332.65	19.36	19.42	-0.30
Std dev (%)	0.36	342.82	30.51	30.63	-0.40
Maximum (%)	1.22	352.59	45.86	46.16	-0.64
RMS (kPa)	0.61	363.13	69.34	69.83	-0.70
		373.00	99.20	100.43	-1.22

Table C- 5: Comparison between experimental and calculated vapour pressure data for 0.5M NaCl solution

Error Analysis		T(K)	P_{expt}(kPa)	P_{calc}(kPa)	ΔP(kPa)
Average (%)	0.72	332.50	19.229	19.02	1.08
Std dev (%)	0.34	342.30	29.842	29.56	0.95
Maximum (%)	1.08	352.32	45.405	45.05	0.78
RMS (kPa)	0.30	362.65	68.050	67.66	0.58
		372.81	98.634	98.43	0.21

Table C- 6: Comparison between experimental and calculated vapour pressure data for 2M NaCl solution

Error Analysis		T(K)	P_{expt}(kPa)	P_{calc}(kPa)	ΔP(kPa)
Average (%)	0.71	332.57	18.005	18.05	-0.27
Std dev (%)	0.42	342.65	28.270	28.39	-0.42
Maximum (%)	1.36	353.20	43.861	44.15	-0.67
RMS (kPa)	0.62	362.84	63.915	64.46	-0.85
		372.78	91.783	93.03	-1.36

C.2 DENSITY

Table C- 7 to Table C- 9 shows a comparison between the experimental and the literature densities for the three NaCl solutions

Table C- 7: Comparison between measured and literature density data for 0.35M NaCl solution

Error Analysis		T(K)	P_{expt}(kPa)	P_{calc}(kPa)	ΔP(kPa)
Average (%)	0.65	332.65	19.36	19.42	-0.30
Std dev (%)	0.36	342.82	30.51	30.63	-0.40
Maximum (%)	1.22	352.59	45.86	46.16	-0.64
RMS (kPa)	0.61	363.13	69.34	69.83	-0.70
		373.00	99.20	100.43	-1.22

Table C- 8: Comparison between measured and literature density data for 1.10M NaCl solution

Error Analysis		T(K)	P_{expt}(kPa)	P_{calc}(kPa)	ΔP(kPa)
Average (%)	0.72	332.50	19.23	19.02	1.08
Std dev (%)	0.34	342.30	29.84	29.56	0.95
Maximum (%)	1.08	352.32	45.41	45.05	0.78
RMS (kPa)	0.30	362.65	68.05	67.66	0.58
		372.81	98.63	98.43	0.21

Table C- 9: Comparison between measured and literature density data for 2.33M NaCl solution

Error Analysis		T(K)	P_{expt}(kPa)	P_{calc}(kPa)	ΔP(kPa)
Average (%)	0.71	332.57	18.005	18.05	-0.27
Std dev (%)	0.42	342.65	28.270	28.39	-0.42
Maximum (%)	1.36	353.20	43.861	44.15	-0.67
RMS (kPa)	0.62	362.84	63.915	64.46	-0.85
		372.78	91.783	93.03	-1.36

C.3 ELECTRICAL CONDUCTIVITY

Table C- 10 to Table C- 12 shows a comparison between the experimental and the literature electrical conductivities for the three NaCl solutions

Table C- 10: Comparison between measured and literature conductivity data for 0.01M NaCl solution

Error Analysis		T(K)	κ_{expt} (S m^{-1})	κ_{calc} (S m^{-1})	$\Delta\kappa$(%)
Average (%)	1.63	293.15	0.106	0.107	-0.866
Std dev (%)	1.14	303.15	0.132	0.132	-0.142
Maximum (%)	3.06	313.15	0.155	0.158	-1.947
RMS (kPa)	0.00	323.15	0.180	0.186	-3.057
		333.15	0.211	0.215	-2.123

Table C- 11: Comparison between measured and literature conductivity data for 0.1M NaCl solution

Error Analysis		T(K)	κ_{expt} (S m^{-1})	κ_{calc} (S m^{-1})	$\Delta\kappa$(%)
Average (%)	1.68	293.15	0.953	0.960	-0.735
Std dev (%)	0.74	303.15	1.162	1.177	-1.298
Maximum (%)	2.67	313.15	1.386	1.409	-1.629
RMS (kPa)	0.03	323.15	1.621	1.655	-2.089
		333.15	1.866	1.916	-2.672

Table C- 12: Comparison between measured and literature conductivity data for 0.5M NaCl solution

Error Analysis		T(K)	κ_{expt} (S m^{-1})	κ_{calc} (S m^{-1})	$\Delta\kappa$(%)
Average (%)	0.77	293.15	4.193	4.204	-0.261
Std dev (%)	0.55	303.15	5.156	5.135	0.407
Maximum (%)	1.47	313.15	6.103	6.130	-0.443
RMS (kPa)	0.07	323.15	7.098	7.187	-1.259
		333.15	8.188	8.308	-1.466

APPENDIX D: EXPERIMENTAL DATA OF HYDROLYSED URINE

This appendix presents the experimental data of the vapour pressure, osmotic pressure, density and electrical conductivity of hydrolysed urine.

Table D- 1: Vapour pressure and osmotic pressure data for urine solutions at varying temperatures and concentration

X = 4.5 %			X = 7.7 %			X = 10.4 %		
T (K)	P(kPa)	π (Mpa)	T (K)	P(kPa)	π (Mpa)	T (K)	P(kPa)	π (Mpa)
332.53	19.10	2.67	332.74	19.04	4.65	332.52	18.61	6.54
342.61	30.00	2.73	342.49	29.46	4.77	341.91	28.37	6.69
352.85	46.06	2.79	352.77	45.31	4.89	353.20	45.52	6.87
362.67	67.70	2.85	363.11	67.93	4.99	362.93	66.57	7.18
368.08	82.85	2.88	368.09	81.80	5.04	367.91	80.19	7.25
372.74	98.13	2.91	373.13	98.20	5.09	373.11	96.80	7.32

X = 14.5 %			X = 18.4 %			X = 21.3 %		
T (K)	P(kPa)	π (Mpa)	T (K)	P(kPa)	π (Mpa)	T (K)	P(kPa)	π (Mpa)
332.63	18.23	10.47	333.03	18.02	14.99	332.57	17.08	19.79
342.73	28.63	10.76	342.85	27.90	15.55	342.31	26.41	20.46
353.23	44.40	11.03	353.40	43.35	15.94	352.44	40.39	20.92
363.54	66.34	11.45	363.14	63.36	16.44	363.53	62.30	21.55
367.55	77.05	11.54	368.13	76.33	16.58	367.83	73.18	21.68
373.08	94.20	11.64	373.26	91.93	16.70	373.37	89.48	21.82

X = 25.4 %			X = 29.2 %			X = 32.2 %		
T (K)	P(kPa)	π (Mpa)	T (K)	P(kPa)	π (Mpa)	T (K)	P(kPa)	π (Mpa)
332.65	16.23	28.11	332.65	15.56	34.52	332.55	14.62	43.16
342.54	25.25	28.92	342.72	24.39	35.45	342.67	23.01	44.21
352.81	38.87	29.34	352.49	36.71	36.33	352.76	35.14	45.02
363.15	58.23	30.16	363.13	55.78	36.99	363.29	53.16	45.75
368.18	70.26	30.46	368.05	67.02	37.39	368.19	63.86	46.12
373.37	84.79	30.72	373.36	81.28	37.62	373.36	77.11	46.30

Table D- 2: Density data in kg m^{-3} of urine solutions at varying temperatures and concentration

T	Total salts concentration (wt %)								
(K)	4.5	7.7	10.4	14.5	18.4	21.3	25.4	29.2	32.2
293.15	1025.5	1044.3	1060.4	1085.1	1107.8	1125.5	1151.3	1173.8	1191.7
298.15	1023.1	1042.8	1058.7	1083.2	1105.9	1123.6	1149.2	1171.7	1189.6
303.15	1022.5	1041.0	1056.9	1081.3	1103.6	1121.5	1147.1	1169.6	1187.4
308.15	1020.8	1039.2	1055.0	1079.3	1101.8	1119.4	1145.6	1167.4	1185.2
313.15	1018.7	1037.2	1052.9	1077.2	1099.7	1117.2	1142.8	1165.1	1183.2
318.15	1016.6	1035.0	1050.7	1075.0	1097.7	1115.4	1140.4	1162.9	1180.7
323.15	1014.0	1031.4	1048.4	1072.7	1095.1	1112.5	1138.1	1160.6	1178.4
328.15	1009.6	1028.0	1046.0	1070.2	1093.1	1110.3	1135.7	1158.2	1176.1
333.15	1008.0	1026.7	1041.6	1067.7	1090.5	1108.1	1133.3	1155.9	1173.7

Table D- 3: Electrical Conductivities data of urine solutions in S/m at varying temperatures and concentration

T(K)	Total salts concentration (wt %)								
	4.5	7.7	10.4	14.5	18.4	21.3	25.4	29.2	32.2
293.15	5.40	8.52	11.06	14.59	17.35	19.26	21.61	23.03	23.82
298.15	5.93	9.31	12.09	15.89	18.95	20.92	23.48	25.13	25.98
303.15	6.50	10.22	13.17	17.26	20.57	22.65	25.37	27.19	28.17
308.15	7.08	11.23	14.27	18.66	22.19	24.41	27.39	29.32	30.33
313.15	7.68	12.08	15.35	20.11	23.82	26.17	29.36	31.44	32.52
318.15	8.26	13.04	16.47	21.54	25.49	27.94	31.35	33.52	34.68
323.15	8.89	13.89	17.55	22.86	27.19	29.56	33.06	35.53	36.76
328.15	9.44	14.71	18.86	24.47	28.69	31.31	35.07	37.55	38.96
333.15	10.03	15.61	19.82	25.84	30.30	33.06	37.02	39.53	41.01

APPENDIX E: CORRELATIVE MODELING DATA

This appendix contains the correlative data for the vapour pressure, Osmotic Pressure, Density and Electrical conductivity of hydrolysed urine.

The following information for each property is presented in the tables;

1. Coefficients for the correlative equation
2. Calculated values using the correlation equations
3. The percent error between the calculated and experimental data
4. Analysis of the percent error

Table E- 1: Correlation calculations for vapour pressure

Coefficients	Value
A_0	6.998
A_1	-0.0013
A_2	-3.68E-5
A_3	5.03E-6
B_0	-1573.8
B_1	0.6706
B_2	-0.0709
B_3	-0.00263
C_0	-108439
C_1	-142.800
C_2	19.120
C_3	0.246

Statistical Analysis (%)	
Average	0.1880
Standard deviation	0.1991
Minimum	0.0003
Maximum	0.6050
Range	0.6047

Calculated Pressure values in kPa

	Total dissolved solids (wt %)								
T (K)	**4.5**	**7.7**	**10.4**	**14.5**	**18.4**	**21.3**	**25.4**	**29.2**	**32.2**
333	19.102	19.040	18.610	18.227	18.017	17.085	16.229	15.556	14.621
343	29.998	29.460	28.365	28.633	27.904	26.406	25.246	24.395	23.007
353	46.058	45.306	45.522	44.399	43.345	40.390	38.875	36.713	35.143
363	67.700	67.926	66.573	66.341	63.357	62.304	58.229	55.781	53.163
368	82.852	81.804	80.186	77.053	76.332	73.177	70.259	67.024	63.859
373	98.127	98.204	96.800	94.204	91.927	89.483	84.785	81.281	77.112

Percent Error (%)

	Total dissolved solids (wt %)								
T (K)	**4.5**	**7.7**	**10.4**	**14.5**	**18.4**	**21.3**	**25.4**	**29.2**	**32.2**
333	0.053	-0.096	-0.031	-0.009	0.270	0.001	-0.582	0.605	-0.206
343	0.051	-0.095	-0.012	0.022	0.206	-0.047	-0.596	0.587	-0.216
353	0.046	-0.091	0.011	0.058	0.250	0.013	-0.408	0.508	-0.174
363	0.046	-0.080	-0.074	-0.016	0.183	-0.044	-0.519	0.535	-0.157
368	0.049	-0.070	-0.062	0.000	0.214	0.000	-0.531	0.465	-0.200
373	0.051	-0.059	-0.050	0.030	0.252	0.064	-0.524	0.496	-0.138

Table E- 2: Correlation calculations for Osmotic pressure

Coefficients	Value
A_0	-220.39
A_1	1.9108
A_2	-0.0054
A_3	5.00E-6
B_0	7973.5
B_1	-68.189
B_2	0.1935
B_3	-0.0002
C_0	-25080
C_1	213.86
C_2	-0.5978
C_3	0.0006

Statistical Analysis (%)	
Average	0.333
Standard deviation	0.287
Minimum	0.018
Maximum	0.985
Range	0.967

Calculated Pressure values in MPa

	Total dissolved solids (wt %)								
T (K)	**4.5**	**7.7**	**10.4**	**14.5**	**18.4**	**21.3**	**25.4**	**29.2**	**32.2**
333	2.71	4.73	6.64	10.62	15.17	20.00	28.36	34.82	43.48
343	2.73	4.77	6.69	10.77	15.55	20.45	28.92	35.44	44.22
353	2.79	4.89	6.87	11.03	15.94	20.91	29.35	36.32	45.02
363	2.85	5.00	7.18	11.45	16.44	21.55	30.16	36.98	45.75
368	2.88	5.04	7.25	11.54	16.57	21.68	30.47	37.38	46.12
373	2.91	5.09	7.32	11.64	16.70	21.82	30.73	37.61	46.31

Percent Error (%)

	Total dissolved solids (wt %)								
T (K)	**4.5**	**7.7**	**10.4**	**14.5**	**18.4**	**21.3**	**25.4**	**29.2**	**32.2**
333	-0.24	0.21	0.18	0.12	-0.39	-0.09	0.73	-0.97	0.46
343	-0.20	0.21	0.12	0.05	-0.34	-0.05	0.75	-0.99	0.44
353	-0.20	0.20	0.12	0.06	-0.31	-0.04	0.60	-0.83	0.40
363	-0.16	0.14	0.15	0.04	-0.36	-0.02	0.72	-0.90	0.39
368	-0.16	0.14	0.16	0.03	-0.36	-0.08	0.76	-0.84	0.34
373	-0.15	0.14	0.16	0.02	-0.38	-0.11	0.83	-0.82	0.30

Table E- 3: Correlation calculations for Density

Coefficients	Value
A_0	-2.796934
A_1	0.253424
A_2	-0.009988
A_3	0.000017
B_0	6.695057
B_1	-0.057674
B_2	0.001042
B_3	-0.000005
C_0	-0.008441
C_1	0.001271
C_2	-0.000026
C_3	0.0000001

Statistical Analysis (%)	
Average	0.0317
Standard deviation	0.0286
Minimum	0.0002
Maximum	0.1338
Range	0.1337

Calculated Densities values in kg m^{-3}

	Total dissolved solids (wt %)								
T (K)	**4.5**	**7.7**	**10.4**	**14.5**	**18.4**	**21.3**	**25.4**	**29.2**	**32.2**
293	1025.1	1044.2	1060.3	1084.9	1108.3	1125.8	1150.6	1173.7	1192.0
298	1023.9	1042.7	1058.7	1083.1	1106.4	1123.8	1148.5	1171.6	1189.9
303	1022.4	1041.1	1056.9	1081.2	1104.4	1121.7	1146.4	1169.5	1187.8
308	1020.6	1039.2	1055.0	1079.2	1102.3	1119.6	1144.3	1167.3	1185.6
313	1018.5	1037.1	1052.9	1077.1	1100.2	1117.5	1142.1	1165.1	1183.3
318	1016.1	1034.8	1050.6	1074.8	1098.0	1115.3	1139.9	1162.8	1181.0
323	1013.4	1032.2	1048.2	1072.5	1095.7	1113.0	1137.6	1160.5	1178.7
328	1010.4	1029.4	1045.5	1069.9	1093.2	1110.6	1135.2	1158.2	1176.3
333	1007.1	1026.3	1042.6	1067.2	1090.7	1108.1	1132.8	1155.8	1173.9

Percent Error (%)

	Total dissolved solids (wt %)								
T (K)	**4.5**	**7.7**	**10.4**	**14.5**	**18.4**	**21.3**	**25.4**	**29.2**	**32.2**
293	0.04	-0.08	0.01	0.02	0.03	0.05	0.06	-0.08	0.09
298	0.02	0.00	-0.01	0.00	0.01	0.02	-0.08	-0.13	0.03
303	0.00	0.00	0.00	0.00	0.00	0.00	0.02	0.05	-0.09
308	0.02	0.01	0.01	0.01	0.01	0.02	0.02	0.03	0.04
313	-0.05	-0.04	-0.07	-0.05	-0.05	-0.02	-0.05	-0.01	-0.02
318	-0.02	-0.02	-0.02	-0.02	-0.03	0.01	-0.05	-0.03	0.00
323	0.06	0.06	0.06	0.11	0.06	0.05	0.05	0.04	0.04
328	0.01	0.01	0.01	0.01	0.01	0.01	0.01	0.01	0.01
333	-0.02	-0.03	-0.03	-0.04	-0.01	-0.03	-0.02	-0.02	-0.02

Table E- 4: Correlation calculations for Electrical Conductivity

Coefficients	Value
A_0	703.775
A_1	29.612
B_0	-1003.13
B_1	-97.756
C_0	3779.229
C_1	211.388
D_0	-8990.6
D_1	-199.344

Statistical Analysis (%)	
Average	0.3460
Standard deviation	0.3018
Minimum	0.0007
Maximum	1.2011
Range	1.2005

Calculated Electrical Conductivity values in S m^{-1}

	Total dissolved solids (wt %)								
T (K)	**4.5**	**7.7**	**10.4**	**14.5**	**18.4**	**21.3**	**25.4**	**29.2**	**32.2**
293	53.2	85.9	110.9	145.1	173.9	192.9	215.5	230.9	238.0
298	58.7	94.4	121.4	158.3	189.3	209.8	234.4	251.5	259.7
303	64.1	102.9	132.2	172.0	205.2	227.1	253.5	272.1	281.6
308	70.4	112.3	143.6	186.0	221.5	245.0	273.5	293.4	303.3
313	76.1	121.1	154.7	200.0	237.8	262.8	293.2	314.5	325.2
318	82.0	130.3	166.2	214.2	254.3	280.7	312.8	335.4	346.7
323	87.7	139.1	177.2	227.9	269.8	297.3	330.8	354.9	367.7
328	93.4	148.4	189.1	242.8	286.6	315.2	349.8	375.2	389.8
333	99.0	157.0	199.8	256.3	302.5	332.6	369.1	395.6	410.1

Percent Error (%)

	Total dissolved solids (wt %)								
T (K)	**4.5**	**7.7**	**10.4**	**14.5**	**18.4**	**21.3**	**25.4**	**29.2**	**32.2**
293	1.77	-0.30	0.26	1.03	0.11	0.07	0.26	-0.40	-0.09
298	0.86	-0.43	-0.46	0.31	0.04	-0.40	0.01	-0.21	-0.07
303	0.68	-1.20	-0.72	0.13	0.07	-0.48	-0.11	-0.21	0.06
308	0.69	0.06	-0.77	0.15	0.09	-0.39	0.24	0.04	0.07
313	0.98	0.40	0.99	0.42	0.14	0.33	0.38	0.22	0.16
318	0.98	0.10	-0.89	0.53	0.35	-0.27	0.56	0.25	0.16
323	1.45	-0.18	-1.09	0.14	0.65	-0.70	-0.12	0.09	-0.07
328	1.06	-0.68	0.00	1.00	0.21	-0.65	0.12	-0.03	0.05
333	1.13	-0.61	-0.80	0.86	0.21	-0.64	0.20	-0.23	-0.21

APPENDIX F: PREDICTIVE THERMODYNAMIC MODELING DATA

This appendix contains the thermodynamic modeling data for the vapour pressure, Osmotic Pressure, Density and Electrical conductivity of hydrolysed urine.

The following information for each property is presented in the tables;

1. Calculated values using the correlation equations
2. The percent error between the calculated and experimental data
3. Analysis of the percent error

Table F- 1: Thermodynamic model correlation calculations for Density

Statistical Analysis (%)	
Average	2.107
Standard deviation	2.373
Minimum	-7.279
Maximum	0.070
Range	7.348

Calculated Vapour Pressure values in kPa

	Total dissolved solids (wt %)								
T (K)	**4.5**	**7.7**	**10.4**	**14.5**	**18.4**	**21.3**	**25.4**	**29.2**	**32.2**
333	19.09	19.03	18.60	18.29	18.18	17.43	16.91	16.29	15.69
343	29.98	29.44	28.35	28.73	28.17	26.95	26.30	25.52	24.65
353	46.03	45.28	45.49	44.55	43.76	41.21	40.43	38.43	37.60
363	67.67	67.88	66.53	66.57	63.96	63.56	60.55	58.33	56.78
368	82.81	81.75	80.14	77.32	77.05	74.62	73.06	70.02	68.08
373	98.08	98.14	96.74	94.52	92.76	91.20	88.13	84.83	82.07

Percent Error (%)

	Total dissolved solids (wt %)								
T (K)	**4.5**	**7.7**	**10.4**	**14.5**	**18.4**	**21.3**	**25.4**	**29.2**	**32.2**
333	0.05	0.07	0.06	-0.32	-0.93	-2.04	-4.20	-4.70	-7.28
343	0.05	0.06	0.06	-0.35	-0.95	-2.05	-4.17	-4.63	-7.14
353	0.05	0.06	0.06	-0.35	-0.96	-2.04	-4.00	-4.69	-6.99
363	0.05	0.06	0.06	-0.35	-0.95	-2.02	-3.98	-4.57	-6.80
368	0.05	0.06	0.06	-0.35	-0.94	-1.98	-3.98	-4.47	-6.61
373	0.05	0.07	0.06	-0.34	-0.91	-1.92	-3.95	-4.37	-6.43

Table F- 2: Thermodynamic model correlation calculations for Density

Statistical Analysis (%)	
Average	3.271
Standard deviation	3.654
Minimum	-0.110
Maximum	10.694
Range	10.804

Calculated Osmotic Pressure values in MPa

	Total dissolved solids (wt %)								
T (K)	**4.5**	**7.7**	**10.4**	**14.5**	**18.4**	**21.3**	**25.4**	**29.2**	**32.2**
333	2.74	4.76	6.63	9.99	13.59	16.75	21.90	27.59	32.56
343	2.81	4.87	6.79	10.23	14.08	17.32	22.60	28.45	33.55
353	2.88	4.98	6.96	10.48	14.42	17.72	23.14	29.09	34.33
363	2.94	5.09	7.28	10.88	14.90	18.32	23.84	29.75	35.10
368	2.97	5.15	7.35	10.97	15.05	18.48	24.08	30.25	35.65
373	3.00	5.20	7.43	11.09	15.20	18.68	24.33	30.56	36.02

Percent Error (%)

	Total dissolved solids (wt %)								
T (K)	**4.5**	**7.7**	**10.4**	**14.5**	**18.4**	**21.3**	**25.4**	**29.2**	**32.2**
333	-0.07	-0.11	-0.10	0.49	1.40	3.04	6.21	6.93	10.61
343	-0.08	-0.10	-0.09	0.53	1.47	3.14	6.31	7.00	10.66
353	-0.08	-0.10	-0.10	0.55	1.52	3.20	6.21	7.24	10.69
363	-0.08	-0.10	-0.10	0.57	1.54	3.23	6.32	7.23	10.64
368	-0.09	-0.11	-0.10	0.57	1.52	3.20	6.38	7.14	10.46
373	-0.08	-0.11	-0.10	0.55	1.50	3.13	6.40	7.06	10.29

Table F- 3: Thermodynamic model correlation calculations for Density

Statistical Analysis (%)	
Average	0.0317
Standard deviation	0.0286
Minimum	0.0002
Maximum	0.1338
Range	0.1337

Calculated Density values in kg m^{-3}

	Total dissolved solids (wt %)								
T (K)	**4.5**	**7.7**	**10.4**	**14.5**	**18.4**	**21.3**	**25.4**	**29.2**	**32.2**
293	1025.9	1045.4	1062.0	1087.7	1112.2	1130.3	1157.1	1179.6	1198.3
298	1024.5	1043.8	1060.3	1085.8	1110.1	1128.1	1154.8	1177.2	1195.9
303	1025.9	1045.4	1062.0	1087.7	1112.2	1130.3	1157.1	1179.6	1198.3
308	1021.6	1040.6	1056.7	1081.6	1105.5	1123.2	1149.5	1171.9	1190.6
313	1020.0	1038.8	1054.7	1079.4	1103.0	1120.6	1146.7	1169.0	1187.8
318	1018.2	1036.8	1052.6	1077.1	1100.4	1117.9	1143.8	1166.1	1184.9
323	1016.1	1034.6	1050.3	1074.6	1097.8	1115.1	1140.9	1163.2	1181.9
328	1013.7	1032.2	1047.8	1072.0	1095.1	1112.4	1138.1	1160.3	1179.0
333	1010.9	1029.3	1045.0	1069.3	1092.4	1109.7	1135.4	1157.5	1176.1

Percent Error (%)

	Total dissolved solids (wt %)								
T (K)	**4.5**	**7.7**	**10.4**	**14.5**	**18.4**	**21.3**	**25.4**	**29.2**	**32.2**
293	-0.04	-0.10	-0.15	-0.24	-0.39	-0.42	-0.51	-0.49	-0.55
298	-0.14	-0.10	-0.15	-0.23	-0.38	-0.40	-0.48	-0.47	-0.53
303	-0.15	-0.18	-0.19	-0.25	-0.35	-0.44	-0.50	-0.55	-0.45
308	-0.09	-0.13	-0.16	-0.22	-0.33	-0.34	-0.34	-0.39	-0.46
313	-0.13	-0.15	-0.17	-0.20	-0.30	-0.30	-0.34	-0.33	-0.39
318	-0.16	-0.18	-0.19	-0.19	-0.25	-0.22	-0.30	-0.28	-0.36
323	-0.21	-0.31	-0.18	-0.18	-0.24	-0.24	-0.25	-0.22	-0.30
328	-0.41	-0.40	-0.17	-0.17	-0.19	-0.19	-0.21	-0.18	-0.25
333	-0.28	-0.26	-0.33	-0.15	-0.18	-0.15	-0.18	-0.15	-0.21

Table F- 4: Thermodynamic model calculations for Electrical Conductivity

Statistical Analysis (%)	
Average	0.3460
Standard deviation	0.3018
Minimum	0.0007
Maximum	1.2011
Range	1.2005

Calculated Electrical Conductivity values in S m^{-1}

	Total dissolved solids (wt %)								
T (K)	**4.5**	**7.7**	**10.4**	**14.5**	**18.4**	**21.3**	**25.4**	**29.2**	**32.2**
293	54.5	58.7	63.6	70.0	75.3	83.3	89.4	94.1	101.6
298	85.7	93.6	102.5	113.2	121.2	131.5	139.5	147.1	156.2
303	110.7	121.6	132.9	144.1	155.3	166.5	177.7	188.9	200.1
308	146.4	159.5	173.6	187.6	201.7	215.8	229.8	245.4	258.9
313	174.2	190.4	206.6	222.8	239.0	255.2	272.4	287.6	303.8
318	192.6	210.2	227.7	245.2	262.8	280.3	297.8	315.4	332.9
323	217.7	236.0	254.7	275.9	296.2	316.8	331.8	352.8	372.8
328	230.4	251.9	272.6	294.6	316.5	337.5	357.2	377.1	396.1
333	239.4	261.1	282.7	304.4	326.0	347.7	369.3	391.0	412.6

Percent Error (%)

	Total dissolved solids (wt %)								
T (K)	**4.5**	**7.7**	**10.4**	**14.5**	**18.4**	**21.3**	**25.4**	**29.2**	**32.2**
293	1.06	-1.01	-2.12	-1.05	-2.01	0.79	0.58	-0.27	1.36
298	0.60	0.57	0.33	0.78	0.33	0.86	0.49	0.02	0.06
303	0.13	0.61	0.87	0.93	1.16	1.07	1.27	0.18	0.99
308	0.32	0.40	0.58	0.55	0.28	0.17	0.55	0.32	0.18
313	0.39	0.45	0.42	0.39	0.34	0.12	0.18	0.26	0.26
318	0.00	0.47	0.55	0.45	0.40	0.34	0.77	0.71	0.71
323	0.76	0.50	0.38	0.73	0.87	1.04	0.36	0.60	0.68
328	0.06	0.24	0.24	0.48	0.66	0.70	0.53	0.41	0.21
333	0.52	0.49	0.37	0.35	0.26	0.26	0.48	0.36	0.62

APPENDIX G: REGRESSION CONSTANTS FOR BINARY SALTS

The regression constants used for calculating the density of the individual aqueous salt solutions were extracted from Zaytsev (1992). Table G- 1 shows the regression constants for the density equation (3.25)

Table G- 1: Density constants for Millero's equation for densities extracted from Zaytsev (1992)

Constants	NaCl	Na_2SO_4	KCl	NH_4Cl	$(NH_4)_2SO_4$	NaH_2PO_4
A_0	-0.3644	-8.3164	0.2612	-0.1335	9.0069	5.9502
A_1	-0.0262	0.6213	-0.0759	-0.0049	-1.1340	-0.0484
A_2	-0.0007	-0.0163	0.0013	-0.0006	0.0366	0.0008
$A_3 \times 10^{-4}$	0.1284	1.2964	-0.0732	0.0638	-3.2765	-0.0985
B_0	48.6135	67.5096	53.2533	22.8865	22.4840	43.5883
B_1	-0.1842	-1.6777	0.0250	-0.2794	0.9671	0.0068
B_2	0.0033	0.0405	-0.0026	0.0063	-0.0332	0.0002
$B_3 \times 10^{-4}$	-0.2508	-3.1052	0.2844	-0.4569	3.0428	-0.0299
C_0	-5.6489	-11.4129	-5.9063	-4.2844	-2.2157	-4.5416
C_1	0.0429	0.5897	-0.0638	0.0955	-0.2074	0.0029
C_2	-0.0009	-0.0146	0.0022	-0.0021	0.0071	-0.0002
$C_3 \times 10^{-4}$	0.0693	1.1218	-0.1952	0.1597	-0.6519	0.0147
ARD (%)	0.006	0.005	0.008	0.005	0.118	0.015
SD (%)	0.005	0.003	0.006	0.006	0.105	0.066
MRD (%)	0.022	0.015	0.022	0.042	0.998	0.515

APPENDIX H: DESIGN CALCULATIONS FOR THE QUINTUPLE EFFECT EVAPORATOR

This appendix shows the design calculations for a quintuple effect evaporator.

H.1 DESIGNING A MULTIPLE EFFECT EVAPORATOR

A simple non-iterative algorithm was developed in an excel spreadsheet to calculate the heating transfer area of a triple effect evaporator train. By definition the BPE is the difference in the temperature of a solution to that of water at the same pressure,

$$BPE_i = T_{urine,i} - T_{v,i} \quad \text{(H. 1)}$$

where *BPE* is the Boiling Point Elevation in K, T_{urine} is the temperature of urine in K and T_v is the temperature of the vapour in K and I is the effect number.

The heat transferred by the heating steam to the urine solution is an effect is given by the following expression

$$Q_i = U_i A_i \Delta T \quad \text{(H. 2)}$$

where Q is the heat transferred in kJ, U is the heat transfer coefficient in kW/m^2 K, A is the heating surface area in m^2, and ΔT is the driving force temperature between the heating steam $T_{v,i-1}$ and the urine solution being heated, $T_{urine,i.}$

The heat transferred can also be calculated from the mass and enthalpy of the heating steam by equation below

$$Q_i = m_{v,i} \Delta h_i \quad \text{(H. 3)}$$

where $m_{v,I}$ is mass of the heating vapour in kg and Δh_i is latent heat of vaporisation in effect I of the vapour in kJ/kg.

Combining equations (H-2) and (H.3) and rearranging gives an expression for calculating the specific evaporation rate, SE.

$$\frac{m_{v,i}}{A_i} = \frac{U_i \Delta T_i}{\Delta h_i} \qquad \text{(H. 4)}$$

The total evaporation from the multiple effect evaporator can be calculated by the equation below

$$m_{v,T} = m_{urine,0}\left(1 - \frac{X_0}{X_n}\right) \qquad \text{(H. 5)}$$

where $m_{v,T}$ is the total mass of the vapour evaporated in kg/h, and $m_{urine,0}$ is the mass flow of urine in kg/h, X is the salt weight fraction of the dissolved salt in urine in kg/kg.

The heat transfer area of each effect is calculated as follows

$$A_i = \frac{m_{v,i}}{SE_i} \qquad \text{(H. 6)}$$

Where A_i is the heating surface area in m^2, SE is the specific evaporation rate in kg/m^2 h. The total heating area, A_T, of the multiple effect evaporator is the sum of the individual areas

$$A_T = \sum_{i=1}^{n} A_i \qquad \text{(H. 7)}$$

H.2 CALCULATION PROCEDURE AND INPUT PARAMETERS

The excel spreadsheet for calculating the surface area of the multiple effect evaporator was constructed using the equations (H.1) – (H-7)

- A plant processing 12 m^3/d of urine was considered with a supply saturated steam at 200kPa.
- The following additional inputs were considered in modelling the distribution of the heating surface areas of the effects
- The temperature of the urine solutions in each effect at a given pressure were calculated using the Antoine equation

- The heat transfer coefficient of each effect were assumed to have the following fixed values 3100, 2000 and 1200 W/m^2 K.
- The initial and final concentration of the urine solutions were the limit values studied in this work, i.e. 4.7 and 32.2%
- The optimum distribution of the heating surfaces was calculated by maximizing the total specific evaporation rate SET, using the Solver function of MS Excel. The total specific evaporation rate was calculated by summing the individual Ses of the effects.

$$SE_T = \frac{\sum_{i=}^{n} m_{v,i}}{\sum_{i=1}^{n} A_i} \qquad (9.1)$$

Table H- 1: Design calculations for the quintuple effect evaporator

INPUT PARAMETERS

Volumetric flow	m^3/d	12
Density	kg/m^3	1025.5
Mass flow	kg/h	512.8
Inlet Temp	(°C)	298.15
Urine inlet TDS	(%)	4.7
Final urine TDS	(%)	32.2
Pressure (kPa)	Steam	200
	Vacuum	15

OUTPUTS

Area (m²)	26538.7
SE (kg/m² h)	16.5
Steam Required (t/h)	166.8
TDS rate (t/h)	74.8
Total Evaporation (t/h)	437.9

Effect	P	T_{H2O}	T_{urine}	B.P.E	ΔT	(Δh)	OHTC	S.E	Area	Steam Req	Evap	Urine Flow	TDS
	(kPa)	(K)	(K)	(K)	(K)	(kJ/kg)	(W/ m² K)	(kg/m² h)	(m²)	kg/h	(kg/h)	kg/h	kg/h
0	200.0	393.3				2202.6						512.8	4.7
1	159.3	386.5	387.03	0.50	6.3	2223.2	2600	26.6	5654.3	151.7	91.1	421.6	5.7
2	120.5	378.4	378.90	0.52	7.6	2245.7	1600	19.5	4637.0	91.1	90.2	331.4	7.3
3	83.5	368.2	368.92	0.69	9.5	2271.7	1220	18.3	4887.7	90.4	89.3	242.0	10.0
4	48.3	354.1	355.58	1.50	12.6	2305.4	850	16.8	5270.5	89.8	88.5	153.6	15.7
5	15.0	327.2	333.06	5.86	21.0	2367.5	450	14.4	6089.2	89.9	87.6	66.0	32.2

APPENDIX I: PAPERS

This appendix contains two unpublished papers that are ready for submission. The title of the papers are as follows

1. Thermodynamic Properties Urine. Vapour Pressure, Osmotic Pressure, Density and Electrical conductivity measurements.
2. Modeling of the Thermodynamic Properties Urine. Vapour Pressure, Osmotic Pressure, Density and Electrical conductivity.

PAPER 1

Thermodynamic Properties Urine. Vapour Pressure, Osmotic Pressure, Density and Electrical conductivity measurements.

K P Dube*, S Septien*, Velkushanova*, D Ramjugernath K and C A Buckley***

*Pollution Research Group, Department of Chemical Engineering, Howard College Campus, University of KwaZulu-Natal, Durban 4041, South Africa (khonzaphidube@gmail.com)
**Thermodynamic Research Group, Department of Chemical Engineering, Howard College Campus, University of KwaZulu-Natal, Durban 4041, South Africa

ABSTRACT

Very little information is available in literature on the thermodynamic properties of hydrolysed urine. The aim of this study is to determine the thermodynamics properties of hydrolysed urine required for the engineering design of thermal, membrane and electrochemical separation processes. The investigated properties include vapour pressure, osmotic pressure, density and electrical conductivity. Measurements for vapour pressure, osmotic pressure, density and electrical conductivity for hydrolysed urine are presented ranging from 4.5 to 32.2 wt% in concentration and 293 to 373 K in temperature. The thermodynamic properties were fit into correlative models as functions of concentration and temperature. The accuracy of the models was validated by comparing model calculations with experimental data. These equations can be conveniently integrated into computer software for design, modeling and optimization of urine treatment processes.

Keywords: hydrolysed urine, thermodynamic properties, vapour pressure, osmotic pressure, density, electrical conductivity.

INTRODUCTION

The treatment of source separated urine using chemical engineering principles has received increasing attention over the years (Maurer *et al.*, 2006). This concept has been investigated as early as the 1990s as a sustainable option, since urine is abundant with nutrients which can be used as a fertiliser (Kirchmann & Pettersson, 1994; Larsen & Gujer, 1996; Otterpohl *et al.*, 1999). In 2011, the Bill and Melinda Gates Foundation initiated the Reinvent the Toilet Challenge (RTTC) to improve sanitation in the developing world by funding research projects into delivering a "reinvented toilet". The aim of the challenge was to use fundamentals of chemical engineering processes to design and develop a low cost toilet, not connected to the water or sewer or electricity grid, which could sanitize the waste and recover valuable components like nutrients, water and energy(BMFG, 2011). A few examples of the RTTC funded projects include the complete recovery of nutrients from urine through nitrification and distillation (Udert & Wächter, 2012), use of membrane processes (microfiltration, nanofiltration and forward osmosis) to treat urine (PRG, 2014), and generation of electricity from urine using a microbial fuel cell (ref). The development, design and optimization of these processes requires knowledge of the thermodynamic properties of urine.

Treatment technologies for urine must take into account the spontaneous transformative processes that change the composition of source separated urine(Udert *et al.*, 2006). Fresh urine is biologically unstable as it contains urea which is readily hydrolysed into ammonia and bicarbonate, by the enzyme urease produced by most bacteria found in faeces and urine collecting systems (Hellström *et al.*, 1999; Udert *et al.*, 2003a). The increase in ammonia and bicarbonate concentration raises the pH to 9 and prompts the precipitation of struvite ($MgNH_4PO_4 \cdot 6H_2O$), hydroxyapatite ($Ca_5(PO_4)_3(OH)$) and calcite ($CaCO_3$). Table 1 shows the composition of hydrolysed urine found in literature.

PAPER 2

Modeling of the Thermodynamic Properties Urine. Vapour Pressure, Osmotic Pressure, Density and Electrical conductivity.

K P Dube*, S Septien*, Velkushanova*, D Ramjugernath K and C A Buckley***

*Pollution Research Group, Department of Chemical Engineering, Howard College Campus, University of KwaZulu-Natal, Durban 4041, South Africa (septiens@ukzn.ac.za)
**Thermodynamic Research Group, Department of Chemical Engineering, Howard College Campus, University of KwaZulu-Natal, Durban 4041, South Africa

ABSTRACT

Hydrolysed urine is a complex multicomponent aqueous solution containing cations, anions and neutral complexes. The aim of this paper was to incorporate the chemical equilibria of hydrolysed urine in the thermodynamic equations used for calculating vapour pressure, osmotic pressure, density and electrical conductivity. The activity coefficients of the ionic species in the solution were calculated using the B-dot model, which is an extension of the Debye-Hückel law. The model predictions were compared to the data in literature for a concentration range of 4.5 to 32.2 wt% and temperature range of 293 to 373 K. Vapour pressure and osmotic pressure were predicted from the activity of water in urine, and the model was accurate up to a concentration of 14 wt%. The speciation model can be reliably used for the calculation of density and electrical conductivity with good predictions.

Keywords: hydrolysed urine, speciation, Ionic equilibria, vapour pressure, osmotic pressure, density, electrical conductivity

INTRODUCTION

The design and optimisation of engineering processes involving multicomponent electrolyte systems requires suitable models that can accurately predict the thermodynamic properties of the electrolyte solutions. Literature is abundant with thermodynamic models developed for this purpose which include the Davies equation (Davies, 1962), the B-dot equation (Helgeson *et al.*, 1969), the specific-ion equation (Guggenheim & Turgeon, 1955) and the Pitzer (Pitzer & Mayorga, 1973). These models are empirical extensions of the Debye-Hückel law expressed in terms of ionic strength. The thermodynamic models can be coupled with speciation of the electrolyte solutions to improve their predictions. In relation to aqueous solutions, chemical speciation is the distribution and concentration of physicochemically distinct entities at molecular level. The knowledge of the activity coefficients of the species and the true ionic strength obtained from speciation calculations, can be extended to calculate vapour pressure (Gibbard Jr & Scatchard, 1972; Mariah *et al.*, 2006), osmotic pressure (Brouckaert, 1993; May *et al.*, 2010), density (Appelo *et al.*, 2014; Krumgalz *et al.*, 1994; Millero, 1985) and electrical conductivity (Brouckaert, 1995; McCleskey, 2011; McCleskey *et al.*, 2012; Pawlowicz, 2008; Visconti *et al.*, 2010).

In the previous work, Dube et al (2016), the thermodynamic properties of urine were expressed in terms of correlative equations as functions of temperature and total dissolved salts. The contribution of the components constituting the urine was not investigated in calculating the thermodynamics properties. Urine contains the following ionic species with concentrations greater than 0.1mM; Na^{+}, K^{+}, NH^{4+}, Ca^{2+}, $C1^{-}$, SO_4^{2-}, PO_4^{3}- and HCO_3^{2-}(Kirchmann & Pettersson, 1994). This current work is aimed at including the thermochemical equilibria in the equations for calculating the vapour pressure, osmotic pressure, density and electrical conductivity of urine.